Juhani Vihavainen

VVER-440 Thermal Hydraulics as a Computer Code Validation Challenge

Thesis for the degree of Doctor of Science (Technology) to be presented with due permission for public examination and criticism in the Auditorium 1383 at Lappeenranta University of Technology, Lappeenranta, Finland on the 12th of December, 2014, at 13 o'clock.

Acta Universitatis
Lappeenrantaensis 618

Supervisor Professor Juhani Hyvärinen
Department of Energy Technology
School of Technology
Lappeenranta University of Technology
Finland

Reviewers Professor Henryk Anglart
School of Engineering Sciences
KTH Royal Institute of Technology
Sweden

D.Sc. (Tech.)
Harri Tuomisto
Fortum Power and Heat Oy
Finland

Opponent D.Sc. (Tech.) Harri Tuomisto
Fortum Power and Heat Oy
Finland

ISBN 978-952-265-716-9
ISBN 978-952-265-717-6 (PDF)
ISSN-L 1456-4491
ISSN 1456-4491
Lappeenrannan teknillinen yliopisto
Digipaino 2014

Abstract

Juhani Vihavainen
VVER-440 Thermal Hydraulics as a Computer Code Validation Challenge
Lappeenranta 2014
175 pages
Acta Universitatis Lappeenrantaensis 168
Diss. Lappeenranta University of Technology
ISBN 978-952-265-716-9, ISBN 978-952-265-717-6 (PDF), ISSN-L 1456-4491, ISSN 1456-4491

This thesis concentrates on the validation of a generic thermal hydraulic computer code TRACE under the challenges of the VVER-440 reactor type. The code capability to model the VVER-440 geometry and thermal hydraulic phenomena specific to this reactor design has been examined and demonstrated acceptable.

The main challenge in VVER-440 thermal hydraulics appeared in the modelling of the horizontal steam generator. The major challenge here is not in the code physics or numerics but in the formulation of a representative nodalization structure. Another VVER-440 specialty, the hot leg loop seals, challenges the system codes functionally in general, but proved readily representable.

Computer code models have to be validated against experiments to achieve confidence in code models. When new computer code is to be used for nuclear power plant safety analysis, it must first be validated against a large variety of different experiments. The validation process has to cover both the code itself and the code input. Uncertainties of different nature are identified in the different phases of the validation procedure and can even be quantified.

This thesis presents a novel approach to the input model validation and uncertainty evaluation in the different stages of the computer code validation procedure. This thesis also demonstrates that in the safety analysis, there are inevitably significant uncertainties that are not statistically quantifiable; they need to be and can be addressed by other, less simplistic means, ultimately relying on the competence of the analysts and the capability of the community to support the experimental verification of analytical assumptions. This method completes essentially the commonly used uncertainty assessment methods, which are usually conducted using only statistical methods.

Keywords: nuclear power plants, thermal hydraulics, VVER-440 reactors, experiment facilities, thermal hydraulic computer codes, validation, TRACE code, uncertainties
UDC: 621.311.25:621.039.58:004.942:621.039:621.039.51

Acknowledgements

This work was carried out in the department of LUT Energy at Lappeenranta University of Technology, Finland, between 2009 and 2014. The research work has received funding from the Finnish Research Programmes on Nuclear Power Plant Safety: SAFIR2010 and SAFIR2014.

I want to express my deepest gratitude to my supervisor Professor Juhani Hyvärinen for his guidance and helpful instructions during compilation of this thesis. Also, his inspiring ideas and our discussions enhanced my understanding of nuclear engineering and safety.

I am deeply thankful to my pre-reviewers, Professor Henryk Anglart and Dr. Harri Tuomisto, for their proficient comments and valuable suggestions. I especially appreciate their capability to proceed the review process in very tight schedule.

I also wish to thank Professor Riitta Kyrki-Rajamäki for her encouragement during all these years and giving me opportunity to complete this work.

All my colleagues in the Laboratory of Nuclear Engineering and in the Nuclear Safety Research Unit deserve my special thanks for their professional support, not forgetting the bond of friendship with them.

Finally, I wish to thank my wife Maija for her loving care and having persistent faith in my endeavour.

Juhani Vihavainen
November 2014
Lappeenranta, Finland

"It doesn't matter how beautiful your theory is,
it doesn't matter how smart you are.
If it doesn't agree with experiment, it's wrong"

Richard P. Feynman

Contents

Nomenclature

Latin alphabet

A	area	m^2
D	diameter	m
g	acceleration due to gravity	m/s^2
h	height	m
L	length	m
m	mass	kg
p	pressure	Pa
T	temperature	K
t	time	s
v	velocity magnitude	m/s
x	x-coordinate (width)	m

Greek alphabet

α	void fraction
Δ	change in the following variable

Dimensionless numbers

Fr	Froude number
Gr	Grashof number
Nu	Nusselt number
Pr	Prandtl number
Re	Reynolds number

Abbreviations

AER	Atomic Energy Research
AIAA	American Institute of Aeronautics and Astronautics
AP-1000	Advanced Pressurized Water Reactor 1000 concept of Westinghouse
AP-600	Advanced Pressurized Water Reactor 600 concept of Westinghouse
Apros	Advanced Process Simulator
APEX	Advanced Plant Experimental Facility
ATHLET	Analysis of THermal-hydraulics of LEaks and Transients; Computer code developed by GRS
ASME	American Society of Mechanical Engineers
ATWS	Anticipated Transient Without Scram
BE	Best Estimate
BEPU	Best Estimate Plus Uncertainty

BETHSY	Boucle d'Etudes Thermalhydrauliques Systèmes; French test facility for pressurized water reactor modelling
BDBA	Beyond Design Basis Accident
BWR	Boiling Water Reactor
CATHARE	Code for Analysis of THermalhydraulics during an Accident of Reactor and safety Evaluation
CCC	Containment Cooling Condenser
CCFL	Counter Current Flow Limitation
CFD	Computational Fluid Dynamics
CIAU	Code with capability of Internal Assessment of Uncertainty
CMT	Core Make-up Tank
CSAU	Code Scaling, Applicability and Uncertainty
DBA	Design Basis Accident
DEC	Design Extension Condition
ECC	Emergency Core Cooling
EC	Emergency Condenser
EM	Evaluation Model
EOP	Emergency Operating Procedure
ESBWR	Economic Simplified Boiling Water Reactor
GDCS	Gravity Driven Cooling System
GRS	Gesellschaft für Anlagen- und Reaktorsicherheit; German research organization
HA	Hydro-Accumulator
HPI	High Pressure Injection
HPIS	High Pressure Injection System
HSG	Horizontal Steam Generator
IAEA	International Atomic Energy Agency of United Nations
ICS	Isolation Condenser System
ICARE	French code for the simulation of severe accidents
IET	Integral Effect Test
IL	Injection Line
IMTHUA	Integrated Methodology for Thermal–Hydraulics Uncertainty Analysis
IP	Intermediate Pressure
IRWST	Internal Refueling Water Storage Tank
ISP	International Standard Problem of OECD/NEA
ITF	Integral Test Facility
KERENA	AREVA BoilingWater Reactor design
LOCA	Loss-of-Coolant Accident
LPIS	Low Pressure Injection System
LSTF	Large Scale Test Facility
LUT	Lappeenranta University of Technology
NC	Natural Circulation
NPP	Nuclear Power Plant
OECD	Organisation for Economic Co-operation and Development

/NEA /	Nuclear Energy Agency
/CSNI /	Committee on the Safety of Nuclear Installations
OTSG	Once Through Steam Generator
PACTEL	Parallel Channel Test Loop; a test facility at LUT
PBL	Pressure Balancing Line
PCCS	Passive Containment Cooling System
PIE	Postulated Initiating Event
PIRT	Phenomena Identification and Ranking Table
PKL	Primärkreislauf; German test facility for pressurized water reactor modelling
PMK	Hungarian test facility for VVER-440
PPPT	Passive Pressure Pulse Transmitters
PRISE	Primary to secondary leak
PSHR C	Passive System of Heat Removal from Containment
PSHR SG	Passive System of Heat Removal from Steam Generators
PSIS	Passive Safety Injection System
PWR	Pressurized Water Reactor
RCP	Reactor Coolant Pump
RELAP	Reactor Excursion and Leak Analysis Program
REWET	Series of test facilities at LUT
RHR	Residual Heat Removal
ROSA	Rig of Safety Assessment
RPV	Reactor Pressure Vessel
SBLOCA	Small Break Loss-of-Coolant Accident
SCDAP	Severe Core Damage Analysis Package
SET	Separate Effect Test
SETF	Separate Effect Test Facility
SG	Steam Generator
SNAP	Symbolic Nuclear Analysis Package; graphical user interface
Stdst	Steady state
STUK	Radiation and Nuclear Safety Authority of Finland
SV	Sensitivity value
SWR-1000	Siedewasser Reaktor 1000
TMI-2	Three Mile Island reactor unit 2
TRACE	TRAC/RELAP Advanced Computational Engine
UMAE	Uncertainty Methodology based on Accuracy Evaluation
UQ	Uncertainty quantification
UPTF	Upper Plenum Test Facility
UTSG	U-Tube Steam Generator
VEERA	Test facility for VVER studies at LUT
VVER	Russian pressurized water reactor type
VVER-440	Russian pressurized water reactor

1 Introduction

Nuclear power differs significantly from other energy forms because it generates radioactive materials that would pose a health hazard if they were released into the environment in large quantities. For this reason, the nuclear community devotes a lot of attention to the safety or prevention of damage of nuclear power plants and the minimization of radioactive releases. The safety aspect is continuously present throughout the lifecycle of a nuclear power plant. The safety of nuclear power plants must be maintained continuously and reviewed periodically at defined intervals (IAEA, 2009a). Such reviews involve safety analyses: the analysis of nuclear power plant behaviour under normal, abnormal and even quite extreme conditions The adequate safety assessment requires, that also the tools needed for the safety analysis have to be always available and in good condition.

It is not possible or desirable to run tests at the nuclear power plant to cover all possible situations of interest in the safety analysis. However, accident conditions can be replicated in dedicated experimental facilities, such as the PACTEL facility at Lappeenranta University of Technology (LUT). Safety analysis of actual power plants is performed using theoretical means: using computer code calculations that are supported by (mainly) model experiments. With model experiments the physical phenomena in reality can be observed and analysed. The computer codes solve the relevant physical equations with numerical methods.

When computer code models are validated against experiments, confidence in code models can be achieved. Therefore, if a new tool, like a new computer code, is to be used for the nuclear power plant safety analysis, it must first be validated against a large variety of different experiments. The validation process has to cover both the code itself (for the adequacy of physics and numerics) and the code input (for the adequate representation of the plant or model in question). Uncertainties of different nature can be identified in the different phases of the validation procedure, and under certain constraints, the uncertainties can even be quantified.

This thesis focuses on the validation of a new thermal-hydraulic system analysis code TRACE for VVER-440 reactor applications. The TRACE code has been developed in the United States by the U.S. Nuclear Regulatory Commission (NRC) for the generic thermal-hydraulic safety analysis of light water reactors (LWRs). The Finnish interest in TRACE stems from the authority requirement to maintain diverse safety analysis tools for the safety analysis of Finnish reactors.

The development of VVER-440, the first widely built Russian pressurized water reactor type, started already in the 1950s when its first generation and prototype reactors were introduced. The second generation of VVER reactors was designed in the 1970s. These reactors are still in operation and located in Russia, Eastern Europe and also two of them in Finland. Loviisa Unit 1 started commercial operation in 1977 and Loviisa Unit 2 in 1981. The principal specific feature in VVER reactor cooling systems are the

horizontal steam generators, but it also has hot leg loop seals. Western PWRs typically have vertical steam generators and straight hot legs.

The thesis presents the results of the TRACE validation effort for VVER-440 reactor related experiments. Thermal hydraulic modelling is always an optimization task: different modelling options have to be evaluated and decisions have to be made to reach the most applicable solution. As always in numerical modelling, the model accuracy is competing with the need to have reasonable computing times.

This thesis presents a novel approach to the input model validation and uncertainty evaluation in the different stages of the computer code validation procedure. In particular, the new framework allows a clear identification, which uncertainties are statistically quantifiable and which are not. This thesis also shows that in the safety analysis, there are inevitably significant uncertainties that are not statistically quantifiable; they need to be and can be addressed by other, less simplistic means, ultimately relying on the competence of the analysts and the capability of the community to support the experimental verification of analytical assumptions. This method completes essentially the commonly used uncertainty assessment methods, which are usually conducted using only statistical methods.

1.1 Contribution of the author

The author has validated the thermal hydraulic TRACE code against unique VVER-440 specific thermal-hydraulic phenomena, as represented by the PACTEL facility. This is a novel application of the TRACE code; it has not been used in Finland for VVER-440 type reactor analysis purposes.

As far as the author knows, the only other study where the TRACE code has been applied to VVER-440 analysis was conducted in the Czech Republic. The TRACE code has been applied to the Dukovany VVER-440 reactor pressure vessel to evaluate mixing factors under normal operation conditions (Heralecky and Blaha, 2010). The purpose of these analyses was to assess the capability of the TRACE code and the developed input deck to solve coolant mixing problems in VVER-440 type reactors.

The VVER-440 specific phenomena pertain to hot leg loop seals and horizontal steam generator behaviour at natural circulation conditions. Being VVER-440 specific but well represented in PACTEL, these phenomena constitute challenging validation cases for TRACE because the code was initially developed for western PWRs, where such geometric features do not exist. On the basis of its design, as a generic thermal hydraulic modelling code, TRACE should be capable of reproducing PACTEL (VVER) behaviour.

The author has published the essential aspects of the works utilized in this thesis in the following publications:

- *Vihavainen, J., Riikonen, V., Kyrki-Rajamäki, R., TRACE code modeling of the horizontal steam generator of the PACTEL facility and calculation of a loss-of-feedwater experiment, Annals of Nuclear Energy, 2010.*
  This paper describes the modelling of a horizontal steam generator with the TRACE code and the calculation results of a loss-of-feedwater experiment at the PACTEL facility. Modelling options are discussed. The author of this thesis was the principal author of this publication.

- *Vihavainen, J., Riikonen, V., Puustinen, M., Kyrki-Rajamäki, R., Modeling of the PACTEL Facility and Simulation of a Small Break LOCA Experiment with the TRACE v5.0 code, Nureth-14 conference proceedings, 2011.*
  This paper presents a full simulation model of the PACTEL facility prepared with the TRACE code. The paper discusses the PACTEL experiment SBL-30 as a TRACE code validation case. The author of this thesis was the principal author of this publication.

- *Kouhia, V., Purhonen, H., Riikonen, V., Puustinen, M., Kyrki-Rajamäki, R., Vihavainen, J., PACTEL and PWR PACTEL test facilities for versatile LWR applications, Science and Technology of Nuclear Installations, 2012.*
  This paper includes a description of the PACTEL facility set-up and a presentation of specific facility characteristics. The experimental work with PACTEL is introduced based on the PACTEL natural circulation experiments. The paper also introduces the PWR PACTEL facility set-up and specific characteristics. The author of this thesis has acted as a co-author of this publication.

- *Purhonen, H., Puustinen, M., Riikonen, V., Kyrki-Rajamäki, R., Vihavainen, J., PACTEL integral test facility—description of versatile applications, Annals of Nuclear Energy, 2006.*
  This paper presents PACTEL experiments that have been carried out during the whole operating period of the facility. The role of PACTEL facility has been significant in VVER-440 thermal hydraulic investigations. The author of this thesis has acted as a co-author of this publication.

1.2 Subjects of the thesis

In this monograph, the author has compiled the main findings of these publications and added a complementary analysis and discussion to provide a comprehensive presentation of the validation of TRACE against PACTEL data representing VVER-440 specific thermal hydraulics. The author also presents a comparison of the inherent thermal hydraulic behaviour of VVER and western U-tube steam generators.

Chapter 2 focuses on reactor safety and thermal hydraulics, enlightening all main aspects of thermal safety analysis practice. Traditional validation methods for computer

codes are presented and a new, more comprehensive approach for system code validation is presented.

Chapter 3 discusses the thermal hydraulics of VVER-440 reactor type and focuses on phenomena arising due its specific geometric features. Previous research work related to VVER-440 thermal hydraulics is presented for all phenomena of interest.

Chapter 4 presents the PACTEL facility and a matrix of experiments selected for the TRACE code and input validation purposes.

Chapter 5 presents the TRACE code. The input model and results of the validation calculation cases are presented.

Chapter 6 discusses uncertainty quantification. The most interesting validation insights relevant to uncertainty identification and quantification are discussed as well.

Chapter 7 discusses the primary side natural circulation in the horizontal steam generator of VVER-440 and compares it to the vertical U-tube steam generators typical in western reactors. Surprisingly, despite their geometric differences, both steam generator types display some common behaviour: under natural circulation, the tube flow reverses in part of the tube bundle, even though the net flow remains in the normal direction.

Chapter 8 discusses the sense of validated code in more depth.

Chapter 9, Conclusions, summarizes all the main findings of this thesis. In particular, this validation effort shows that in the thermal hydraulic safety analysis, some uncertainties are statistically quantifiable, but there also are significant uncertainties (uncertainty categories) that are not quantifiable at all by statistical means.

2 Reactor safety and thermal hydraulics

The safety requirements of International Atomic Energy Agency (IAEA) define three fundamental safety functions for nuclear power plants: "*(1) control of reactivity, (2) removal of heat from the reactor and from the fuel store and (3) confinement of radioactive material, shielding against radiation and control of planned radioactive releases, as well as limitation of accidental radioactive releases"* (IAEA, 2012). The fulfilment of these functions shall be ensured for all plant states. The fourth fundamental safety function has been suggested to define the avoidance of fast exothermic chemical reactions (Kyrki-Rajamäki and Talus, 2013).

Thermal hydraulics is the main tool to be used to investigate the fulfilment of the second safety function. Thermal hydraulics is a term specifically introduced for nuclear power applications. The term combines heat transfer and fluid flow. Thermal hydraulics contains specific heat transfer and fluid flow types needed in the frame of nuclear power analysis. Thermal hydraulic accident analysis focuses on the coolant behaviour in the primary system and the coolability (or overheating limitation) of the reactor core. Such analysis needs to include all components of the primary system, which usually requires some compromises on the detailed geometrical description to keep the analyses in reasonable size and feasible.

The IAEA safety requirements provide also a basis for the safety analysis for the nuclear power plant. The safety analysis has to be conducted by applying the methods of both deterministic analysis and probabilistic analysis to enable the challenges to safety in the various categories of plant states to be evaluated and assessed.

Continuous development of safety is a prerequisite for reliable use of Nuclear Power Plants (NPPs). Safety issues have to be taken care of from the very first plans up to the finishing line of NPP operation and beyond that to the decommissioning and final disposal of spent fuel. The adequacy and scope of the nuclear power plant design basis must be reviewed at regular intervals as stated in Finnish legislation concerning the assessment and verification of safety (Government Decree, GD 717/2013, Chapter 2, Section 3): *"The safety of a nuclear power plant shall be assessed when applying for a construction license and operating license, in connection with plant modifications, and at regular intervals during the operation of the plant. Unless compliance with safety regulations can be directly verified on the basis of the nuclear power plant's design solution, compliance must be demonstrated. Nuclear power plant safety and the technical solutions of its safety systems shall be substantiated by using experimental and calculation methods. Analyses shall be maintained and revised if necessary, taking into account operating experience, the results of experimental research, plant modifications and the advancement of calculation methods."*

This thesis serves to fulfil these legislation requirements concerning experimental and calculation methods and attends the use of research results and advancement of calculation methods. The legislation gives a strong recommendation that the thermal

hydraulic analysis has a key role in the nuclear power plant safety assessment. The knowledge of the thermal hydraulic behaviour has an important role in the safety management in all operating situations.

The analysis methods are defined in nuclear regulations by the Radiation and Nuclear Safety Authority of Finland (STUK) (YVL B.3, 2010), which state that "if sufficiently reliable calculation methods are not available, the analysis shall be justified by experiments".

Another methodology regulation is defined concerning the analysis of power plant behaviour. The analysis is to be used either using conservative analysis methods with an additional sensitivity analysis or using the best estimate (BE) method with a statistical uncertainty analysis.

The term best estimate (BE) method is defined as a safety analysis method, where the physical modelling of a specific phenomenon is as realistic as possible and the initial assumptions for the calculation are chosen realistically.

The conservative approach refers to an analysis method where uncertainties are included in the parameters chosen for the analysis. In the conservative approach, parameters are chosen from its range of variation in such a way that the choice is least favourable for the analysis results. The analyses shall take into account that it is not always possible to define unambiguously in advance how the influence of the uncertainties connected to the calculation models, parameters or initial assumptions is conservative considering the final results.

Sensitivity analyses have to map the sensitivity of the final results according to the used analysis models, the initial condition and significant parameters. When the BE method is used, the uncertainty analysis has to be performed using suitable statistical methodology.

The IAEA safety report (IAEA, 2008) states that computer programs, analytical methods and plant models used in the safety analysis shall be verified and validated and adequate consideration shall be given to uncertainties.

Moreover, the use of BE codes is generally recommended for the deterministic safety analysis. Two options are offered to demonstrate sufficient safety margins when using BE codes:

> (a) The first option is the use of the codes *"in combination with a reasonably conservative selection of input data and a sufficient evaluation of the uncertainties of the results."* In this statement, the evaluation of uncertainties is understood more in the deterministic sense: code to code comparisons, code to data comparisons and expert judgments in combination with sensitivity studies are considered as typical methods for the estimation of uncertainties.

(b) The second option is the use of the codes with realistic assumptions on initial and boundary conditions. However, for this option *"an approach should be based on statistically combined uncertainties for plant conditions and code models to establish, with a specified high probability, that the calculated results do not exceed the acceptance criteria."*

Both options should be complemented by sensitivity studies, which include systematic variations of the code input variables and modelling parameters with the aim of identifying the important parameters required for the analysis and *"to show that there is no abrupt change in the result of the analysis for a realistic variation of inputs ('cliff edge' effects)"*(IAEA, 2008).

All these previous statements give explicit guidelines on how the safety analysis procedure should be carried out. The experiments, computer codes with sensitivity analyses and uncertainty assessment methods form a combination for the sufficient safety analysis.

2.1 Nuclear power plant behaviour in normal, transient and accident situations

The normal operation mode of the nuclear power plants is identical in most of the reactors requiring forced circulation by pumping for fluid motion and heat transfer. However, due to the exceptional nature of nuclear power, its safe operation requires preparedness to all deviations from the normal operation including incidents and accidents. The legislation (GD 717/2013) defines a classification for the different abnormal situations according to their expected occurrence as follows:

- *"Anticipated operational occurrence (AOO) shall refer to such a deviation from normal operational conditions that can be expected to occur once or several times during any period of a hundred operating years (frequency at least 10^{-2} / year).*
- *Accident shall refer to postulated accidents, design extension conditions (DEC) and severe accidents (SA).*
- *Postulated accident shall refer to such a deviation from normal operating conditions that can be assumed to occur more rarely than once during any period of a hundred operating years and which the nuclear power plant is required to withstand without severe fuel damage.*
    - *Class 1 postulated accidents, which can be assumed to occur less frequently than once during any period of a hundred operating years, but at least once during any period of a thousand operating year (frequency 10^{-3}…10^{-2} / year).*
    - *Class 2 postulated accidents, which can be assumed to occur less frequently than once during any period of a thousand operating years (frequency less than 10^{-3} / year)."*

These situations correspond to the Design Basis Accident (DBA) of older literature. The DBAs are used as the dimensioning basis for the power plant safety systems.

- *"Design extension condition (DEC) shall refer to a situation caused by a rare external event, or a situation where the initiating event of an anticipated operational occurrence or Class 1 postulated accident involves a common-cause failure in the safety systems, or a complex combination of failures, and which the facility is required to withstand without severe fuel damage.*
- *Severe accident (SA) shall refer to a situation where a considerable part of the fuel in the reactor is damaged."*

These extreme situations are also dimensioning events (and thus part of plant design basis), but with the criteria relaxed (DEC) or different (severe accidents) from the postulated accidents. In some older literature, these extreme situations have been called Beyond Design Basis Accidents (BDBA), indicating that they were initially not an explicit part of the dimensioning of the plants.

2.2 Design and dimensioning of safety systems

From the first steps in the nuclear power history the necessity and importance of safety systems have been recognized. Nuclear power plants are equipped with safety systems, which activate on demand. Safety systems are designed to perform safety functions, which were stated in the beginning of Chapter 2.

One of the main safety functions is the removal of the decay heat in all circumstances. This requires that the pressure control and coolant inventory must be taken care of. The inventory can be maintained (or restored) by coolant injection systems at different pressure stages, sometimes in combination with depressurization systems. Consecutive closed loop cooling chains perform the decay heat removal. Maintaining the core cooling prevents fuel damage and minimises possible radioactive releases.

The dimensioning of Emergency Core Cooling Systems (ECCS) is based on the DBA scenarios according to GD 717/2013 Class 1 and 2 postulated accidents. The ECCSs have to be able to provide cooling in case of loss-of-coolant accidents (LOCA). The large break LOCA (LBLOCA) is an ultimate case for the dimensioning of the safety systems. The LBLOCA leads to a rapid and complete loss of original coolant during violent depressurization. The TMI-2 accident showed that also a small break LOCA (SBLOCA) can lead to severe core damage. Slow coolant loss can result in core uncovery due to the coolant redistribution so that the liquid remains elsewhere in the reactor circuit while the core dries out.

The ECCSs are usually divided into separate systems, which activate in different pressure stages, like high pressure (HP), intermediate pressure (IP) or low pressure injection (LP) systems. High pressure injection systems are required in cases where inventory loss is relatively small and primary side pressure remains near the operating pressure. Thus, the required flow rate is small, but pump head is high. On the contrary, the low pressure injection systems have to provide a high flow rate with low head aiming to quickly restore the lost coolant and maintain long term single phase cooling.

The initiation of safety systems is usually automated, and they are designed to operate without any operator actions requirements at the early stages of an accident. In some cases, such as large break LOCAs in PWRs, the events are taking place so fast that operator actions are not even possible.

Safety systems have usually been active systems, consisting of pumps and valves, which require external energy, usually electrical power, for their operation. Active systems can be controlled and their performance is known and verifiable by start-up and periodic testing, but they also tend to be relatively complex, requiring automated controls and safety-grade external power supplies to function.

Some new nuclear power plant concepts are designed with simplified systems that are as little as possible dependent on external energy. These kinds of systems are called passive systems. The energy required for the initiation and operation of passive systems can be self-contained and operated by gravity, natural circulation or stored energy of pressurized gas. These safety systems are usually called passive, even though they often activate automatically. Passive systems can be separated in two categories based on whether they require electrical control or not. The advantages of passive systems are considered to be the independence of external energy and low costs both during the construction and operating periods.

Safety systems with passive features have been used also in earlier reactor concepts, like hydro accumulators and decay heat removal via natural circulation. The evolutionary designs of the nuclear power plants contain passive safety systems, which do not require outside energy for their operation. New passive systems have been developed in many new reactor concepts. They are either replacing the earlier active systems or operating as backup if active system initiation fails. New passive systems often involve natural circulation as their operating mechanism.

2.3 Role of natural circulation

Natural circulation is based on the density difference created by the temperature difference between the heat source and heat sink. The role of natural circulation in PWRs is to remove the decay heat from the core to the steam generators. If pumping is not available, the reactor has to be shut down, but the decay heat can still be transferred with natural circulation. Thus, natural circulation is a very important method for removing residual heat from the reactor core.

The natural circulation is a function of the primary side inventory. When the inventory is full, the coolant stays in a single phase and the driving force for the fluid motion is the temperature difference between heating and cooling. Thus, the induced single phase natural circulation flow is then a function of the sensible heat. When the inventory is reduced, the coolant changes into two phase condition. The induced two phase natural circulation flow is a function of the latent heat in case of the boiling of coolant. The primary side inventory defines the different modes of natural circulation. The mass flow rate of the natural circulation is controlled by the different heat removal mechanisms. In pressurized water reactors, the natural circulation modes are single phase, two phase and boiling condenser or reflux mode.

Usually natural circulation is taking place after the reactor scram, when pumps are stopped. The reactor scram is a typical consequence of a postulated initiating event. For example, leakages on the primary side, loss-of-feedwater to steam generators and station blackout initiating events will cause a reactor scram.

In LOCA situations, the primary side pressure decreases rapidly to the pressure corresponding to the hot leg saturation temperature. Single phase natural circulation mode continues until the inventory on the primary side decreases and the collapsed level goes down to the hot leg level. The flow to the steam generator then changes to a two phase flow. The heat is removed when steam is condensed and also cooled in the steam generator. Continued inventory reduction changes the condition of the hot leg fluid eventually to steam only. This phase is called the boiler condenser mode in once through steam generators (OTSG) or reflux condenser mode in U-tube steam generators (UTSG). In UTSG reflux natural circulation only steam flows to the steam generator.

The VVER-440 geometry with the hot leg loop seals produces a specific behavior during natural circulation. The single phase natural circulation in VVER-440 is similar to that of the western PWR reactors. The difference appears when the inventory on the primary side decreases to the hot leg connection level. The flow to the steam generator then changes to two phase flow. The steam at the hot leg start section forms a block, and natural circulation stagnates. This causes essential degradation of heat transfer, and primary pressure begins to rise. The primary side pressurization continues until the loop seals (or only one or some of them) clear and natural circulation is recovered. The loop seal clearance is due to the dual effect of inventory reduction and steam pushing the liquid forwards from the bottom of the loop seal. After the loop seal clearance, the steam flow towards the steam generators can continue in the cleared loops.

Typically, strong primary flow oscillations occur due to the loop seal clearance. Due to the horizontal structure, the reflux flow can occur, when condensate in the heat exchanger tubes flows backwards to the bottom of hot leg loop seal. Part of the condensate water can flow towards the cold leg, and can be considered as the boiler condenser mode. The feature of horizontal steam generator allows the condensate to flow both to cold leg and back to hot leg. However, the feature of hot leg loop seals does not allow reflux flow to reach the core region. The backward condensate can fulfil

the loop seal and then cause flow stagnation and pressure rise. The distribution of condensate between hot and cold legs is difficult to measure and thus poorly known.

Continuing fluid loss decreases the primary pressure to the secondary side pressure if the leakage removes enough energy from the primary system. This weakens the heat removal capability. When the temperature difference between the primary and secondary side disappears, the natural circulation flow rate decreases correspondingly.

2.4 Safety systems relying on natural circulation

Natural circulation is also an essential driving force in various safety systems, which, as stated previously, are often called passive safety systems. In the following subsections, some of the well-known reactor design concepts containing passive safety features are described shortly. The equipment proposed in these reactor concepts includes natural circulation phenomena as the main mechanism that determines the passivity of the entitled function. These new designs rely very much on natural circulation and are thus worth of closer look. The VVER-440 specific thermal hydraulic phenomena are quite similar to what would be expected in passive safety systems presented below. Their heat exchangers may exhibit asymmetric tube bank behaviour similar to the horizontal steam generators.

2.4.1 AP-1000

The AP-1000 concept by Westinghouse and the earlier AP-600 as well contain several passive safety applications, which operate by natural circulation (Schulz, 2006). Four units of AP-1000 are under construction in China and four in the USA. The AP-1000 concept has active systems for normal operation. It has no traditional active safety systems for ECC or containment cooling, but does have an active non-safety RHR system for normal operation.

Passive safety injection system (PSIS) is designed to replace the high pressure injection system. This gravity driven system consists of core makeup tank (CMT), pressure balancing line (PBL) and injection line (IL). The CMT is situated above the reactor vessel. The CMT tank is pressurized at the reactor pressure continuously during normal operation via PBL connected from cold leg to the top of the CMT. On demand a valve is opened and the cold borated water circulates naturally from the CMT to the downcomer of the reactor vessel. At the first stages of PSIS operation, the warm water flows to the top of the CMT tank replacing the cold water inventory and forms an insulating layer preventing the direct contact of the entering steam and cold water in the later operating mode of the system. The actual operation starts when the cold leg is voided and steam enters trough the PBL to the top of the CMT. This phase provides the largest injection flow rate due to significantly increased density difference between PBL and IL. The AP-1000 with passive core cooling systems is presented in Figure 1.

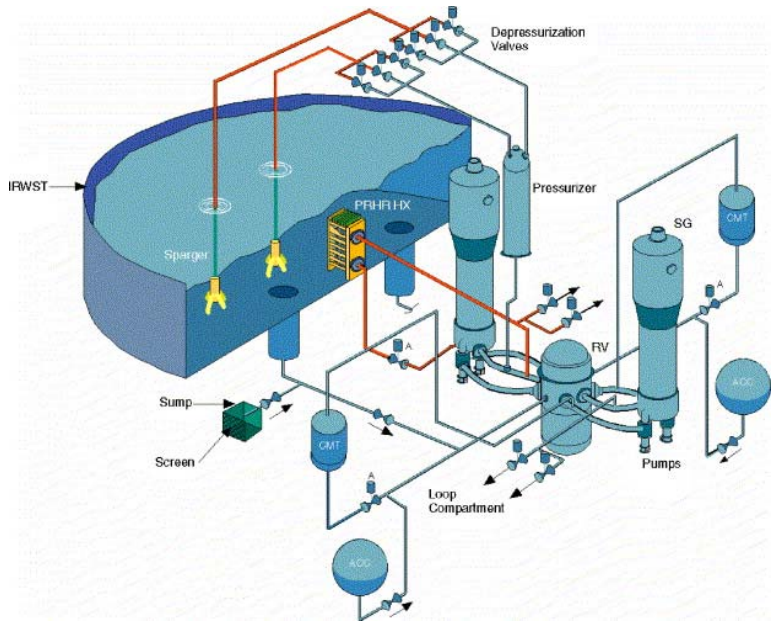

Figure 1: AP1000 RCS and passive core cooling system (Schulz, 2006).

2.4.2 **AES-2006**

The AES-2006 reactor, formerly known as VVER-1200, is designed by OKB Gidropress for 3200 MW thermal and 1200 MW electrical output. It is the result of the further improvement of the VVER-1000 reactor with the insertion of additional passive systems.

Safety functions are realized using both active and passive systems. The reactor contains traditional passive safety system for ECCS using hydraulic accumulator tanks, but also new features for beyond DBA (BDBA) management systems:

1. The passive system of heat removal through the steam generator (PSHR SG, see Figure 2, item 28) is intended for prolonged residual heat removal absorbed through the second circuit in case of BDBA. The natural circulation is the driving force in the operation of this system.
2. The passive heat removal system from the containment (PSHR C, see Figure 2, item 27).

Both of these systems remove the heat to the PSHR emergency heat removal tank (see Figure 2, item 28), which is located at high elevation and between the inner and outer containment. This tank is connected to the atmosphere through a hydraulic lock (see Figure 2, item 30).

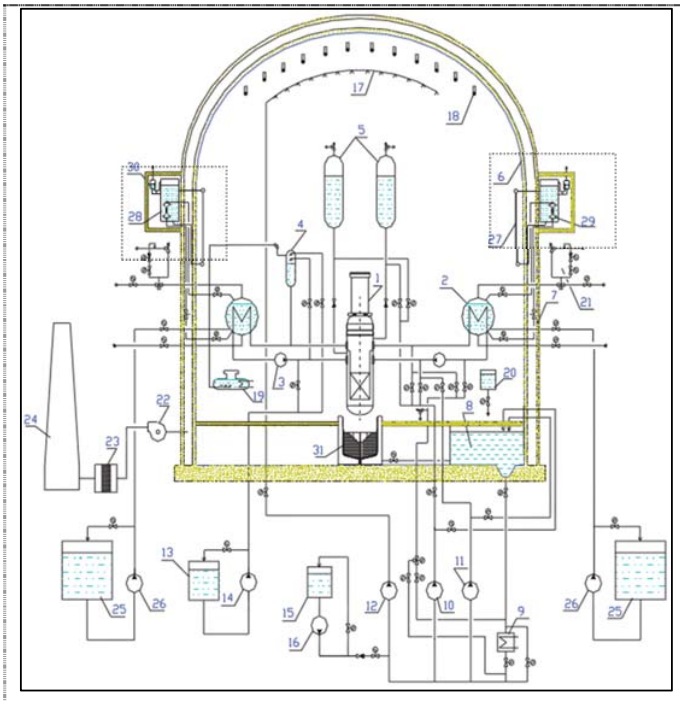

Magnified parts

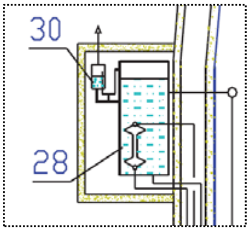

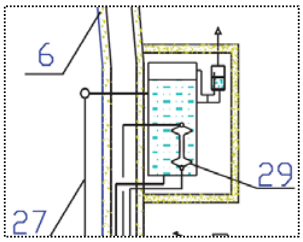

1. Reactor
2. Steam generator
3. RCPS
4. Pressurizer
5. ECCS tanks
6. Containment
7. Outer containment
8. Sump tank
9. Heat exchangers
10. Low pressure emergency injection pump
11. High pressure emergency injection pump
12. Spray pump
13. Boric water storage tank
14. Emergency boron injection pump

…

18. Passive hydrogen recombiner
19. Bubbler

…

25. Desalted water storage tank
26. Emergency injection pump
27. **PSHR C condenser heat exchanger**
28. **PSHR emergency heat removal tank**
29. **PSHR SG heat exchanger**
30. **Hydraulic lock**
31. Core melt localizing facility

Figure 2: AES-2006 schematic diagram of safety systems (selected explanations) (Rosatom, 2011).

2.4.3 KERENA™

The Kerena™ concept (formerly known as SWR-1000) is Generation III+ boiling water reactor (BWR) design by AREVA with the thermal output of 3370 MW and net electrical output of 1250 MW (Leyer and Wich, 2012). This reactor concept is equipped with both active and passive safety systems. Most safety functions are performed by active systems having passive systems as backup. In the event of failure of the active safety equipment, the passive system will bring the plant to a safe condition. Passive systems do not need any external power, even for the activation. The active and passive

safety features complement each other, resulting in a simplified system design. Passive safety systems in the Kerena^{TM} concept (see Figure 3) are described as follows:

Emergency condensers (EC) function, in case of an accident, is to remove the decay heat generated in the reactor as well as any sensible heat stored in the reactor to the core flooding pools. No coolant inventory is lost from the reactor. Thus, the system replaces the high-pressure coolant injection systems used in existing boiling water reactor plants.

Containment cooling condensers (CCC) remove by passive means the decay heat from the containment. The four condensers activate during accidents leading to the release of steam inside the drywell. This way the containment pressure increase is limited.

The passive core flooding system is a low-pressure system for controlling passively the effects of loss-of-coolant accidents (LOCAs). The installation elevation of this system enables reactor core flooding by gravity flow after automatic depressurization of the reactor.

Passive pressure pulse transmitters (PPPT) are passive switching devices that are used to directly initiate the safety functions of reactor scram, containment isolation at the main steam line penetrations, and automatic depressurization of the reactor. The PPPT activates when reactor water level is decreased or increased or if reactor pressure is increased. For activating the various safety functions, PPPTs are installed at three elevations. The upper PPPTs, situated at an elevation beneath that of the normal water level of the reactor pressure vessel, are responsible for initiating reactor scram. The lower PPPTs activate automatic depressurization of the reactor as well as closure of the main steam containment isolation valves. Other PPPTs are installed at appropriate locations responding to rising reactor water level and activating reactor scram and containment isolation.

Kerena^{TM} concept is considered to be exceptional compared to the other passive design concepts. It is to be the only passive design that is capable of initiating all main safety functions without any intervention of plant automation.

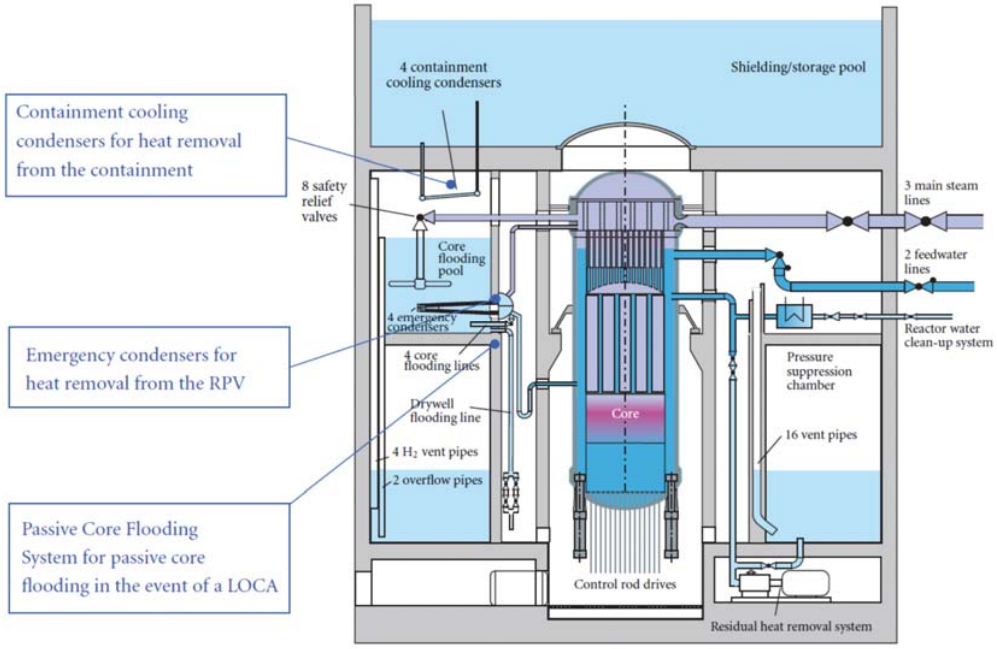

Figure 3: Section of the KERENA containment with passive safety systems (Leyer and Wich, 2012).

2.4.4 **ESBWR**

The Economic Simplified Boiling Water Reactor (ESBWR) concept (GE Hitachi, 2011) is designed to operate in the natural circulation mode without recirculation pumps. Thus, ESBWR is simplified having no pumps and associated motors, piping, valves, heat exchangers, controls and electrical support systems that exist with forced circulation reactors. Natural circulation in the ESBWR also eliminates the risk of flow disturbances resulting from recirculation pump anomalies. However, the benefits associated with the pumps are lost. The possibility to run the reactor within a large flow range is not available. This has straightforward effects on the fuel economy and also on safety. Despite these disadvantages, natural circulation is a proven technology. Long operating experience has been gained from previously employed natural circulation BWR designs. Power plants like Humboldt Bay plant in California and the Dodewaard plant in the Netherlands used only natural circulation, and they operated for 13 and 30 years, respectively. The ESBWR has features that enhance the natural circulation performance (see Figure 4). It has a tall open downcomer and reduced core resistance providing circulation driving head, partitioned chimney above the reactor core to stabilize and direct the steam and water flow above the core as well as a large water inventory for Loss of Cooling Accident (GE Hitachi, 2007).

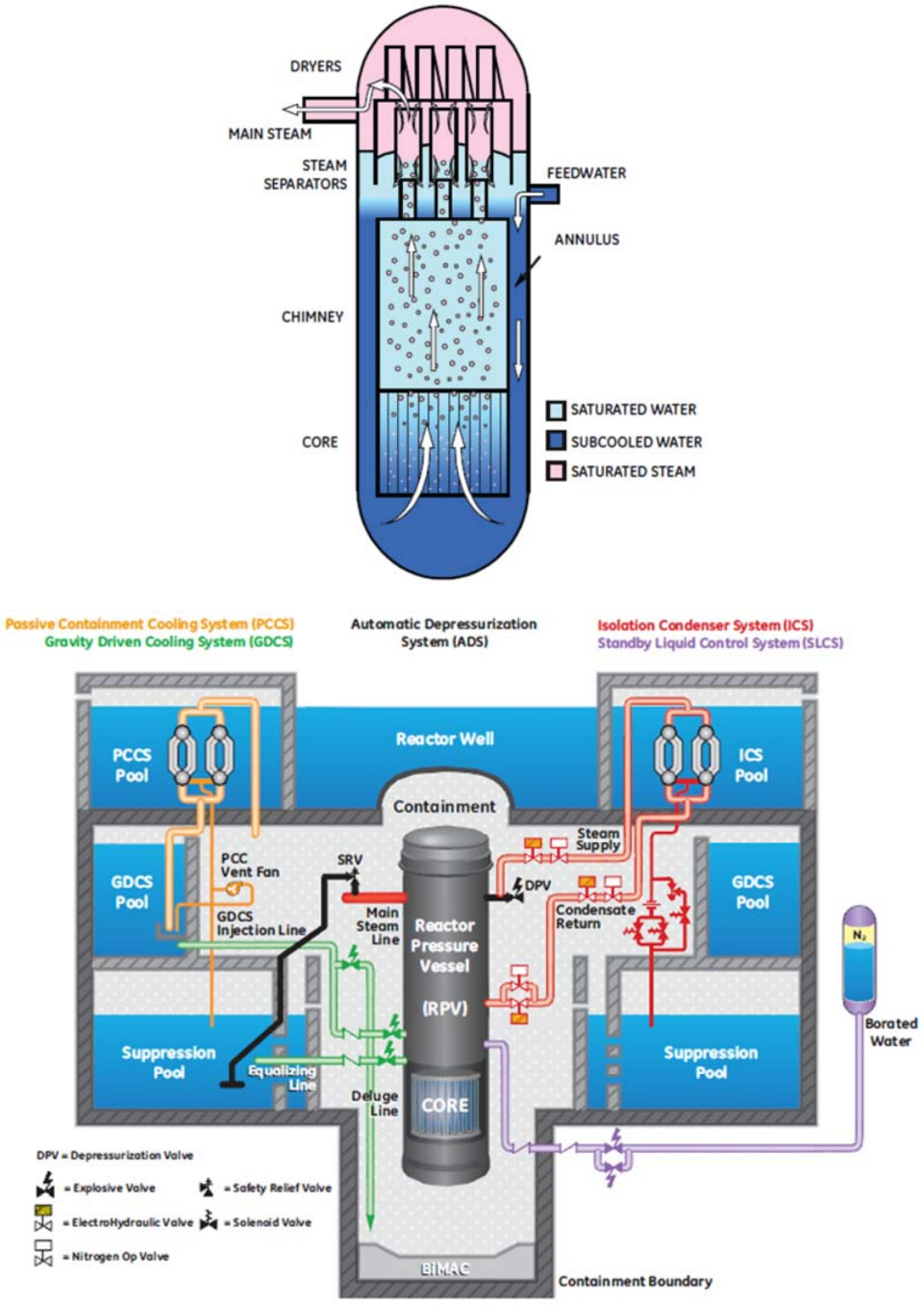

Figure 4: ESBWR reactor in natural circulation (top) and ESBWR safety systems (below) (GE Hitachi, 2007; GE Hitachi, 2011).

2.5 System codes in safety analysis

The performance analyses of nuclear power plants usually require complex computer codes. They include many types of codes, ranging from specialized reactor physics codes to mechanistic system thermal hydraulic codes.

The NPP thermal hydraulic safety analysis is performed using thermal hydraulic models to predict the plant behaviour under normal, transient or accidental situations. The computer codes used for the modelling of all events are usually called system codes.

System thermal hydraulic codes are typically not reactor design specific and can be applied to a wide variety of designs and conditions. A number of these codes are widely used around the world by regulatory, research and industry organizations.

Today, the system code modelling is almost exclusively performed using best estimate (BE) codes. The general BE modelling methodology process comprises different steps, from capturing the reality to conceptual models to convert those models to computerized BE codes. The system codes that are used nowadays are typically BE codes and do not contain specific models for conservative analysis. The thermal hydraulic codes are characterized by mechanistic models for two fluid, non-equilibrium hydrodynamics, point and multidimensional reactor kinetics, control systems and other system components such as pumps, valves and accumulators. These codes can typically be used to model a wide range of configurations for single pipes, experimental facilities and full plants and, in many cases, have been applied to most reactor designs around the world. The behaviour of two-phase mixtures in thermal hydraulics involves the simultaneous presence or the occurrence of phase change, transient conditions, non-developed flows, heated surfaces at different temperatures and complex geometries (D'Auria, 2010).

For advanced reactor designs with passive coolant systems, the codes are typically used to describe both the reactor coolant system, emergency systems and the thermal hydraulic behaviour of the containment. Recent developmental activities have focused on the development of more integrated graphics—user interfaces and the application of the codes to a wider variety of reactor designs. Some work has been focused on the development of fast-running simulator versions of these codes.

2.5.1 System codes as tools for safety analysis

Computer codes have been developed and used during the whole history of NPPs. Thermal hydraulic computer programs play an important role in this development. The models of computer codes must be validated by comparing the results of experiment measurements against the calculation results. Comparisons provide confidence in the code capability and information about uncertainty estimates.

Thermal hydraulic codes are used in multiple steps of nuclear power plant life cycle starting from the preliminary design of the power plant concept and their detailed subsystem analysis. In the licensing procedure of new power plants, the safety authorities require thermal hydraulic analysis (IAEA, 2009 b). Analyses relating to the behaviour of nuclear power plants shall cover the normal operational states, anticipated operational occurrences (AOO), postulated accidents, design extension conditions and severe reactor accidents (STUK, 2013).

The IAEA Specific Safety Guide (IAEA, 2009b) states the requirements for the safety analysis preparation. A comprehensive listing of postulated initiating events (PIEs) should be prepared to ensure that the analysis of the plant behaviour is complete. An initiating event is an event that leads to anticipated operational occurrences (AOO) or accident conditions. "Postulated initiating events and the consequential transients should be specified to ensure that all possible scenarios are being addressed. When performing deterministic safety analyses for anticipated operational occurrences, design basis accidents and beyond design basis accidents, all postulated initiating events and associated transients should be grouped into categories" (IAEA, 2009b).

Examples of initiating events to be analysed are faults that have the following consequences (STUK, 2003):

- Leak from the primary circuit during power operation, change in operational state, refuelling and/or outage,
- Leak from secondary circuit (PWR),
- Leak from primary to secondary circuit (PWR),
- Disturbance in the reactor power control or other disturbance, which causes a change in reactivity,
- Disturbance in primary circuit flow, pressure control or water volume control,
- Disturbance in steam pressure or steam flow and
- Disturbance in feedwater flow or temperature.

Also, the planning of NPP power upgrades requires a new safety analysis using thermal hydraulic codes. The licensing work contains the quantification of necessary safety margins.

Codes are validated against experiment data from downscaled facilities. The scaling tries to maintain prototypic heights while reducing volume by the factor of 1 to approximately 100. For this reason, test facilities end up being tall and slim. When computer code model is constructed using a system code for tall and slim type experiment facility, the one dimensional flow formulation is enough to model the actual flow phenomena with sufficient accuracy. In real power plants, the component dimensions are truly three dimensional, and for example pipe diameters are extensively larger than in experiment facilities, and thus, the flow phenomena in three dimensions

are more likely to take place in real size reactors than in experiment facilities. The slim facility gives mostly a one dimensional view of the phenomena. This standpoint could lead to an excessive optimism when 1-D results are interpreted.

In the modelling of large diameter vessels, the flows can be modelled to some extent with one dimensional flow elements using multiple flow paths and cross-flow junctions. However, this pseudo-two/three dimensional method cannot present realistic flow characteristics. The secondary side of the horizontal steam generator has clearly 3-D effects. Usually, the detailed modelling of these effects is not considered essential in the sense of safety analysis. However, Zarifi et al. (2009) have presented semi 2-D nodalization studies for the VVER-1000 horizontal steam generator using the RELAP5 code. The model contained semi 2-D modelling with lots of cross-flow connections on the secondary side. These studies contained only the steady state analysis.

The Upper Plenum Test Facility (UPTF) was a geometrical full-scale test rig of the primary system of a four loop 1300 MWe Siemens PWR (NUREG, 1993). The major objective of the UPTF 2D/3D program was to study multidimensional flow phenomena in the primary system of a PWR end of blowdown, refill and reflood phases following a postulated loss-of-coolant accident with a hot or cold leg break considering various ECC injection modes of different ECC systems. Thus, the UPTF experiments provided exceptional large-scale data.

2.5.2 Code modelling of the nuclear power plant

In system codes, the usual flow model approach is a one dimensional formulation. Although most of these codes focused initially upon the one dimensional representation of the reactor vessel and piping, two and three dimensional representations of the vessel and other coolant system structures are now being used more widely. In real reactors, the physical phenomena and thus the flow directions are almost always three-dimensional (3-D). However, the 3-D modelling of the whole power plant requires huge computing resources, and it is not always necessary to achieve appropriate results.

Considering the dimensions of components at different parts of the power plant, the adequacy of the modelling can be assessed. The length (L) over diameter (D) parameter can be calculated from the dimensions of different components on the primary and secondary sides of the NPP. With the help of this L/D parameter it can be concluded whether the dominant flow is in the axial direction and one-dimensional modelling is sufficient (large L/D) or the main flow direction cannot be clearly determined (L/D is near or slightly larger to unity) and the component requires 2- or 3-D modelling. Table 1 presents the values for the L/D parameter that were calculated using the average dimensions of the Loviisa power plant. These results show that the one-dimensional flow modelling is often a sufficient modelling approach in various parts of the power plant. For the core region, coolant pipelines and steam generator heat exchanger tubes, 1-D modelling is an adequate method. Luckily, these are the regions that dictate the heat transfer performance.

There are certain regions like the upper and lower plenum of the reactor vessel that clearly require 3-D modelling if mixing and recirculating flows inside these volumes need to be resolved.

Table 1: Length vs. diameter (L/D) parameter calculated for Loviisa NPP.

Component or region	L/D	Required Dimensions
Fuel bundle sub-channel	2440/3 = 813	1
Upper plenum	3500/3500 = 1	3
Hot and cold legs	(8000/500 = 16) ~20	1
Collectors	3200/800 = 4	3
HSG tubes	10000/13 = 769	1
Downcomer	7000/100 (10000) = 70 or 0.7	1 or 2
Lower plenum	2630/3000 = 0.75	3

2.5.3 Formation of nodalization

Thermal hydraulic behaviour is described by a system of differential conservation equations. A discrete representation of the system to be modelled is needed to solve the system of equations numerically. The structure of the facility or system is defined by nodalization. The nodalization defines how the system and its volume should be divided into smaller pieces. These pieces are usually called nodes or cells or in some cases control volumes.

Most thermal hydraulic system codes use a staggered grid nodalization. The calculation node or cell is the smallest piece of structure where the scalar quantities like pressure and temperature are defined and the assumption is made that the quantity is concentrated to the centre point of the node. The node value of the quantity represents the average value in the whole volume. The vector quantities like velocity and flow rates are defined on the edge of the inlet and outlet of the node.

Four different aspects concerning the formation and choosing the nodalization are:

1) Node sizing,
2) Connecting small and large nodes,
3) Branching and
4) Lumping.

These aspects are discussed further here. The aspects 1) and 2) are usually well managed and instructed by code guidelines. The aspect 4), lumping, is the most dependent of user decisions.

The first aspect concerns the node sizing. The chosen nodalization fixes the amount of information that can be obtained from the calculation. It is important to gain the necessary amount of data from the process or system to be modelled, especially when information from the changes in time and in space in the system is required. Usually,

there is a need for comparison of the data gained from the calculation model to the measurement results from the facility. To be able to compare the calculated and measured results as accurately as possible, the planning of nodalization is essential. In experiment facilities, as well as in real power plants, the amount of measurements is limited, and practical arrangements also restrict where the measurements can be situated in the facilities. However, data from the calculation model is huge compared to the experiment. To ensure the best comparison of calculation and measurement, the centre point of the node is usually defined according to the location of the experiment measurement point. Then the size of the node, that is, the surrounding volume around the point to be measured, is planned and concerned by the user.

The node temperature represents the average temperature throughout the total node volume. The temperature measurement in a facility represents the local temperature only in one single point. Therefore, in the calculation model, the surrounding volume of this measurement point is desired to be kept as small as possible in order to achieve the best possible correspondence between the states of the node. The need how well the calculation model should correspond to the measurements in the facility gives the requirement for the size of the nodes and for the density of the nodalization scheme. An example of how the renodalization can improve the calculation correspondence to actual measurement device locations is presented in Figure 5.

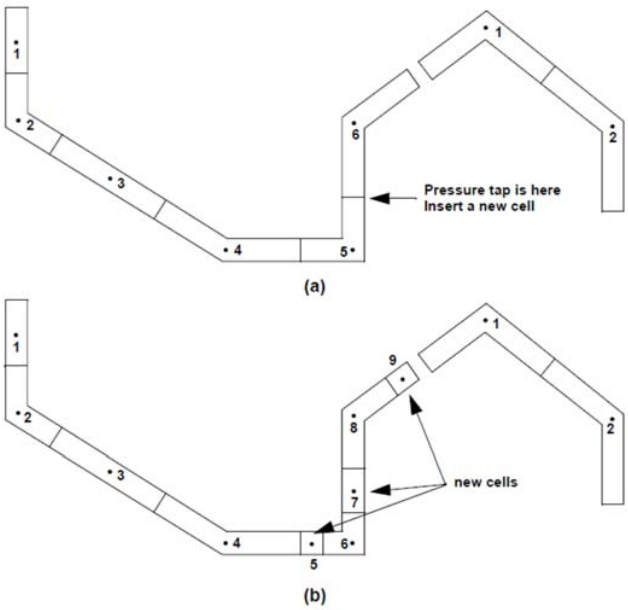

Figure 5: Sample nodalization used to demonstrate the impact of noding choices in the component model. Schematic (a) shows a component before the renodalization. Schematic (b) is renodalized and shows one possible way of adding new mesh segments in the vicinity of the cell bends (TRACE V5.830 User's Manual, 2013).

The second aspect concerns the connection of different sized nodes to each other. Very often the thermal hydraulic calculation codes (system codes) contain restrictions and recommendations for the largest allowed changes in the volume and flow area in relations between concatenating nodes. It is usually necessary to meet these requirements and recommendations to maintain a reasonable calculation capability and validity of the resolution. However, exceptions to the modelling recommendations have to be made sometimes. For example, connecting a small diameter pipe to a large volume tank is will most probably produce at least a warning or a suggestion for changes in the system modelling (see examples in Figure 6 and Figure 7). The codes are able to cope to some extent with the extending situations beyond the recommendations. The codes have also recommendations for the minimum and maximum node sizes and restrictions for the changes in the size of concatenating nodes.

When the nodal size is derived based on the layout of the instrumentation and its locations, the code recommendations would require relatively small changes in geometric parameters of succeeding nodes. This would be an ideal resolution in the frame of the calculation code geometry definition. The nodalization with equal deviation and thus probably rather small sized nodes would lead to problems in the frame of the usability of the code model. The total number of the nodes in the model would inevitably increase, and the solution time of one time step could become intolerable. Also, the small sized nodes lead to promptly meet the Courant limit in the solution. In system code solutions, this means that the maximum available time step has to be decreased. Both of these factors affect the slowing advancement in the calculation ending up to very long calculation times, which is clearly weakening the usability of the code.

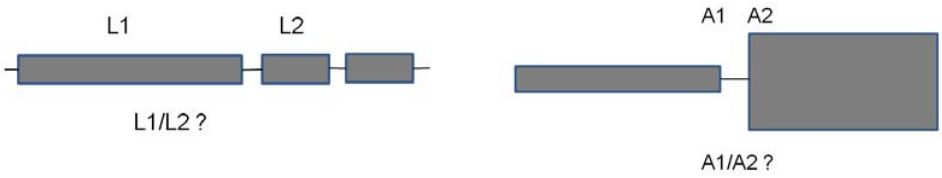

Figure 6: Selecting the rate of node size change.

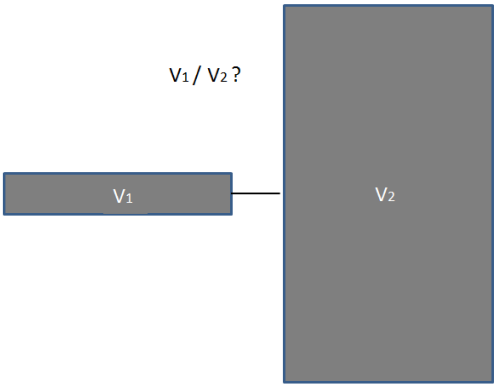

Figure 7: Connecting a small node to a large (vessel).

The third aspect concerns branching, that is, how the sideways connections for different nodes are defined. In many modelling cases, there is a need for the connection of the sideway flow to the main flow. The first option is usually to connect the node from the sideway flow to the main flow node with a cross-flow connection. In this connection mode, the inlet or outlet of the sideway node is connected to the middle point of the main flow node. The user has to define the cross-flow connection with a specific action from the sideway pipe to the centre point of the main flow node. Some codes can provide a special TEE component for this connection mode. Then, the TEE component contains a ready-made side node. The second option is that the inlet or outlet of the sideway node is connected to the inlet or outlet of the main flow node by directing the sideway node perpendicularly or with the defined angle from the main flow node. The difference between these two options is the momentum transfer. In the first option with cross-flow connections, the momentum transfer is not calculated. With the second option with straight connections, the momentum transfer is calculated (see Figure 8).

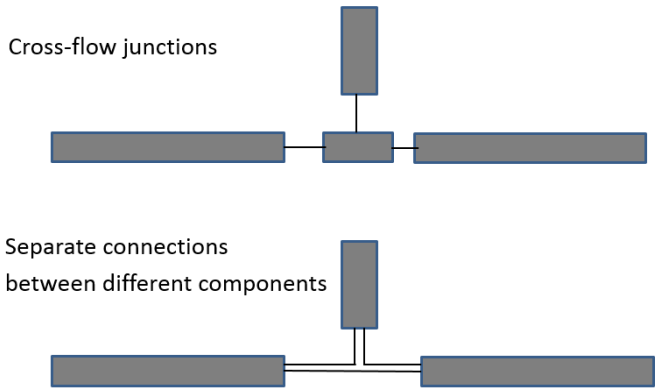

Figure 8. Modelling branching flow.

The fourth aspect is concerning the rate of the lumping of small channels. This question of how detailed modelling is needed arises almost always when the real reactor core and steam generators are modelled. The reactor core is usually formed of tens of thousands fuel rods and sub-channels for the coolant flow. Steam generators, both the horizontal and vertical type, contain typically thousands of heat exchanger tubes. The problem is similar to the modelling of experimental facilities as well. Usually in thermal hydraulic codes, multiplication factors can be used in the modelling. Only one fuel rod and the corresponding sub-channel can be described and then multiplied by a necessary factor. With this modelling option, an assumption is made that all fuel rods and sub-channels behave equally. It is apparent that with this approach the possibility for the modelling of power and flow distributions in the radial direction of the core is lost.

In the modelling of horizontal steam generators, tubes or more often tube rows are lumped together and multiplication factors are used also here. Ultimately, the representative modelling of the tube bank would require the separate modelling of each tube. One tube row contains tubes with different lengths. One tube row could be presented with one average length. Even the separate modelling of each tube row in a real reactor is impractical; for example, in the VVER-440 steam generator, there are 77 tube rows in the vertical direction. Hence, these approaches are hardly possible. If the other ultimate modelling approach is presented and the total tube bank is lumped together, then no row definitions are introduced. This description of tubes is not able to bring out any information about vertical differences in heat transfer and flow distributions. To reach a more truthful and detailed description of the horizontal steam generator behaviour, at least tube rows with a certain rate of lumping should be introduced. Of course, it is not necessary to model every tube or every tube row either in detail if calculating times are to be kept reasonable. In vertical U-tube steam generators, the lumping of tubes is also essential. The tubes have different lengths, which means

that pressure losses are different between the tubes. With too much lumping of tubes it is not possible to find out for example the asymmetric behaviour related to the flow reversal between different tubes. See examples of lumping in Figure 9.

It can be concluded that certain phenomena can be observed only when enough details are presented in the modelling. Hence, if detailed information from steam generator or core behaviour is necessary to reveal, optimization between lumping and detailed modelling is required.

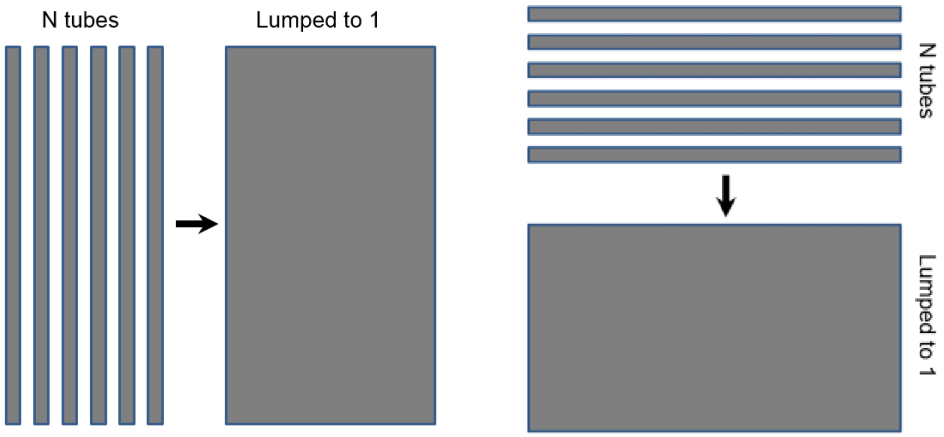

Figure 9. Lumping parallel sub-channels, vertical and horizontal case.

2.6 Scaling of system test facilities

D'Auria and Galassi (2010), among others, have discussed widely the scaling issues in nuclear reactor thermal hydraulics. The origin of the scaling issue can be characterized as follows: it is infeasible (or cost prohibitive) to perform meaningful experiments at the full scale, and the ability of numerical tools designed to simulate the performance of nuclear reactors can be proven only at the reduced scale.

Ishii et al. (1998) have proposed a scaling approach especially dedicated to the PUMA integral facility. The scaling method consists of three levels of scaling analysis, namely the integral system scaling, control volume scaling and local phenomena scaling. The first two levels correspond to the top-down scaling while the third level represents the bottom-up scaling. Ishii et al. (1998) have concluded this issue as follows: "The design of a test facility cannot completely satisfy all the scaling requirements. Thus, scaling distortions are inevitable. Distortions are encountered for two major reasons: difficulty to match the local scaling criteria and lack of understanding of the local phenomenon itself. Therefore, the direct extrapolation of the local experimental data to the prototypic conditions is often quite difficult or impossible."

Nuclear power plant concepts are usually modelled with scaled down experiment facilities. Three basic type of scaling methods have been introduced (Navahandi et al., 1982):

1) Time-reducing (or linear),
2) Time-preserving (or volumetric) and
3) Time preserving idealized model/prototype.

Additionally, many thermal and fluid based dimensionless quantities, for example Re (Reynolds), Pr (Prandtl), Nu (Nusselt), Fr (Froude) or Gr (Grashof), are widely used as preserved quantities in the scaling of facilities. The first method implies to the reduction of the linear dimensions of the prototype by a given factor and, in transient conditions, the reduction of time by the same factor. In this case, the amount of power transferred to the fluid is reduced as the square of the linear dimension factor. The second method contains the preserving of the dimensionless design factors, and the third method resembles the second, with more flexibility left to the designer, being the 'time preserving' the main objective for the application (D'Auria and Galassi, 2010).

The facility can be designed for the modelling of separate effect tests (Separate Effect Test Facility, SETF) or integral testing (Integral Test Facility, ITF). The computer code models are then created with system codes for the facility, and models are validated against a large set of experiments simulating various transient and accident scenarios. The validation results can be scaled up to the models of a full size power plant. The computer codes are then in most cases the only link between the experiments and real power plants. Then the operational and safety analysis of a full NPP can be considered reliable enough.

The integral test facilities are in most cases scaled down by using the volumetric scaling approach. The component elevations and heights are often kept equal compared to the reference reactor. This scaling approach leads to an experiment facility that is tall and slim, as stated in previous chapters. In many experimental situations, the flow processes are driven by natural circulation, and fluid is in two-phase state. Gravitational forces dominate in these processes. Equal heights, and thus hydrostatic pressures, are considered necessary to achieve results representative of the real reactor. However, two-phase critical flow phenomenon is considered non-scalable due to the thermal non-equilibrium phenomena. This is due to the differences in local geometric properties at the break location, which are usually not scalable. Table 2 presents selected thermal hydraulic ITFs with their scaling factors. It can be noted that the majority of presented facilities have 1 to 1 height factors, and the volumetric scaling factors are greater than hundred. Thus, they represent the typical tall and slim type of facilities.

Table 2: Scaling factors of selected thermal hydraulic test facilities.

Facility	Volume	Height	Reference reactor, power
APEX	1:192	1:4	AP-1000 (Reyes et al., 2003)
PKL	1:135	1:1	Konvoi KWU (Umminger et al., 2012)
PACTEL	1:305	1:1	VVER-440
PMK	1:2070	1:1	VVER-440 (Ezsöl et al., 2012)
REWET-III	1:2333	1:1	VVER-440
ROSA-IV/LSTF	1:48	1:1	Westinghouse, Tsuruga-2, 1160 MWe (Yonomoto, 2005)
BETHSY	1:100	1:1	Framatome PWR 900 MWe (Noël, 1999)

2.7 Code validation – Traditional approach

There is normally a regulatory requirement that codes should be assessed or validated in relation to relevant experimental data for the major phenomena expected to occur (IAEA, 2002). The validation relates to the confidence that can be placed on the accuracy of the values predicted by the code. The specifications of what is required will vary according to the facts of the safety assessment under consideration. Four sources of data are generally used to validate these codes:

- phenomenological data,
- separate effect data (component data),
- integral data and
- power plant operational data.

For accident conditions, the availability of data is limited. Integral data are available for the early phases of accidents, but data for the later phases are obtained primarily from experimental facilities for separate effects, using simulant materials in many cases. Exceptional data from the accidents at Three Mile Island in the USA in 1979, Chernobyl in the USSR in 1986 and Fukushima in Japan 2011 are available for the validation of models for severe accidents.

For validation, certain quantities are selected for the comparison of calculations with experimental data (IAEA, 2002). “These quantities serve as ‘indicators’ for determining whether or not a code provides satisfactory results”; that is, indicators that can be used to measure the ‘level of validation’ of a code. The identification or choice of indicators is, therefore, a crucial step in the validation. The quantification of the validation can be expressed in terms of the accuracy with which a code predicts an indicator, and it must relate to the agreement between the values of the indicators as predicted and as measured experimentally. The indicators are directly related to the physical driving phenomena of the response to the accident and are usually those code output quantities that are compared with the acceptance criteria in accident analysis.

Traditionally, the validation of many codes has included the formulation of a model design according to the validation experiment facility, collection of experimental data,

analysis of this data, comparison of the experimental data with code predictions, and reformulation of the model. The need for the reformulation of the model and reiteration depends on whether or not the code is decided to have met the validation criteria. Because many of the experimental programmes have been completed so far, the validation of new models and codes has to rely on the data sources from the archives. However, it is necessary to validate the code against as many experiments as possible, which have not been used directly to support the models of the code.

Some peculiarities have been observed in the code performance. A code can occasionally predict results with high degree accuracy for certain data set and might still result in extreme inaccuracy for other data sets. This has led to the need to develop a 'validation matrix' for each code through which different types of experimental facilities and different sets of conditions in the same facility are used for code validation (IAEA, 2002).

Most internationally recognized codes have been subjected to systematic validation procedures through a number of international programmes, with system thermal hydraulic codes receiving the most attention. Under these programmes, which include those of the IAEA and the OECD/NEAs CSNI, extensive experimental matrices for code validation have been established, and the codes have been assessed in relation to many of the experiments that are included in those matrices. The validation exercises have also included comparisons with relevant data from plant operations and participation in international standard problems.

The validation of a thermal hydraulic computer code is an extensive procedure. Code developers have usually their own sets of specific test cases, which are carried out every time new major changes are implemented in the code. After the code version is launched to the users it is necessary to broaden the code testing to larger experimental databases. This validation phase is not possible without international co-operation. Thus, OECD NEA's CSNI has coordinated and gathered databases of the existing experiments and test facilities into validation matrices. To reach the best possible coverage, a validation matrix usually consists of data from four types of tests mentioned earlier.

These experiments have been set available for developing the models in computer codes and validating them to be used in different situations. However large these databases are, they do not completely cover all the situations of accidents and transients needed for code validation.

The OECD/CSNI working group formulated a validation matrix based on separate effects tests (SET) for the assessment of large thermal hydraulic codes. This matrix (Aksan et al., 1994) completed the earlier Code Validation Matrix by CSNI (OECD, 1987).

Later, also the Integral Test Facility Validation Matrix (OECD, 1997) and Validation Matrix for the Assessment of Thermal Hydraulic Codes for VVER LOCA and Transients (OECD, 2001) have been prepared. The contents of these reports are considered to represent the international state of the art of experimental thermal hydraulic research for computer code validation, listing the facilities, available experimental data for certain types of phenomena as well as the integral test facilities for a certain type of NPP. Also the missing experimental data of the phenomena are indicated. The matrices have been widely used for choosing validation cases for computer code models and for testing the overall performance of the codes. The facilities of LUT have also been included in the separate effects test matrix. They are REWET-I, REWET-II and VEERA. The VVER validation matrix includes REWET-II, VEERA and PACTEL facilities. This matrix is presented in APPENDIX I.

Regardless of the large number of thermal hydraulic experiments conducted with many different facilities, the need for good quality data from integral test facilities has not yet reached saturation. Over the last twenty-five years, the International Standard Problem (ISP) exercises have been organized under the OECD/NEA umbrella. The ISPs are exercises in which the predictions of different computer codes for a given physical problem are compared with each other or with the results of a carefully controlled experimental study. The main goal of the ISP exercises is to increase confidence in the validity and accuracy of the tools, which are used in assessing the safety of nuclear installations. They enable code users to gain experience and demonstrate their competence. These exercises are performed as open or blind problems. In an open ISP exercise, the results of the experiment are available to the participants before performing the calculations while in a blind standard problem exercise, the results are not disclosed until the calculation results are made available for comparison. Experiments selected to support ISP exercises must be well documented; they provide the framework for several code validation matrices. More than 50 ISPs have been introduced thus far, containing a wide range of in-vessel thermal hydraulics and versatile cases of severe accident scenarios.

Collaboration on VVER safety has been realized also in the VVER operator forums and in the Atomic Energy Research (AER) working groups. Computer code benchmark problems have been conducted and analysed for example by Hämäläinen (2005).

2.8 TMI-2 as a code validation case

The accident at Three Mile Island Unit 2 (TMI-2) nuclear power plant in 1979 led to a partial core melt. TMI-2 primary system layout and pressurizer connection to the hot leg are presented in Figure 10. Even though TMI-2 had severe consequences, it provided a unique opportunity to assess the analysis methods and computer simulation capabilities. OECD/NEA organized an exercise, where several participants contributed to benchmark analyses with different codes (OECD/NEA, 1992). The TMI-2 accident scenario had certain limitations on the analysis precision. Although the operational sequence of the events is well known, phenomenological events are based on indirect data, core end

state conditions and analyses. Another limitation is the lack of knowledge of boundary flows. They were also estimated indirectly from the measurements. The codes used in this exercise represent a broad spectrum of codes and were developed for different purposes. They were grouped into three categories:

1. Thermal hydraulic codes with detailed models of thermal hydraulics with extended severe accident regimes (ATHLET, CATHARE/ICARE, SCDAP/RELAP).
2. Severe accident codes with simple thermal hydraulics (e.g. MELCOR, MAAP).
3. Special purpose codes with segments of the accident progression (e.g. FLOW3D)

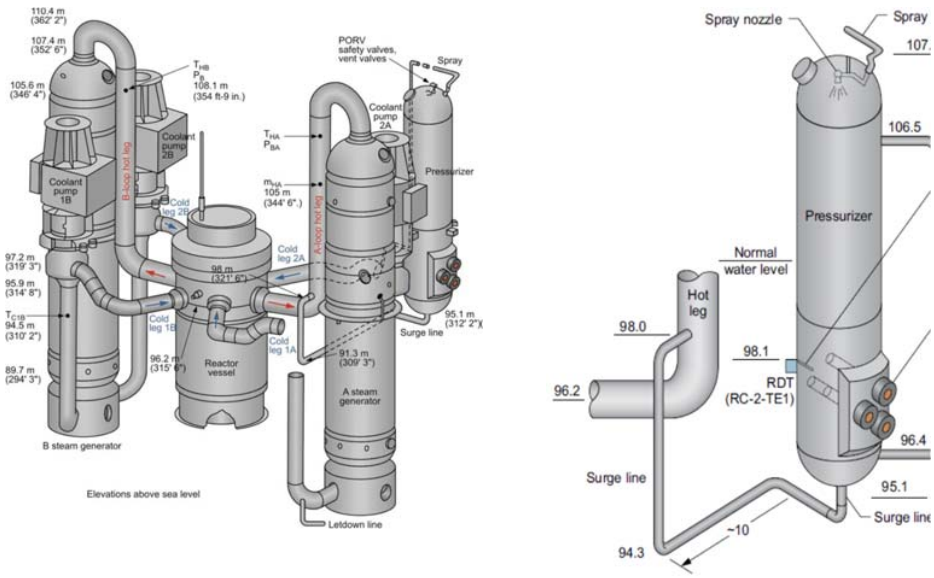

Figure 10: TMI-2 primary system layout (left) and pressurizer connection to hot leg (right) (Rempe and Knudson, 2013).

The accident scenario has been described in many references (OECD/NEA, 1992; Rempe and Knudson, 2013). The TMI-2 accident is generally divided into four distinct phases for analysis purposes:

Phase 1. (0–100 min) is an SBLOCA with the RCS pumps on.
Phase 2. (100–174 min) continues the SBLOCA with RCS pumps off along with initial core heat-up, melting and in-core relocation.
Phase 3. (174–200 min) is the RCS pump transient short term cooling effects.
Phase 4. (200–300 min) is the re-establishment of safety injection and the relocation of molten core materials and termination of core degradation.

Due to the different nature of the codes, they could not be used similarly to model the entire accident sequence. To model all four phases of the accident, the code should include models for all different phenomena occurring throughout these phases. Codes like SCDAP/RELAP and CATHARE/ICARE feature detailed physics models for both thermal hydraulic and severe accident phenomena. Thus, this kind of code should be able to reproduce the accident sequence consistently, given the known boundary conditions.

The calculation results revealed some interesting features in code modelling especially during Phase 2. None of the used codes could predict that the core overheats and melts after the stuck-open Pilot Operated Relief Valve (PORV) was manually closed by operators at time 139 min. During the accident, the pressurizer level remained constant. However, the calculations could not predict this pressurizer liquid hold-up with the specified boundary condition of makeup flow. Almost all codes drained the pressurizer. SCDAP/RELAP was not able to reproduce the liquid hold-up in the base case calculation. Once the reduced makeup flow in the parametric sensitivity case was introduced, the approximate results were obtained (see Figure 11). Also, CATHARE was able to produce the desired result after the analyst had inserted an additional valve in the surge line and closed it before the pressurizer draining could occur.

Some code analysts reported that inadequate RELAP modelling of the counter-current flow limitation (CCFL) at the pressurizer surge line junction would have partially explained the deviations in the results. This was argued by the reviewers of the analysis. The modelling of the surge line itself might have had a significant role in the pressurizer level behaviour. The surge line configuration forms a loop seal between the pressurizer and hot leg (see Figure 12). The pressurizer surge line declines about 3 m below the hot leg and is also one modelling detail that could have affected the results. In the CATHARE code, the connection was implemented with a special TEE component. In RELAP, the connection from the hot leg to the surge line appeared to be a straight connection from the hot leg pipe outlet, which is different from the connection used in CATHARE.

This particular modelling case suggests severe challenges to the codes as well as to the analysts. It was recognized that the uncertainties in the boundary conditions worsen the problem solving. Reasonably small variations in the boundary conditions, in similar but not identical code versions, or used by different analysts, could lead to significantly diverging results. This is particularly relevant for actual plant calculations because they are in most cases done “blind”, without prior knowledge of how the plant would behave in reality. According to the initial TMI-2 analysis results, the accident should never have happened.

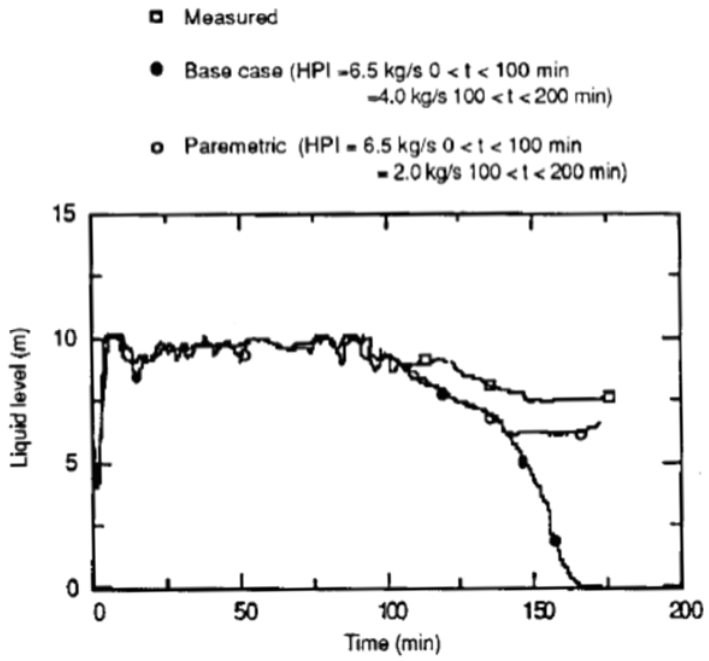

Figure 11: Pressurizer collapsed levels in measurement, base case and parametric study case calculations of the TMI-2 accident with RELAP/SCDAP code by DOE/INEL (TMI-2 Analysis Exercise, 1991).

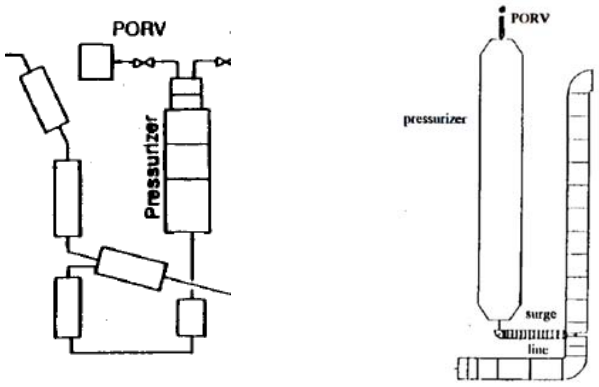

Figure 12. TMI-2 hot leg, surge line and pressurizer connections in schematic drawings, on left RELAP/SCDAP model and CATHARE/ICARE model on right (TMI-2 Analysis Exercise, 1991).

2.9 Generic validation and verification for software

Thermal hydraulic code validation can learn from generic software validation procedures. When new model is created to describe a certain phenomenon, it must be tested and proved to correspond to reality. This leads at first to the concept of verification. The equations describing the phenomenon must be verified, and therefore, the first test concerns solving the "equations right". After the verification, the model must be validated. The validation concept concentrates on the assessment of solving "right equations". These concepts for the verification and validation were launched by Roache (1998). He stated also that "verification deals with mathematics; validation deals with physics."

Oberkampf and Trucano (2007) quote the definitions of verification and validation adopted especially for the needs of CFD by AIAA and ASME as following statements:

- *"Verification*: The process of determining that a model implementation accurately represents the developer's conceptual description of the model and the solution to the model."
- *"Validation*: The process of determining the degree to which a model is an accurate representation of the real world from the perspective of the intended uses of the model."

2.9.1 Validation

General definitions for validation have been stated for many different disciplines, including e.g. in medicine. Formal definition of validation of any analytical method is presented by US Pharmacopeia as follows: "Validation is the process that establishes, by laboratory studies, that the performance characteristics of the method meet the requirements for the intended analytical applications."

According to the ISO 9001 standard (ISO 9000, 2005), validation is defined as follows: "*Validation is a process. It uses objective evidence to confirm that the requirements, which define an intended use or application, have been met. Whenever all requirements have been met, a validated status is achieved. The process of validation can be carried out under realistic use conditions or within a simulated use environment."*

Software validation is a part of the design validation for a completed device, but is not separately defined in the quality system regulations. General principles have been suggested even by U.S. Food and Drug Administration (FDA, 2002). Software validation is considered to be "confirmation by examination and provision of objective evidence that software specifications conform to user needs and intended uses, and that the particular requirements implemented through software can be consistently fulfilled."

The definition of verification is similar to that of the validation (ISO 9000, 2005). The purpose of verification is to provide objective evidence that the design outputs of a particular phase meet all the specified requirements for that phase. “Software verification looks for consistency, completeness, and correctness of the software and its supporting documentation, as it is being developed, and provides support for a subsequent conclusion that software is validated” (FDA, 2002).

The quality system regulation is harmonized with ISO 8402 (1994) treating “verification” and “validation” separately. However, in many software engineering publications "verification" and "validation" are used reciprocally. In some contexts, "verification, validation, and testing (VV&T)" are treated as if they would form a single concept, with no division among the three terms.

Software validation activities can occur at all stages of software development life cycle to ensure that all requirements have been fulfilled. The conclusion that software is validated is reliant on wide-ranging software testing and other verification tasks performed at each stage of the software development. The testing of software functionality can be carried out in a simulated or in a user site testing environment. They are typically included as a component of an overall design validation program.

Software verification and validation are usually difficult tasks because testing cannot be continued endlessly. Also, it is difficult to decide how much proof is needed. Software validation can be considered as a matter of developing a “level of confidence” that all requirements and user expectations are met for the software functions and features. Measures such as defects found in specification documents, estimates of defects remaining, are used to develop a sufficient level of confidence before launching the end product. The sufficient confidence means that some uncertainty is acceptable and is to be covered by the confidence interval.

The relationship between verification and validation can be described with a software development life cycle diagram, which is usually called the V-model and it is presented in Figure 13. At the bottom of the diagram is the code that is being developed. On the left hand side are the requirement definitions that the code should fulfil and cover. On the right hand side are the steps of validation. Hence, arrows from right to left at each validation step describe the respond that the validation gives questions that requirements are asking at different levels.

The V-model has been in use for long and is well established, but experience also suggests that it could be improved. Herzlich (Gerrard, 2002) introduced the W-Model approach to do this. Rather than focusing on specific dynamic test stages, the W-Model focuses on the development products themselves. Essentially, every development activity that produces a work product is “shadowed” by a test activity. The purpose of the test activity specifically is to determine whether the objectives of a development activity have been met and the deliverable meets its requirements. In its most generic form, the W-Model presents a standard development lifecycle with every development

stage mirrored by a test activity. On the left hand side, typically, the deliverables of a development activity are accompanied by a test activity "test the requirements".

Based on experiences, Spillner (2002) has listed deficiencies that commonly used V-models contain:

- Test activities start too late,
- Connection between test stages and the basis for the test is not clear and
- Test, debug and change tasks are not explicit.

In line with the Herzlich approach, Spillner has proposed an alternative W-model without these deficiencies. In the W-model, the weak links of the left and right hand sides in the V-model are removed. The W-model proposes that only testable requirements should be implemented. Also, concerning the architectural design, the model proposes that the architectural design should be kept simple and testable.

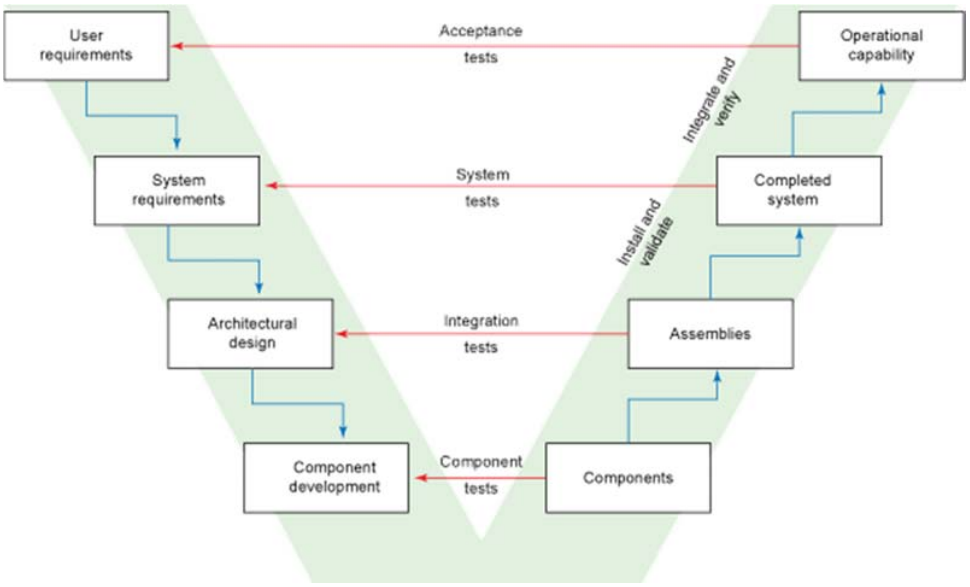

Figure 13: V-model process for validation and verification (IBM, 2013)

2.10 Proposed improvements to thermal hydraulic code validation

The traditional thermal hydraulic code validation process focuses on the code itself. The code performance and its abilities to describe the required physical phenomena are of the main concern. An essential part of the code validation is that the input is prepared according to the recommendations and the input itself is validated and it fulfils certain

qualification criteria. Due to this, a novel approach for the input deck validation is proposed here in the following sub-section. There are similarities to the pure code validation approach. However, it presents the validation process from a new perspective.

2.10.1 **Input validation**

The code validation brings out usually aspects, which are mostly related to the software performance and its abilities. However, much of the work in code validation processes is included in the modelling capabilities or even decision procedures that are usually called engineering judgment that the individual users imply according to their knowledge and experience background. To enhance the validation process, an input validation procedure is introduced here. The V-model and W-model approaches were considered as the basis for the input validation approach. Usually, input models are prepared for a certain purpose and can thus be very case-specific. The development of a generic and all-purpose input model for an experiment facility would require a large amount of data.

Figure 14 presents a novel approach for system code input validation in the form of a V-model. The entrance to the V-model is at top left. The exit of the model is at top right with a valid input model. The valid input model means that it has passed all stages of the validation process and the uncertainties of different nature at different steps have been recognized and assessed. The final stage should be that the user has an impression of the error margins when the calculations are carried out and they run as planned. Thus, the user is confident that the calculations results are representative and conclusions can be drawn from all matters that were defined at the beginning. The conclusions should give answers to the requirements concerning for example how much the margin for critical heat transfer should be if a certain type of reactor core has a specific loading pattern and power history. One purpose of this approach is that it allows “emergency exit” to a totally different approach of methods if in the validation process it is found in any level that the used approach does not satisfy the original definitions of requirements. These different methods could be CFD or perhaps spectral methods.

The flow direction of the “waterfall” from top left downwards includes the preparation of the input splitting all necessary process components into detailed nodes and setting all necessary geometric and different parameters defining coefficients for additive losses, flow discharge, weighing factors for different correlations etc. The methodology presented here is iterative. An optimal or best estimate input model usually requires testing both the verifying and validating nature. The arrowed circle in Figure 14 describes the iterative nature of the method.

When rising from the basement of the parameter set level to right upwards, the validation rate of the input is increased. Next, short explanations are presented of each part of this V-model proposal.

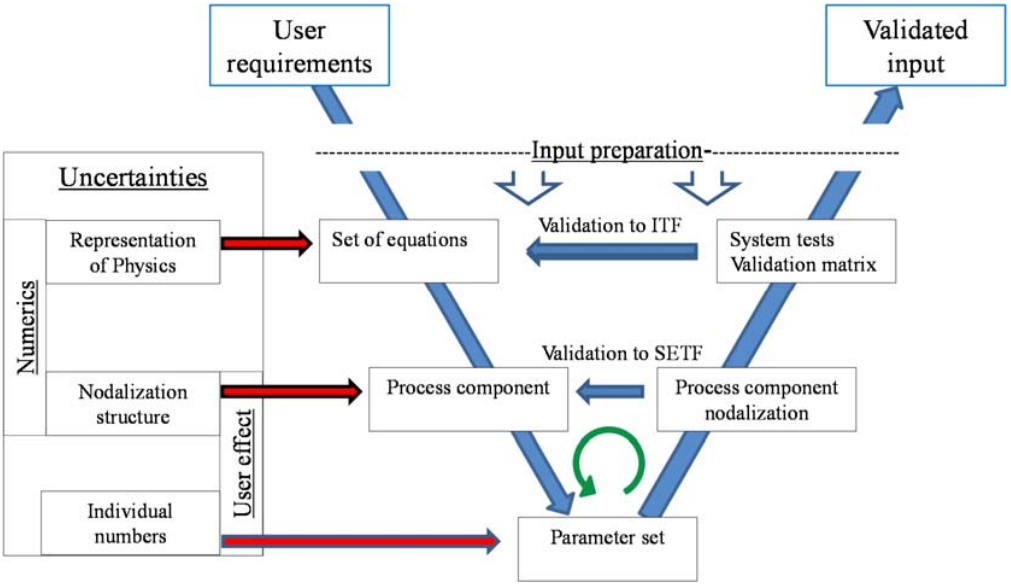

Figure 14: V-model approach for input validation.

User requirements

At the entrance level, the user defines the problem to be solved. The question asked here is: What kind of case is to be calculated (LOCA, non-LOCA transient, etc.). From this level below the actual input preparation is executed.

Set of equations

At this level, the decisions are made about the accuracy requirements that the model should be able to fulfil. The main question here is: What physics is included and what excluded in the chosen code models?

Process component

Modelling decisions concerning for example the number of loops, sub-channels in reactor core, lumping rate of steam generator heat exchanger tubes, that is, fixing the structure of nodalization.

Parameter set

At this level, the user sets the parameters that the code requires for the input. The parameter set can contain factors for friction and other flow losses, discharge

coefficients etc. The main questions asked here are: Which parameters may vary and how much?

Process component nodalization

This level performs the validation concerning different parts of the model separately. Usually, it is practical and convenient to run these validation cases with necessary boundary conditions and thus without the disturbance of surrounding components or other parts of the facility. The cases should contain the pressure difference and heat loss assessments if available. The separate effect tests are usable for validation calculations.

System tests and Validation matrix

When components are separately verified and validated against suitable data, the model is compiled and full structure is then decided and defined. The full model has to be validated against versatile data, by which the general behaviour of the input model is proven to be confident. Also, the input model should be validated against data that contain challenging transient phenomena. The integral test facilities form the essential database for this phase of validation.

Uncertainties

The uncertainties in the input validation appear at different stages and in different nature. Generally, uncertainties can be divided into two basic categories:

1) Numerical uncertainties and
2) User effects.

Both of these categories contain issues that cannot be clearly separated to belong in only one category. This classification of uncertainties produces three sources:

1. Representation of physics. It is essential to realize how the code is able to model physics. The physical representation can contain only limited pressure and temperature ranges. The physics can also contain phenomenological shortage. Approximations such as including only some terms in the field equations (e.g. the viscous stress terms are sometimes not included), ignoring minor components (dissolved non-condensible gases) or the assumption that fully developed flow exists in the system are included in this group of uncertainties. These uncertainties are generally *not statistically quantifiable* because their impact does not depend on any individual variable or parameter that could be varied.
2. Uncertainties related to the structure of the system, that is, nodalization or spatial discretization to obtain the control volumes that are represented by the field equations. For example, the nodalization could be too coarse to describe

flow or temperature distributions in multiple parallel flowpaths. These uncertainties are generally *not statistically quantifiable* either because the lumping of parallel channels is a modelling choice, not a random variable.

3. Individual numbers. This means the input parameters that the user can choose more or less freely and that often have a known range and/or distribution of values, for instance empirical factors in friction and heat transfer correlations. This uncertainty *can be assessed with statistical uncertainty evaluation* methods developed.

As the graphical set-up in Figure 14 presents, both the representation of physics and structure of nodalization contain numerical uncertainties.

The user effect is the most complex uncertainty category. This effect is included in various ways during the input preparation. The user decides the structure of nodalization and sets values to the parameters. Thus, the user effect can be called "user induced uncertainties" due to the choices the user makes.

At least the sources of uncertainties should be recognized. The quantification of uncertainties is hardly ever possible at all levels. The parametric uncertainties are the most recognizable type and can be quantified with specific methods developed for this purpose. The user effect uncertainties can hardly be quantified with any reasonable method.

Validated model

After passing all stages, the model should have a reasonably small or acceptable uncertainty. The uncertainties have been quantified if possible or necessary. The limitations of the model are also understood. The limitations stemmed by physics and numerics as well as lumping in the modelling are understood and accepted.

3 VVER-440 specific thermal hydraulics

The VVER-440 reactor type has features that are different from the western type pressurized water reactors. The layout of VVER-440 containment and schematic drawing of the main safety systems are presented in Figure 15 and Figure 16. From structural and geometrical point of view the differences can be listed as follows (OECD, 2001):

- Horizontal steam generator with two collectors,
- Six loops of primary circuit,
- Loop seals in hot legs,
- Elevation of the top of steam generator tubes related to the top of the core (~4 m, PWR ~ 10 m),
- Shrouded fuel assemblies with hexagonal fuel rod arrangement,
- ECC injection points,
- Secondary side water volume in steam generators compared with nominal thermal core power is larger,
- Two isolation valves in each main loop,
- Special pressure suppression system (ice condenser, only at Loviisa VVER-440),
- Each control rod consists of two parts: lower fuel assembly and upper absorber and
- Lower plenum volume larger and different core internal structures.

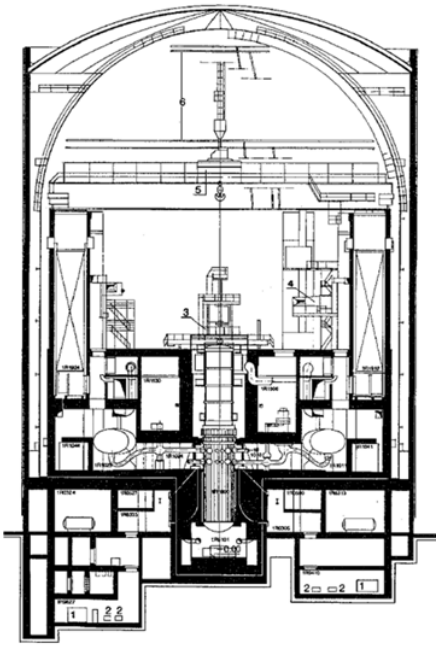

Figure 15: Containment layout in Loviisa VVER-440 power plant (Routamo et al., 2004).

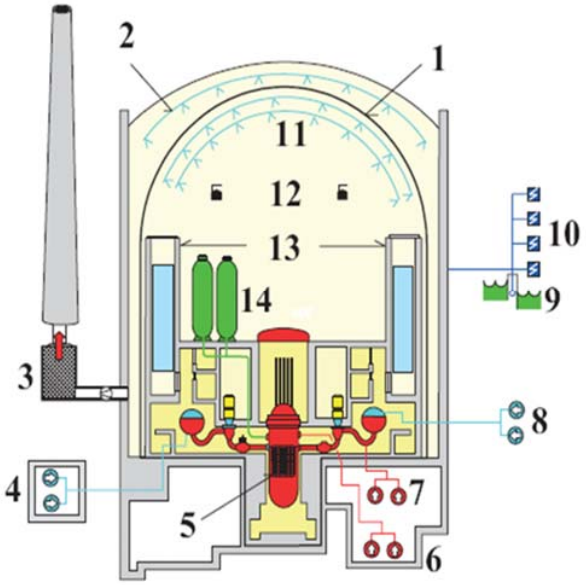

Safety systems:

1. Steel containment
2. Containment's external spray system
3. Air filters
4. Additional emergency feed water pumps
5. Uranium fuel core
6. Emergency cooling pumps
7. Emergency make-up water pumps
8. Emergency feed water pumps
9. Electricity connection from the hydropower plant
10. Emergency diesel generators
11. Containment spray system
12. Hydrogen igniters and recombinators
13. Ice condensers
14. 14. Emergency accumulators

Figure 16: Schematic view of safety systems in Loviisa VVER-440 power plant (Fortum, Loviisa power plant's most important safety systems).

These geometrical differences lead also to differences in thermal hydraulics. Thus, specific thermal hydraulic features in VVER-440 are horizontal steam generators and hot leg loop seals. The horizontal steam generators are cylinders placed horizontally; in the middle of the cylinder two primary collectors, large-diameter pipe headers, enter the vessel from bottom (see Figure 17 and Figure 18). The heat exchange surface consists of 5536 tubes, which extend from the collectors towards both ends of the horizontal vessel. Cold leg loop seals are common also in western type PWR concepts due to the set-up of the main circulation pumps at the cold legs. The loop seals are the U-shaped bends in the hot and cold leg piping connecting the upper plenum and downcomer to the steam generators. The VVER-440 reactor has six loops instead of the usual two to four loops in the western reactors. The large number of loops enables multiple paths for reactor cooling. The volume of the steam generators is large providing a larger coolant volume and heat sink compared to the western designs having vertical steam generators. The large coolant volume especially on the secondary side of the steam generator gives inherent thermal inertia and thus more time to adjust in transient situations. The reactor is operable also with 3–5 loops. In these situations, reactor power is limited according to running pumps. In case the pump is not running, the closing valves are remained open in the corresponding loop.

The loop seals in hot legs are a specific feature in the VVER-440 reactor design (see Figure 19). In later VVER designs, like VVER-1000, the hot leg loop seals do not exist anymore. The effect of the loop seals appears especially in the accident cases when the primary side inventory decreases. Usually in these cases, natural circulation has been started. When the inventory has decreased to the connection elevation of the hot leg loops, steam can flow to the hot legs.

The VVER-440 reactor core design is also different from the western designs. The fuel rods in VVER-440 core are arranged in a triangular grid. The fuel rod bundle has therefore a hexagonal form. In western reactor cores, the fuel rods are arranged in square array. This specific feature must be taken into account in the sub-channel analysis. For example critical heat flux (CHF) correlations have a different formulation in hexagonal fuel rod channels from the channels arranged in square array.

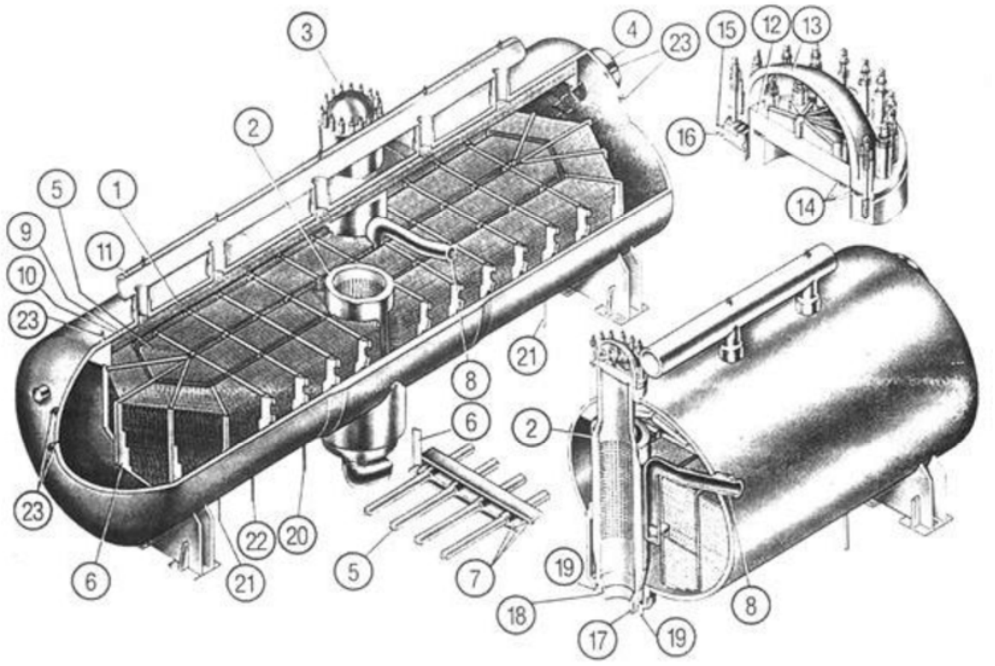

Figure 17: Cutaway diagram of horizontal steam generator of VVER-440 (WWER-440/213 – The secondary circuit). Specifications of numberings are not presented here.

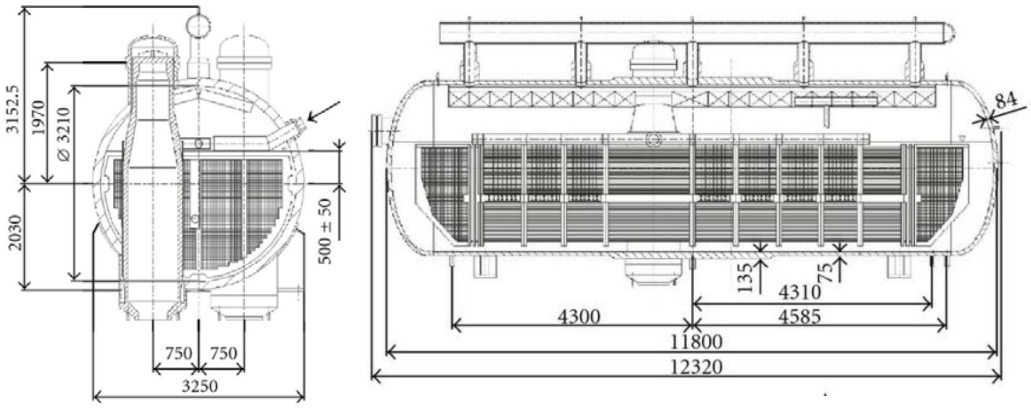

Figure 18: VVER-440 Horizontal Steam Generator (Degmova et al., 2012).

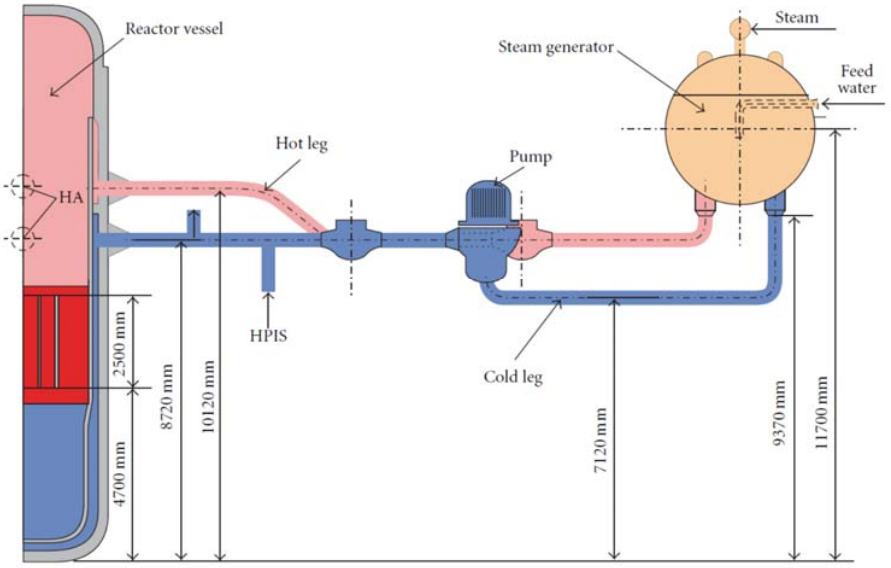

Figure 19: Schematic drawing of the primary circuit of the VVER-440 reactor. Notice the hot leg and the cold leg loop seals (Ezsöl et al., 2012)

3.1 Previous research work of VVER-440

The Loviisa power plant is exceptional since the design is a modified version of the original Russian design having for instance ice-condensers in the containment building. Nevertheless, the basic characteristics are the same as in the original design and almost equivalent to the other VVER-440 model 213 type reactors.

Various studies of the VVER-440 reactor type have been carried out over a number of years. Publicly funded research programmes, for example SAFIR, have been in the key role of safety research in Finland since 1990s. For example at Lappeenranta University of Technology, the thermal hydraulics of the VVER-440 reactor type has been studied almost for 40 years with different experiment facilities and computer codes. These studies include experiments, which started with REWET-I, REWET-II and REWET-III paving the way towards the PACTEL facility. The research work with REWET facilities has been described by Kervinen et al. (1980 and 1983), Kervinen and Tuunanen (1987) and Kervinen et al. (1987).

3.1.1 Early natural circulation and horizontal steam generator studies

The natural circulation in the VVER-440 geometry has been studied with several PACTEL facility experiments. The VVER-440 type reactor was addressed the first time by a CSNI International Standard Problem ISP-33. Natural circulation experiment was considered particularly suitable.

The International Standard Problem ISP-33 was carried out with the PACTEL facility in Lappeenranta, and the comparison report of the results was published in the OECD series (Purhonen et al., 1994). The ISP-33 participation contained 19 institutions from 11 countries using a variety of codes like RELAP5, ATHLET and CATHARE, including some of the Russian origin. The PACTEL experiment for ISP-33 concentrated on the natural circulation during a stepwise coolant inventory reduction. The objectives of the ISP-33 were to study:

- the natural convection circulation in a VVER plant,
- the series of quasi steady natural circulation periods,
- single phase natural convection and two-phase natural convection with continuous liquid flow,
- convection flow under reflux -boiler mode conditions and
- "double-blind" pre-test analyses; "open" post-test analyses also processed.

Main findings resulted:

- overall transients reasonably were well predicted,
- main discrepancies noted concerned the predictions of flow stagnations and time of core heat-up,
- two-phase natural circulation flow and refilling rates in general were over-predicted,
- post-test analyses yielded in general improved results due to the inclusion of some experimental problems not known in advance for "double-blind" predictions (e.g. leak of safety valve) and
- loop seal behaviour a problem also for "open" post-test analyses.

Several series of small break loss-of-coolant accident (SBLOCA) experiments have been carried out in the PACTEL facility. All three different natural circulation flow modes, the one-phase liquid flow, the two-phase mixture flow and the boiler-condenser mode were clearly visible in each experiment of the series. The different break sizes and ECC measures had an effect on the duration and timing of the transient events, but the general thermal hydraulic behaviour of the facility was similar throughout the test series.

Tuunanen (1996) has reported studies of horizontal steam generators (HSG) of VVERs. The analyses contained experimental and computer code modelling of HSGs in transient and accident situations. Because HSGs act as heat sink, their performance and availability is essential especially in all transient and accident situations. The computer code modelling of HSGs is still topical since most of the computer codes have been validated against vertical steam generators. The results showed that during the loss-of-feedwater (LOF) event, the RELAP5/MOD3 code model was not capable of simulating steam superheating on the HSG secondary side.

The main findings concluded that VVER-440 reactors have an important inherent safety feature having a large ratio of primary coolant volume compared to the core power. Also, the large coolant volume on the secondary side of SGs gives time for corrective actions for example in the case of LOF and station blackout (SBO) situations. The six coolant loops in the primary system provide multiple cooling paths in LOF and pump failure transients.

Tuunanen (1994) has reported several thermal hydraulic analyses related to the VVER-440 reactor type. Studies include for example boron behaviour during the long-term cooling period in the loss-of-coolant-accident (LOCA) of the VVER-440 type reactor. The results of these studies conclude two main anomalies in boron behaviour. Boric acid crystalizes if borated water is allowed to boil long enough in the reactor core and if the flow out from the pressure vessel is pure steam flow. The crystallized boric acid might block some flow paths in the core leading to overheating and failure of fuel rods.

3.1.2 Horizontal steam generator inherent characteristics

Hyvärinen (1996a, 1996b) has reported fundamental investigations of horizontal steam generator heat transfer performance. Five major findings have been presented:

(1) Under natural circulation conditions, the primary side phenomena determine the overall heat transfer capability when the secondary water level is given. On the secondary side, it suffices to know whether or not a tube layer is wetted; details of the secondary flow patterns are not decisive, on account of the low power input.

(2) The power throughput depends roughly linearly on the inlet mass flow and temperature, but degrades slightly faster than the available heat transfer area if the secondary level is depleted; consequently, under the low secondary inventory regime,

the horizontal steam generator is no longer fully effective in its primary task as a heat exchanger. The deficiency has been quantified for an idealized test case of station blackout. It has been found out that the grace period from the event initiation to the primary pressurization up to the safety valve actuation is 2–3 h, and about 4 h to the point where the primary becomes solid. These times are substantially shorter than the 5–6 h that would be suggested by a simplistic secondary boil-off energy balance analysis, or a system code calculation employing overly simple nodalization.

(3) Under typical low flow conditions, the magnitude of the internal circulation increases with decreasing inlet flow by decreasing tube frictional pressure drop and increasing the density difference between the collectors by increasing gravitational pressure difference.

(4) The vertical distribution of the number of tubes (primary flow and heat transfer area) is a very important factor that affects, among other things, the heat transfer capability and magnitude of internal recirculation.

(5) Two mechanisms that could potentially cause loop flow instability exist: one arises from the non-uniqueness of the steam generator pressure drop-mass flow characteristic, and the other from the incompleteness of backflow mixing in the hot collector. The first mechanism appears possible at exceedingly low powers (less than 0.2 MW per steam generator), while the second mechanism applies under shutdown conditions.

3.1.3 **Noncondensables in VVER loop seals**

Sarrette (2003) has presented studies focused on the presence of non-condensable (NC) gas on the thermal hydraulic behaviour of the coolant of the primary circuit of VVER-440 geometry in abnormal situations. Two different cases were introduced.

(1) The impact of air in the tubes of the horizontal steam generator (HSG) was calculated using the CATHARE2 code. The initial and boundary conditions of the geometry parameters were derived from an experiment carried out on the PACTEL facility with air as the NC gas. A volume of air equivalent to the volume of the primary side of the HSG was injected in the entrance of the hot collector at atmospheric pressure. The calculation showed that the air flows out from the hot collector and stagnates in the second half-length of the primary tubes along the whole height of the tube bundle. The air was gathered to the cold collector and the hot collector contained pure steam during the whole air injection period. The air was also present in the cold leg, mostly in the vertical parts below the cold collector, at the inlet and outlet of the pump.

(2) The degassing of NC gas dissolved in the primary coolant of a VVER-440 was studied using a CATHARE code model developed originally by CEA Grenoble. Potential release of the nitrogen gas dissolved in the water of the accumulators of the emergency core coolant system of the Loviisa NPP was investigated. An experiment

was performed with PACTEL to determine the value of the release time constant of the nitrogen gas in the depressurization conditions representative of the small and intermediate break transients postulated for the Loviisa NPP. Simplified transients were calculated using modified CATHARE code for various values of the release time constant used in the dissolution and release model. For the small breaks, nitrogen gas was gathered in the collectors of the HSGs. The levels oscillated until the low-pressure injection pumps (LPIS) actuated refilling the primary circuit. In the case of the intermediate breaks, most of the nitrogen gas was ejected at the break and hardly any nitrogen was held in the HSGs. The obtained results could be applied to the real safety conditions used in the nuclear power plant.

3.1.4 Horizontal steam generator behaviour in the main steam line break

Hämäläinen (2005) has discussed the modelling of the power plant with 1-D system codes especially concerning the horizontal steam generator modelling. For example, when pipe modelling is considered in radial direction, one node modelling is sufficient in most cases. But with increased diameters, the one node modelling becomes insufficient for describing for example two adjacent flows with different temperatures and possibly having opposite flow directions.

The main steam line break (MSLB) modelling of Loviisa NPP was discussed by Hämäläinen (2005) also. Being different for each plant, MSLB can create in all PWRs the potential hazard of re-criticality due to the strong core cool-down and, consequently, the possible fuel damage. The cooling in the core is strongly asymmetric if several reactor coolant pumps (RCP) are in operation. The accurate plant modelling is a demanding task because various complicated processes, such as asymmetric power generation and mixing in the reactor vessel, as well as various protection and conventional automation signals, contribute to the complexity of the scenario. The plant model for SMABRE code has been introduced. In the nodalization scheme of the secondary system, various break locations were assumed in the analyses. The pipelines can empty the water content into the broken steam generator in one of the calculation cases. The studies included various assumptions on the break size, the operation of the reactor coolant pumps and the performance of other systems. A realistic prediction of the plant behaviour requires careful modelling of details, such as the level measurements in the horizontal steam generators, the feed water system and turbine control. The calculations showed that only a slight return to power after the reactor scram is to be expected under the worst conditions in MSLB at Loviisa.

3.1.5 Hungarian studies with PMK and related work

Hungarian experimental research is mainly related to the PMK-2 facility studies (Ezsöl et al., 2012). The PMK-2 facility is a full-pressure and full scaled power one-loop thermal hydraulic model of the primary and partly the secondary circuit of the Paks nuclear power plant of the VVER-440/213 type. The volumetric scaling ratio is 1:2070; the elevation scale is 1:1; maintaining gravitational forces in natural circulation. The

available power is 2 MW establishing nominal conditions of the plant. All the VVER-specific design features are included in the design of the facility. The PMK-2 experiments provided a database that can be used for code validation in the three main groups of the OECD-VVER code validation matrices: large breaks, small/intermediate leaks and plant transients. Phenomena simulated at the level required by the validation matrices are as follows: break flow, pressurizer thermal hydraulics and surge line hydraulics, heat transfer in SG primary and secondary sides, single- and two-phase natural circulation, mixing and condensation during injection from ECCSs, loop seal behaviour in the hot leg and clearance in the cold leg and the core heat transfer in clearing DNB and dryout.

The codes applied for the safety analysis in Hungary are ATHLET for LBLOCA, RELAP5 for SBLOCA and transients, and CATHARE, which is used as an independent tool to support regulatory authority, and Apros code used by power utility; validation activities in the country are concentrated to these codes. The PMK-2 supported the solution of specific problems encountered during the lifetime of the Paks NPP. They verified the effectiveness of the secondary and primary bleed and feed like post LOCA cool down and large break LOCA during cool down; they continuously supported safety improvement activities in the SG tube and SG header ruptures.

Full power SBLOCA tests demonstrated the possibility of a brief core uncover during loop seal clearing at reduced inventories (Toth, 1988). The coolant distribution in the loop seals prior to clearing created a manometric core level depression, which resulted in increased cladding temperatures near the top of the core. Other natural circulation experiments showed that the transition between the single and two-phase flow is not always smooth, with the nature of this transition depending upon the core power and mass inventory. When the primary side inventory was reduced and the upper plenum water level fell to the hot leg entrances, the loop seals inhibited steam flow into the steam generators. This diminished the natural circulation flow and system re-pressurization was resulted.

3.1.6 **GRS work with horizontal steam generators**

Sonnenburg et al. (1993) have reported of the use of the thermal hydraulic code ATHLET by GRS applied for the analyses of LOCA and transients in VVER plants. The specific design of these plants especially of the horizontal steam generator design requires a specific modelling of the phenomena that may occur under LOCA and transient conditions. Differences in design compared to the design of western reactors have been briefly listed. Specific phenomena occurring under small leak accidents were described. The consideration of the simulation of the boiler-condenser mode of natural circulation (Figure 20) illustrates the modelling requirements for a code. The considered requirements contain predictions of condensate distribution over the horizontal tubes and along the hot and cold legs. Facing the lack of experimental data, the reliability of the ATHLET simulation has been discussed by means of plausibility studies based on the momentum balance for steam and water.

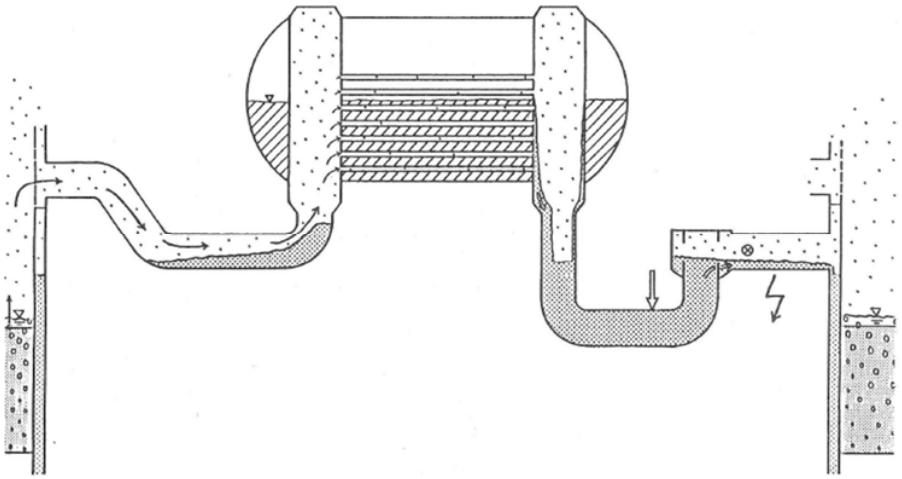

Figure 20: Schematic view of boiler-condenser mode in VVER HSG.

3.2 Conclusions of the previous studies

All presented previous studies indicate that the thermal hydraulics in the VVER-440 reactor geometrics is very different from the other pressurized water reactor designs. These studies served as the basis for the research, which has been performed recently with the TRACE code implementation for the PACTEL facility.

4 PACTEL experiment matrix

This chapter gives an overview of the PACTEL facility and the experiments that have been chosen for the validation studies with the TRACE code.

4.1 PACTEL facility

Parallel Channel Test Loop, PACTEL, is a volumetrically scaled (1:305) model of the VVER-440 type nuclear power plants located in Loviisa. Thus, the geometrical scaling ratio in PACTEL is over ten times larger than in PMK-2 (1:2070). The PACTEL facility was constructed at Lappeenranta University of Technology (LUT) in the beginning of the 1990s. All the main parts of the reference reactor primary loop are included in PACTEL: a pressure vessel, main circulation loops, steam generators and a pressurizer. The main emergency core cooling (ECC) systems, that is, the accumulators and the high and low pressure injection systems (HPIS, LPIS), have been modelled in PACTEL. The original elevations have been kept to preserve the natural circulation pressure heads. The graphical comparison of the PACTEL facility embedded with the figure of reference reactor is shown in Figure 21.

The PACTEL test facility consists of three primary loops while the reference reactor has six primary loops. Therefore, one PACTEL steam generator is representing two steam generators of the reference plant. The number of steam generators and circulation loops was reduced from the original six to three in the PACTEL facility because of the limited space in the laboratory and thus to keep the facility volume within a reasonable range. Also, the choice was a compromise between choosing as many loops as possible and being able to observe asymmetric behaviour of different loops. The length of the loops is about one half of that in the reference plant. If the loop lengths would have been kept original, the use of the volumetric scaling would have led to very small pipe diameters. Thus, the PACTEL hot and cold legs have been scaled intending to preserve the Froude number between the reference plant and PACTEL. Froude number is the ratio of the inertial forces to the gravitational forces:

$$Fr = \frac{v}{\sqrt{gD}}, \tag{4.1}$$

where v is fluid velocity, g is acceleration due gravity, and D is (inner) diameter. Froude number preserving together with volumetric flow scaling ends up to formula:

$$D = D^{*}\left(\frac{n^{*}}{305 \cdot n}\right)^{0.4}, \tag{4.2}$$

where n^{*} refers to number of loops in reference reactor and n to number of loops in the scaled facility. This scaling method gives larger diameters than the plain volumetric scaling. The PACTEL hot and cold leg diameters (52.5 mm) were chosen from standard pipe sizes. Table 3 presents the PACTEL facility characteristics compared to the reference reactor. A general view of the PACTEL facility is presented in Figure 22.

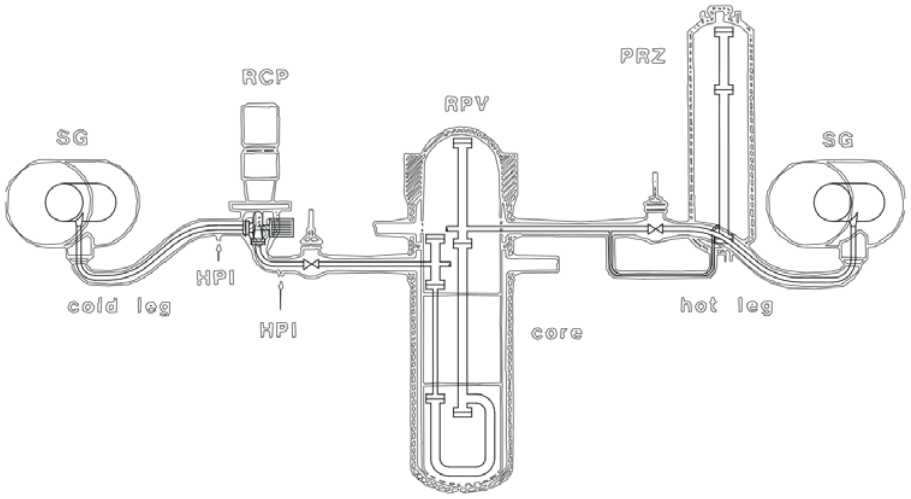

Figure 21: Graphical comparison of Loviisa VVER-440 embedded with the PACTEL facility (Tuunanen et al., 1998).

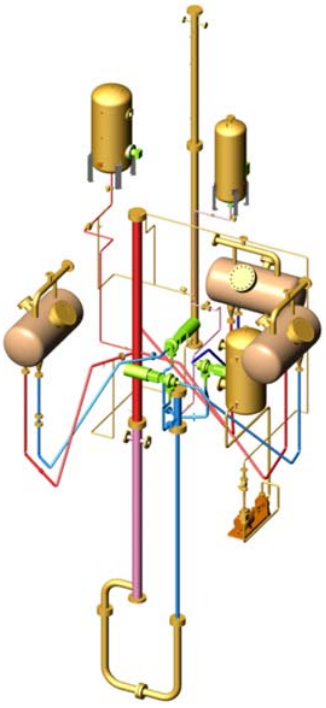

Figure 22: The PACTEL facility.

Table 3: The PACTEL facility design characteristics compared to the Loviisa VVER-440 upgraded design values. Original thermal power of Loviisa reactors was 1375 MW, (served as basis for scaling). Original table values presented by Tuunanen et al. (1998).

	PACTEL	**Loviisa VVER-440**
Volumetric scaling ratio	1:305	-
Scaling factor of component heights and elevations	1:1	-
Number of primary loops	3	6
Length of hot legs (average)	8.3 m	14.7 m
Length of cold legs (average)	9.0 m	16.7 m
Diameter of pipes in hot and cold legs	52.5 mm	494 mm
Maximum heating power/thermal power	1 MW	1500 MW (1375 MW)
Number of rods	144	39438
Outer diameter of fuel rod simulators	9.1 mm	9.1 mm
Fuel rod pitch	12.2 mm	12.2 mm
Heated length of fuel rod simulators	2.42 m	2.42 m
Axial power distribution	Chopped cosine	-
Maximum cladding temperature	800 ºC	-
Primary side pressure	8.0 MPa (max.)	12.3 MPa
Primary side temperature of fluid	300 ºC (max.)	~303 ºC (Core outlet)
Maximum secondary side pressure	5.0 MPa	5.6 MPa (Safety valve opening pressure)
Maximum secondary side temperature	260 ºC	260 ºC
Feedwater tank pressure	2.5 MPa	0.7 MPa
Feedwater temperature	225 ºC	~228 ºC (after pre-heat)
Hydro accumulator pressure	5.5 MPa (max.)	3.5 MPa (updated)
Low-pressure ECC-water pressure	0.7 MPa	0.7 MPa
High-pressure ECC-water pressure	8.0 MPa	11.0 MPa
ECC-water temperature	30 ºC - 50 ºC	30 ºC - 80 ºC

4.1.1 **PACTEL horizontal steam generators**

The PACTEL facility has had two different steam generator configurations: Full Length Steam Generator (FLSG) and Large Diameter Steam Generator (LDSG). The FLSG was the first PACTEL steam generator model. It was constructed with full length heat exchanger tubes. The average length of the tubes was 8.8 m. The tube bundle contained 38 tubes in nine rows. The diameter of the tubes and spaces between them was similar as in the reference steam generator. After a large number of experiments, the idea of a larger diameter steam generator was presented.

The LDSG steam generators were constructed later, and the FLSGs were replaced with these large diameter steam generators. The primary side of the LDSG contains vertical primary collectors and horizontal heat exchange tubes. The average length of the tubes is 2.8 m, which is only one third of the reference SG. The main characteristics of the PACTEL and Loviisa VVER-440 horizontal steam generators are presented in Table 4.

Although the average tube length is much smaller than in the reference steam generator, the heat transfer area of the tube bundle corresponds to two steam generators of the

reference reactor. The secondary side differs from the reference steam generator more than the primary side. Although the height of the shell is only 0.95 m (reference 3.21 m) and the length is reduced to 2.2 m (reference 11.8 m), the volume of the secondary side is larger than it should be according to the scaling factor. Therefore, the coolant inventory is larger, and the transients in the steam generator are slower than in the reference steam generator. This has to be taken into account when the results are scaled to the full scale. Different views of the PACTEL steam generator (LDSG) are presented in Figure 23. The figure on the left shows a cross-sectional view of the steam generator, while the right top figure shows a side view of the steam generator and the right bottom figure shows the thermocouple locations in axial direction in the heat exchange tubes.

Table 4: PACTEL steam generator characteristics compared with the Loviisa VVER-440 steam generator.

	PACTEL HSG	VVER-440 HSG
Number of tubes	118	5536
Tubes layers	14	77
Vertical columns	9	-
Tube outer diameter	16 mm	16 mm
Tube length (average)	2.8 m	9 m
Tube bundle height	624 mm	1.82
Tube horizontal pitch	30 mm	30 mm
Tube vertical pitch	48 mm (doubled)	24 mm
Height of the shell side	0.95 m	3.21 m
Shell length	2.2 m	11.8 m

The structure of the secondary side differs also slightly from the reference steam generator, which has two primary tube bundles and a collector between them in the middle of the steam generator. The PACTEL steam generator has only one tube bundle. This means more empty space in the vicinity of the primary collectors. The scaling and the dimensions of the steam generator cause extra volume on both sides of the tube bundle. The effect of this volume has been reduced by steel plates.

The instrumentation of the steam generator contains mainly temperature measurements. The primary and secondary side temperatures are measured in several tubes. The inlet and outlet temperature of the primary coolant are measured, as well as the primary mass flow rate, mass flow rate of the feed water and the differential pressure on the secondary side. The collapsed level is based on the differential pressure measurement. The uncertainties of the temperature and mass flow rate measurements are ± 1.5 °C and 2.5 %, respectively. The accuracy of the secondary side collapsed level is ± 25 mm.

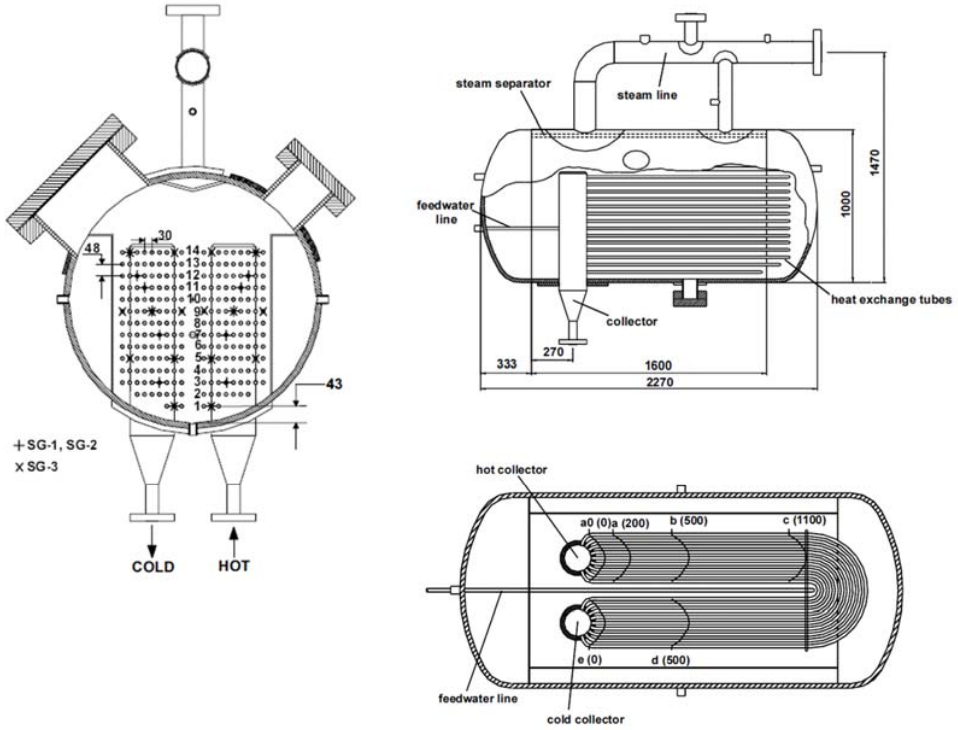

Figure 23: Horizontal steam generator of the PACTEL facility, cross-sectional view (left) and side view the steam generator (right top). Thermocouple locations in axial direction in the heat exchange tubes (right, below).

4.2 Experiment matrix for validation

In this section, the PACTEL experiments used for the validation calculations are described. Table 5 presents the matrix of experiments chosen for the validation. The table lists the objectives and items of interest of different experiments. Also, the table presents the validation item, which presents whether the validation was planned to focus mainly on the code or mainly on the input or in some cases on both. The last column of the table focuses on the observed quantity in the code.

The experiment matrix for validation represents a large variety of different experiment types. It contains tests for the definitions of pressure and heat losses (FLT and HL). The main objectives were to model a diverse range of experiments and validate the model to cover widely different transient types. The main focus was dedicated to enlighten the VVER-440 specific features like the horizontal steam generator behaviour and loop seal effect. The selected PACTEL experiments contained transients with loss-of-feedwater

(LOF), stepwise inventory reduction (SIR), small break LOCA (SBL and IMP), primary-to secondary leakage (PSL) and anticipated transient without scram (ATWS).

The PACTEL SBLOCA experiments contained different break sizes including natural circulation. The intention was to challenge the code and increase the degree of difficulty in every new calculation case. Thus, the increased break size was the main parameter, which challenged the code. The experiments with the break event covered break diameters from 1 mm to 7.8 mm, corresponding to 0.04 %–2.2 % of the cold leg flow area in the PACTEL facility.

Table 6 presents the initial and boundary conditions of both the primary and secondary sides of the PACTEL validation experiments.

An initiative approach to the validation of input model is the definition of pressure and heat losses. They serve as important boundary conditions in all other validation cases. Several PACTEL experiments have been performed to determine the pressure losses over the whole test loop both for normal and for reverse flow direction. The main parts of the facility; three primary circuits, a pressure vessel and a pressurizer surge line; have all been measured separately. Pressure losses have been measured over a large scale of mass flow ranges. The pressure losses in these experiments were presented as a function of mass flow rate in each section of the PACTEL test loop.

The importance of knowing the heat losses has been widely emphasized when the assessment of experiment results has been considered. Therefore, the heat losses of the PACTEL facility were defined. Several possibilities and means exist for this purpose. The overall heat losses were defined using the heat-up and cool-down method presented by Sanders (1991). PACTEL experiment HL-22 was then carried out to gather information for this method. The secondary sides of the steam generators were empty in this transient. This method provided values for the heat losses as a function of the average primary temperature. A similar method for the definition of pressurizer heat losses was used in the separate experiment HL-23. Another method was used to define the heat losses at one operating temperature by measuring the structure temperatures of the insulated parts as well as the temperatures of the fins that are formed by the supporting structures, impulse lines for differential pressure measurements and valves that cannot be insulated. The pump heat losses were defined from separate data. The total heat losses were then calculated by adding up the singular heat losses (Purhonen, 2004).

Table 5: Matrix of PACTEL experiments chosen for TRACE code calculations.

Experiment	Objectives	Item of interest	Validation item	Observed quantity in the code
Form Loss Tests: FLT-04, FLT-08, FLT-11	Pressure losses in normal and reversed directions	Parameters: Local form loss coefficients	Input	• Primary side mass flow
Heat Losses: HL-22 HL-23	Heat losses: Whole facility Pressurizer	Parameters: Insulation properties	Input	• Primary side heat-up and cool-down rate
Loss-Of-Feedwater: LOF-10	Horizontal steam generator behaviour • Only one loop in use	Nodalization: Number of tube layers	Input	• Primary to secondary heat transfer • Cold leg temperature • Steam superheat
Stepwise Inventory Reduction: SIR-21 SIR-23	Natural circulation modes in full and low pressure ranges • Only one loop in use	NC modes Total heat transfer	Code	• System-wide phase separation • Natural circulation modes
Small Break LOCA: SBL-30	Small break LOCA 1 mm break, pressurizer isolated • No HA, HPI, LPI • No feed or bleed	Break flow Loop seals	Code	• Inventory distribution during depletion and recovery • Break flow rate • Hot leg loop seal clearing • Natural circulation modes
SBL-31	SB LOCA 2.5 mm break • HAs • No HPI, LPI • Secondary feed and bleed	Break flow, loop seals, ECCS influence	Code/Input Added: 2 x HA	
SBL-33	SB LOCA 3.5 mm break • HAs • HPIS • No LPIS • Secondary feed and bleed	Break flow, loop seals, ECCS infl., Boiler condenser mode duration	Code/Input Added: HPI	
IMP-06 (IMProved accident management)	• 7.8 mm break • Low HA pressure • LPIS	ECCS influence	Code/Input Added: LPIS	
Primary-to Secondary Leakage: PSL-10, PSL-11	Collector ruptures: 5.5 mm and 2.5 mm • HAs and HPIS • Pressurizer spray	Break	Input	• Break flow • Inventory redistribution • Primary to secondary heat transfer
Anticipated Transient Without Scram: ATWS-32	Simulation of control rod withdrawal, Power feedback • No ECCS	TH dynamic response to varying power	Code	• Inventory redistribution • High power natural circulation

Table 6: Initial and boundary conditions of the PACTEL validation experiments.

Experiment	Initial conditions		Boundary conditions	
	Primary	Secondary	Primary	Secondary
FLT-04, -08,-11	p = 0.1 MPa T = 25 °C	Not in use	Constant	Not in use
HL-22	p = 0.1 MPa T = 25 °C	p = 0.1 MPa	Power ramp up, stdst, cool-down	Constant
HL-23	p = 0.1 MPa T = 25 °C Prz. level = 4.5 m	Not in use	Power ramp up, stdst, cool-down	Not in use
LOF-10	p = 7.3 MPa	p = 4.0 MPa SG level = 0.712 m	Constant p Constant power 75 kW Flow rate	Constant p
SIR-21	p = 1.6 MPa	p = 0.3 MPa	Constant power 115 kW Six inventory reductions ~40 kg steps every 1000 s	Pressure Feed water
SIR-23	p = 7.5 MPa	p = 4.2 MPa	Constant power 115 kW Six inventory reductions ~40 kg steps every 1000 s	Constant p Feed Water
SBL-30	p = 7.31 MPa	p = 4.19 MPa	Constant power 160 kW 1mm break	Constant p
SBL-31	p = 7.46 MPa	p = 4.35 MPa	Constant power 160 kW 2.5 mm break	Pressure
SBL-33	p = 7.31 MPa	p = 4.26 MPa	Constant power 160 kW 3.5 mm break, HPI	Pressure
IMP-06	p = 7.3 MPa Core power 940 kW	p = 4.0 MPa	Core power, residual heat after initiation of 5.5 mm break 7.8 mm break, LPI	Pressure
PSL-10	p = 7.3 MPa Core power 1000 kW	p = 4.3 MPa	Core power, residual heat after initiation of 5.5 mm break, HPI	Relief valve openings
PSL-11	p = 7.3 MPa Core power 1000 kW	p = 4.3 MPa	Core power, residual heat after initiation of 2.5 mm break, HPI	None
ATWS-32	p = 5.8 MPa 50 kW	p = 2.9 MPa	Core power Pressurizer safety valve openings	Constant Feed water

4.2.1 Initiation and termination of the experiments

Usually, the data acquisition period in all PACTEL experiments was initiated with a 1000 s steady state period. This time period was recorded in order to impose distinct initiation conditions to post-test code calculations. Then, the actual transients were initiated. In the LOCA experiments, the transient contains the opening of the break valve, and if pumps are running, the pump coast down begins simultaneously.

The termination criteria of the experiments were defined beforehand. One main criterion was the core outlet temperature limitation to 300 °C. In some tests, the termination criterion was defined according to the appearance or nonappearance of the phenomenon within the set time limitation.

4.2.2 Loss-of-feedwater

Loss-of-feedwater experiment LOF-10 was a single loop test where low core power was used throughout the experiment. Thus, the test did not simulate the actual loss-of-feedwater transient; it was a boil-off experiment. However, the test data were useful for the verification of the steam generator models used in thermal hydraulic computer codes. Only one primary loop was used (Loop 3) in the experiment. The primary loop isolation valves in the other two loops were closed. Although the pressurizer was connected to Loop 1, it was operable because the pressurizer surge line connection is located before the isolation valve in the direction of the loop flow.

Initially, the water level on the steam generator secondary side was above the entire heat exchange tube bundle. The primary circulating pump was running during the equilibrium. After 1000 seconds, the pump was stopped, and no feedwater was injected to the secondary side. The pressurizer heaters were used to maintain the primary pressure. No operator actions were taken during the test. The experiment was terminated at 16000 seconds. At this point, the four upmost rows had dried out. The heating power in this test was 75 kW, corresponding to 1.5 % power in the reference reactor. Table 7 lists the initial conditions in LOF-10.

Table 7: Initial conditions in the LOF-10 experiment.

Parameter	**Value**
Core power	75 kW ± 5 kW
Upper plenum pressure	7.3 MPa ± 0.03 MPa
Secondary side pressure	4.0 MPa ± 0.02 MPa
Level in SG	71.2 cm ± 1.5 cm
Core outlet temperature	255 °C ± 3 °C
Loop mass flow rate	4.99 kg/s ± 0.15 kg/s

The oscillating secondary pressure caused a fluctuation of ± 2 °C in the temperature measurements. The steam flow rate through the secondary side pressure control valve was so low that the control valve opened and closed periodically.

The secondary side collapsed level was determined with a differential pressure transducer between the bottom of the steam generator secondary side and the steam line. Due to the periodical steam flow, there was an oscillating dynamic component in the pressure difference. This caused oscillation to the collapsed level measurement of approximately ± 2 cm on the secondary side.

When the main circulating pump was halted, the natural circulation flow was established. The loop fluid temperatures reached a re-equilibrium. The constant temperatures were observed until the uppermost layer of heat exchange tubes in the steam generator secondary side uncovered; that is, the swell level on the steam generator secondary side dropped below these tubes. The temperature measurements in the uppermost tube layer showed how the heat transfer started to degrade and the tube row was eventually uncovered. The temperature distribution in the tube became almost uniform, which suggested that the heat transfer from the primary to the secondary side was lost, as expected.

The uncovering of tube rows is clearly visible in CL temperatures, which jump up at every uncover event. When the uppermost layer of tubes in the steam generator secondary side was no longer covered by water, steam on the secondary side started to superheat. At the end of the experiment, steam in the top of the steam generator secondary side was about 10 °C superheated.

The LOF-10 test results revealed new horizontal steam generator features. The steam generator temperature measurements indicated that the internal circulation in the heat exchange tubes had changed when the secondary side level dropped (Hyvärinen, 1996a; Kouhia and Puustinen, 1998). The explanation for this behaviour was the changing pressure head of the collectors. When the whole tube bank was covered, the density was higher in the cold collector. The pressure difference introduced reversed flow in the lower part of the heat exchange tube bundle. Hot liquid emerged to the top of the cold collector when the upper part of the tube cluster started to uncover, and the driving force for the flow reversal decreased. The measurements suggested reversed flow in the lowest tube layer until the end of the experiment.

4.2.3 **Stepwise Inventory Reduction**

The main purpose in the stepwise inventory reduction experiments, SIR-21 and SIR-23, was to study the natural circulation behaviour with different primary inventories (Semken and Tuunanen, 1996). Only one of the three primary-side loops of the PACTEL facility (Loop 3) was used. The experiment SIR-23 was carried out at the nominal PACTEL primary pressure of 7.5 MPa and in the experiment SIR-21 at the pressure of 1.6 MPa. As a standard procedure, the pump was stopped after 1000 s, and

natural circulation flow began. Just before 2000 s, the pressurizer was isolated from the rest of the facility. Almost simultaneously with the pressurizer isolation, the first draining was initiated with roughly 40 kg of primary coolant reduction. This procedure was continued with five additional drains with every 1000 s and with approximately 40 kg reduction at each time. The recording of the experiments was terminated at 8000 s on the inventory of approximately 30 %.

All the natural circulation modes, single-phase, two-phase and boiler-condenser modes were observed. Due to hot leg loop seals, two-phase and boiler-condenser are intermittent.

4.2.4 **Small Break Loss-of-Coolant Accident experiments**

SBL-30

In the SBL-30 experiment, all three loops of the PACTEL facility were in use. The SBL-30 focused on the behaviour of new Large Diameter Steam Generator (LDSG), and it was a comparison experiment for SBL-7, which was carried out earlier with the Full Length Steam Generators (FLSG) (Puustinen, 2002). The main circulation pumps were not running during the whole recording period of the SBL-30 experiment; hence, all the flows were induced by natural circulation. In the beginning of the experiment, the primary side flows were single-phase natural circulation. The initial primary and secondary side pressures were about 7.4 MPa and 4.2 MPa, respectively. The core power set-point was 160 kW. The secondary side inventory was held as constant as possible during each experiment. A steady-state period of 1000 s was recorded before the transient phase began. The initial conditions of the SBL-30 experiment before the opening of the break are presented in Table 8.

Table 8: Initial conditions in the SBL-30 experiment.

Parameter	
Primary pressure [MPa]	7.31
Secondary pressure [MPa]	4.19
Loop 1 / Loop 2 / Loop 3 [kg/s]	0.44 / 0.43 / 0.46
SG1 / SG2 / SG3 feed water flow [l/min]	1.97 / 0 / 1.97
Core inlet temperature [ºC]	257
Core outlet temperature [ºC]	269
Pressurizer level [m]	5.2
SG1 / SG2 / SG3 level [cm]	69.2 / 79.1 / 78.3

There was no ECCS in use in this experiment. The break was located vertically at the bottom of Loop 2 cold leg near the downcomer. A sharp-edged orifice (1 mm diameter) simulated the break. The flow area of the orifice in this experiment corresponded to 0.04 % of the PACTEL cold leg cross-sectional area. Due to the scaling method used, this break size corresponds to 0.1 % in the reference reactor.

The operators controlled manually the feedwater flow to the steam generators. The purpose was to keep the collapsed level constant at the set point of 75 cm. Therefore, the control method was the on/off procedure.

The transient was initiated by opening the blowdown valve downstream of the break orifice. At the same time, the pressurizer heaters were switched off. The pressurizer was disconnected from the rest of the primary system as the break was opened by closing an isolation valve in the pressurizer line. The experiment was terminated when the primary circuit liquid inventory was depleted to the point where the core outlet temperatures started to rise. The cladding temperature exceeded 300 °C at 12301 s, and the experiment was terminated. At the time of the experiment termination, the remaining primary inventory was approximately 25 %. During the primary depletion, all natural circulation modes were observed.

The SBL-30 experiment revealed that the new LDSG design had some effect on the natural circulation behaviour on the local scale, that is, in the SGs themselves and in the loop seals below them. More loop seal clearings and refillings could be observed in SBL-30 than in the reference experiment SBL-7.

The effects on the overall system behaviour were, however, minor. The slightly inclined tube bundles of the new SGs facilitated the flow of the condensed coolant back to the collectors and loop seals. Thus, more facilitated flow caused the intermittent flow peaks observed in SBL-30 than in the reference experiment SBL-7, where the tubes were not inclined.

SBL-31

The experiment SBL-31 was a rehearsal of the feed and bleed procedure, which is an operator action in a LOCA in a power plant and whose function would be simulated later in the boron dilution experiments. In SBL-31, PACTEL operators studied also the performance of the second hydro-accumulator (HA), which was installed before the experiment series. The break was located vertically at the bottom of Loop 2 cold leg near the downcomer. A sharp-edged orifice (2.5 mm diameter) simulated the break. The flow area of the orifice in this experiment corresponded to 0.22 % of the PACTEL cold leg cross-sectional area.

In SBL-31, increased natural circulation mass flow rates were measured in the two-phase flow regime. The peak two-phase flow rate was double the single-phase liquid flow rate. This phenomenon was not observed in the other experiments of the series. Increased mass flows at reduced inventories in the VVER geometry have been reported before only in single loop experiments. Hence, the results of SBL-31 contradict the findings of the earlier multiple loop experiments. However, no hydro-accumulators were used in the earlier experiments.

In SBL-31, a secondary side feeding and bleeding operation was performed at 30 minutes after the break by manually opening the control valves in the steam lines and by increasing the feed water flow to each steam generator in order to simulate the actual operator action in a real plant. The experiment was terminated at 10000 s when the primary pressure had decreased below the low pressure injection system (LPIS) head of 0.7 MPa. The LPIS was not actuated in this test. At the time of the experiment termination, the remaining primary inventory was approximately 25 %.

SBL-33

The break was located vertically at the bottom of Loop 2 cold leg near the downcomer. A sharp-edged orifice (3.5 mm diameter) simulated the break. The flow area of the orifice in this experiment corresponded to 0.44 % of the PACTEL cold leg cross-sectional area. Due to the scaling method used here, the break size corresponded to 1.5 % in the reference reactor.

In SBL-33, the two hydro-accumulators (HA) were in use. Also, the high pressure injection system (HPIS) was in use, and it was actuated when the pressurizer level decreased below 2.8 m.

In SBL-33, the time span between the start of the boiler condenser mode and the drop of the primary pressure below the LPIS head was over 2500 s. This long condensation period was a result of the fact that with the used 3.5 mm break size, the hydro-accumulator injection ceased before the secondary side feed and bleed operation began.

The experiment hence verifies the conclusion of the RELAP calculation of the reference reactor that the break sizes in the range of 1.5 % of the cold leg flow area are favourable for the inherent boron dilution mechanism to occur almost at the maximum effect. The inherent dilution mechanism has been described and discussed in detail by Hyvärinen (1993). The total amount of condensed (boron free) coolant generated in SBL-33 was 177 kg. This estimate was calculated with the help of the secondary side measurements. The experiment was terminated at 6000 s when the primary pressure had decreased below the LPIS head. The LPIS was not actuated in this experiment. At the time of the experiment termination, the primary inventory was approximately 30 %.

4.2.5 **IMPAM VVER T2.3 counterpart experiment**

One PACTEL validation case was chosen from test included in the EC project “Improved Accident Management of VVER nuclear power plants” (IMPAM-VVER). The research activities in the IMPAM VVER project included an experimental investigation using PMK-2 and PACTEL test facilities and pre- and post-test analyses of the experiments using advanced codes. The calculations were performed with thermal-hydraulic system computer codes APROS, ATHLET, CATHARE and RELAP.

In some VVER small break LOCA scenarios it has been found out that there may be problems to depressurize the primary system enough in order to allow the emergency core coolant injection from the low-pressure system. The main objective of this project is to investigate which means and criteria for starting depressurization measures, like feed and bleed, would be most efficient. It will also assess whether the computer codes can adequately predict important phenomena, like the effect of steam generator reverse heat transfer at low primary inventories and at high temperature core processes.

The PACTEL test IMPAM VVER T2.3 (IMP-06) was chosen to be a counterpart test for the PMK-2 facility test. The accumulator pressure was reduced to 3.5 MPa, and the amount of water in the accumulators was increased. The special interest in this test was whether the system pressure reaches the head of LPIS pumps of 0.7 MPa earlier than the core overheating occurs.

The transient was initiated by opening the break valve. The flow area of the 7.8 mm break orifice in this experiment corresponded to 2.19 % of the PACTEL cold leg cross-sectional area. Due to the scaling method used, this break size corresponds to 6.04 % in the reference reactor. At the same moment, scram was also initiated (simulation of decay heat power), and the pressurizer heaters were switched off as well as the main circulation pumps tripped with linear coast-down (lasted 150 s). The secondary side feedwater had been stopped before the break initiation. When the primary pressure decreased below the LPIS head of 0.7 MPa, the LPIS was actuated at 1490 s. The experiment was terminated when the primary circuit liquid inventory was depleted to the point where the core outlet temperatures started to rise at 2464 s. The primary pressure at this point was 0.5 MPa. At the time of the experiment termination, the primary inventory was approximately 25 %.

4.2.6 **Primary-to-secondary leakage**

In both units of the Loviisa Nuclear Power Plant, the construction of the steam generator primary collectors cover has been changed so that if the steam generator collector lid lift-off occurs, the leak flow area will reduce significantly. The cover of the steam generator primary collectors has been replaced with the new cover being furnished with leak restrictors and rings restricting the elevation of the cover. New graphite seals have been installed in the cover to replace the original nickel ring seals. The leak restrictor restricts the leak of coolant into the secondary circuit in the event of damage to the head, thus also restricting the release of radioactive materials into the environment. The largest possible leak size has been reduced to approximately 20 % of the original [STUK, 2007].

The maximum possible flow area will correspond to a rupture of five to six heat exchange tubes. To investigate the effect of the new construction on system behaviour, two primary-to-secondary leak (PRISE) experiments were performed on the PACTEL facility in November 1999.

The first experiment, PSL-10, simulated the original leak area. The second experiment, PSL-11, simulated the reduced leak area. The experiment procedures were based on the current Emergency Operating Procedures (EOPs) in the Loviisa nuclear power plant. The experiments focused on reducing the primary pressure and temperature with fast cooling according to the EOPs that the primary pressure stays below the opening pressure of the steam generator safety valve and the boiling margin in the core is more than 20 °C.

In each experiment, all three steam generators were used: two intact and one broken steam generator. The intact steam generator steam lines were coupled. The main isolation valves in the primary circuits were presumed to be stuck open, which prevented the broken loop isolation. The pressurizer spray and the accumulators were used in all the experiments. The collector construction in PACTEL differs from the prototype; hence, the uppermost heat exchanging tube row was chosen as a break location.

The transients were started by opening a break valve in a heat exchanging tube of the broken loop steam generator. Using volumetric scaling to the full-scale break sizes, the break size Ø 5.5 mm in PSL-10 and Ø 2.5 mm in PSL-11 was chosen. Simulating scram the core power was decreased from 1 MW to 344 kW when the collapsed level in the pressurizer reached 2.8 m. After that the core power followed the decay heat power. When the pressurizer collapsed level reached 2.3 m, the pressurizer heaters were switched off, the main circulation pumps started to coast down and the high pressure injection was initiated.

In PSL-11, the process was slower, and the actions did not begin until after 40 s from the core power reduction. The temperatures on the primary side decreased because of the core power reduction and the HPI. The decreased loop flow reduced the heat transfer between the primary and the secondary side of the facility. Then, the steam generation rate on the secondary side decreased. The secondary side pressure dropped until the pressure control system totally closed the control valve of the secondary side.

The main steam isolation valve of the broken steam generator was closed, and feed water injection into the broken steam generator was terminated at 1150 s in PSL-10 and 245 s later in PSL-11. As the operator intervention, the relief valve in one of the intact steam generators was opened. The collapsed levels in the intact steam generators were maintained by the feed water flow. Also, the pressurizer spray was started. These actions dropped the pressure in the intact steam generator. The pressure in the broken steam generator reached soon the opening pressure of the relief valve. In PSL-10, the safety valve of the broken steam generator cycled few times and released the secondary side inventory to the atmosphere. In PSL-11, the safety valve openings did not occur.

The accumulator injection was turned off in PSL-10 at 2030 s. In PSL-11, they did not inject at all because the boiling margin in the core was more than 10 °C when the

injection was supposed to begin. The HPI was stopped at 2670 s in PSL-10 and 170 s earlier in PSL-11 to prevent losing steam volume in the pressurizer.

These two experiments demonstrated that with reduced collector cover flow area, it is possible to manage the primary-to-secondary leakage without unwanted discharge from the safety valve in the damaged steam generator.

4.2.7 **Anticipated Transient Without Scram**

The PACTEL anticipated transient without scram experiment chosen as the validation case was ATWS-32. The experiment simulated the control rod withdrawal from the core when the core was initially operating with low, almost zero power. The core power was then promptly increased to the maximum value. A special core power feedback control system was developed, which could respond to the changes in the core void fraction. The aim of the experiment was to study slow steam compression and the overall behaviour of the facility. The experiment was performed with all three loops running. None of the primary side ECC systems were in use.

The facility was operating with 1 % core power (about 50 kW). After 1000 s, the core power was raised rapidly to the maximum available power (1 MW). The core power feedback was modelled also. Simultaneously, the steam generator feedwater injection rate was set to a constant value of 1.25 litres/min in each steam generator corresponding to the capacity of one emergency feedwater pump in the Loviisa NPP. Automation controlled the pressurizer heaters.

When the core power increased to the maximum, the average temperature of the primary side increased approaching the level corresponding to the new heat balance. However, the core outlet temperature did not reach the saturation temperature. The primary coolant volume expanded because of the increasing average temperature, which increased the pressurizer collapsed level.

The secondary side feedwater injection into the steam generators could not compensate the high evaporation rate on the secondary sides. Thus, the secondary side collapsed levels decreased. When the water level in steam generators had reached 54 cm, all main circulation pumps began to coast down. Then, the single-phase natural circulation flow was initiated, while the core power was still remaining high.

When the main circulation pumps coasted down and the heat exchanging tube layers in the steam generators uncovered steadily, energy transport from the core to the steam generators degraded. This caused the primary pressure increase and the pressurizer safety valves to open.

In the ATWS-32 experiment, three valves were used for the operation of the pressurizer safety valves. The two small diameter valves of Ø3 mm operated as the pressurizer

safety valve. The large capacity valve of Ø17 mm operated as a pressure cut-off valve. There is no corresponding valve in the power plant.

Due to valve openings, the primary inventory was depleted promptly. The collapsed level in the upper plenum was decreased below the hot leg connection, and all the safety valves closed at 3150 s. The natural circulation changed from single-phase to two-phase flow. Hot leg loop seals in Loop 2 and Loop 3 were clear, and steam could flow up towards the steam generators. Loop 1, to which the pressurizer is connected, was stagnated.

From 2720 s to 6980 s, the core power remained at 1 MW. From 6980 s onwards, the primary inventory depletion led to voiding in the core. The control system with core power feedback started to act according to the changes in core voiding. The primary system began to oscillate. Because of the time constants of the core power control system, there was a 5 s–8 s delay between the set point and the measured core power. This was about half of the whole cycle. Therefore, the core power was all the time in the phase where it amplified the primary system oscillation process. Oscillations continued to the end of the experiment. The timing of the main events in the ATWS-32 experiment is presented in Table 9.

Table 9: Timing of main events in experiment ATWS-32.

TIME [s]/signal	**EVENT**
1000	Core power rises promptly to max. value (1 MW). Feedwater set to 1.25 l/min for each SG
2720 / SG collapsed level < 54 cm	All main circulation pumps start to coast down ⇒ Flow stagnates in Loop 1 ⇒ SG1 level stops decreasing
2920	Pressurizer safety valves started to operate: two Ø3 mm valves and one Ø17 mm valve
3150	All safety valves were closed The collapsed level in the upper plenum was below the hot leg connection
4508	Hot leg loop seal in Loop 1 cleared: flow resumed ⇒ The SG 1 level began to decrease.
6980	Control system of the core power started to act according to the changes in core voiding
10410	SGs almost empty: Only one tube layer (with three tubes) covered with water
12000	Experiment terminated

5 TRACE modelling and validation

The TRACE model construction of the PACTEL facility and validation work has been carried out mainly with the support of Finnish national nuclear safety research programs (SAFIRs). The TRACE code usage in Finland has been required by the Finnish Radiation and Nuclear Safety Authority, STUK, because they need an independent tool to support safety and licensing analysis. The use of the TRACE code enhances the preparedness to give analyses support and improves the education in computational thermal hydraulics.

This work was aimed to develop a complete PACTEL simulation model with the TRACE code and use the model for experiment planning and for pre- and post-test analyses at Lappeenranta University of Technology (LUT). A full calculation model of the TRACE code for the PACTEL facility with horizontal steam generators was developed. The input development contained 15 validation calculations according to the specific PACTEL validation matrix. Additionally, this work has produced a basis for the TRACE model of the PWR PACTEL facility.

5.1 The TRACE code

The TRAC/RELAP Advanced Computational Engine (TRACE—formerly called TRAC-M) is the latest in a series of advanced, best-estimate reactor system codes developed by the for analysing the transient and steady-state neutronic-thermal-hydraulic behaviour in light water reactors. It is the product of a long term effort to combine the capabilities of the NRC's four main system codes (TRAC-P, TRAC-B, RELAP5 and RAMONA) into one modernized computational tool (TRACE Theory Manual, 2013).

The TRACE code has been designed to perform best-estimate analyses of loss-of-coolant accidents (LOCAs), operational transients and other accident scenarios in pressurized light-water reactors (PWRs) and boiling light-water reactors (BWRs). It can also model phenomena occurring in experimental facilities designed to simulate transients in reactor systems. The models used include the multidimensional two-phase flow, non-equilibrium thermo-dynamics, generalized heat transfer, reflood, level tracking, and reactor kinetics. Automatic steady-state and dump/restart capabilities are also provided.

In the TRACE documentation, there is no particular reference or mention about the TRACE code applicability to model the VVER reactor type. Thus, the TRACE code is not especially designed for VVER modelling. The assessment matrices contain a large variety of different phenomena, and the main test facility results used for the validation are PWR test facilities with vertical steam generators like ROSA-IV and BETHSY.

The partial differential equations that describe the two-phase flow and heat transfer are solved using finite volume numerical methods. The heat-transfer equations are

evaluated using a semi-implicit time-differencing technique. The fluid-dynamics equations in the spatial one-dimensional (1-D) and three-dimensional (3-D) components use, by default, a multi-step time-differencing procedure that allows the material Courant-limit condition to be exceeded. The finite-difference equations for hydrodynamic phenomena form a system of coupled, nonlinear equations that are solved by the Newton-Raphson iteration method. The resulting linearized equations are solved by direct matrix inversion.

TRACE takes a component-based approach to model a reactor system. The thermal hydraulic components in TRACE include several components, for example PIPEs, VALVEs, PUMPs and HTSTR (heat structures), among others. With this selection of components, full reactor models can be built. The basic nodalization in TRACE is somewhat different from the formalism used in the RELAP5 code. The main difference is concerning the pipe bend modelling. The node of the PIPE component in TRACE is bended at the centre point of the node. The difference between RELAP5 and TRACE nodalization is presented in Figure 24.

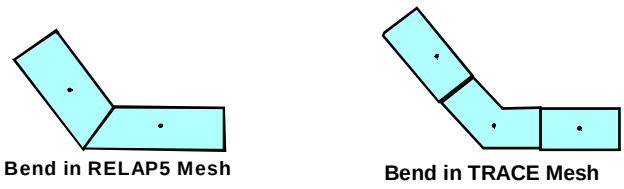

Figure 24: Differences between RELAP5 and TRACE meshing.

TRACE has three different options to solve the two-phase flow equations. Additional to the commonly used semi-implicit method, TRACE has a special improved scheme SETS with two separate options. In semi-implicit schemes, variables are expressed as suitable weighted averages of “old” and “new”. The linearization difficulty can be avoided by lowering the closure terms at the “old” level. If pressure solution is kept fully implicit, the time step is limited only by the material Courant limit $\Delta t < \Delta x/v$, which is often acceptable. Numerical diffusion is present, but much less than in the implicit scheme.

The Stability Enhanced Two-Step (SETS) method eliminates the material Courant limit by first solving a semi-implicit set to obtain intermediate new time step variables and then providing a ”stabilizer” step that uses the intermediate variables to correct the closure and/or linearized relations used in the semi-implicit step. This approach is claimed to provide speedups of up to orders of magnitude for slow transients. The cost of using SETS is high in numerical diffusion, which is inherent in this scheme but support of convergence as well. The default is to use SETS with some restrictions. Another option is SETS without any restrictions. The third option is the semi-implicit method.

5.1.1 **Special TRACE models**

The TRACE code contains a large number of special models, which are important in nuclear power plant thermal hydraulics. Some of the most relevant for the work with PACTEL experiment simulations are presented here; that is, the critical (choking) flow model, water level tracking model and offtake model. These models are described below because they are expected to have an influence on the selected PACTEL modelling cases.

Critical flow model

Critical (choked) flow can occur when the mass flow in a pipe becomes independent of the downstream conditions. Therefore, a further reduction in the downstream pressure will not change the mass flow rate. The reason for choking is that acoustic signals can no longer propagate upstream to affect the boundary conditions that determine the mass flow rate at the choke location. In various operation conditions of a nuclear power plant, the presence of the critical flow can play a significant role in how the plant responds during transients. The predicting of these phenomena during reactor safety simulations can therefore be crucial to achieve an accurate overall understanding of the scenario being simulated.

The critical flow model chosen for computer modelling, like in the TRACE code, has to predict, for a given cell edge, the conditions for which choked flow would be expected to occur. Then, by comparing the momentum solution predictions against these conditions, the code can determine whether the flow is actually choked at a particular cell edge and adjust the velocity and associated pressure derivatives accordingly. Because the predictions of the choking criteria are highly dependent upon the nature of the flow field at the cell-edge and upstream cell-centre, the critical flow model is three separate models in one:

- a subcooled-liquid choked-flow model,
- a two-phase, two-component choked-flow model and
- a single-phase vapour choked-flow model.

The subcooled choked-flow model is a modified form of the Burnell model and is almost the same as that used in RELAP5 (RELAP5 code manual, 2001).

The two-phase, two-component choked-flow model in the TRACE code is an extension of a model developed by Ransom and Trapp. The model assumes that a thermal equilibrium exists between the vapour and liquid phases. An additional inert-gas component and non-equilibrium effects are also possible (TRACE V5.840 Theory Manual, 2013). The single-phase vapour choked-flow model is based on the isentropic expansion of an ideal gas.

Many transient modelling cases include a leakage from the primary side to the atmosphere or to the secondary side. Also most transients in the PACTEL experiments are focused on break modelling situations. Critical or choked flow conditions are expected to take place when fluid is discharged from the primary system and undergoes a large pressure decrease. Choked flow can also appear in valves and throats when the flow area is changed abruptly. The TRACE code has special models available for the critical flow presentation.

The critical flow model in TRACE is implemented as an option. The TRACE code can check for critical flow at the connecting flow junction. To account for any geometry effects, the choked-flow model allows the user to input subcooled and two-phase choked-flow multipliers. Depending on the used choking model (either sub-cooled liquid, two-phase two-component fluid or superheated vapour), these multipliers allow the user to adjust the predicted liquid, steam/gas-mixture, or both, choking velocities to account for the break or nozzle geometry effects.

Water level tracking model

The use of an average void fraction for a computational volume can lead to an erroneous description of a computational volume when it contains a water level. The tracking of water levels is worthwhile in computer code formulations. The search for liquid-gas interfaces is conducted using a series of logical decisions that are based on empirical observations. Once it is determined that an interface exists inside a computational volume, its location inside the volume and its velocity are computed along with the separated sub-volumes. The level tracking method of TRACE consists of two parts:

- A decision making step to locate and follow the water levels and
- Modifications to the field equations and closure models to account for the presence of a water level.

A computational volume consisting of a liquid-gas interface is shown in Figure 25. A void fraction profile decreasing with the increasing height is the simplest case where a stratified interface must satisfy certain conditions between the parameters shown in this figure (TRACE Theory Manual, 2013).

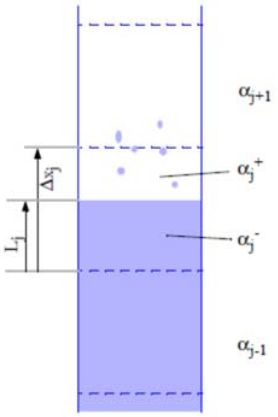

Figure 25: A computational volume with the stratified liquid-gas interface (TRACE Theory manual).

Offtake model

The TRACE offtake model is designed specifically to handle the case of fluid flow through a small break that is made in a larger pipe containing horizontal stratified flow. Such a modelling scenario may exist with the use of a TEE component or a PIPE, VALVE or PUMP with side junctions. One example of a transient that is particularly well-suited for use with the offtake model is a LOCA, in which a small break occurs in one of the large-diameter horizontal pipes of the reactor inlet or outlet legs. During this transient, horizontal stratified flow may occur, and the flow quality discharged at the break will depend on whether the break is above or below the liquid level. To accurately follow the progression of the transient, it is essential that the offtake flow is predicted correctly. The offtake model predicts the offtake flow quality that exits the break based on conditions in the main pipe. In each of the three offtake configurations presented in Figure 26, a critical height (h) at which the gas or liquid entrainment begins may be calculated using major-phase conditions at the entrance plane.

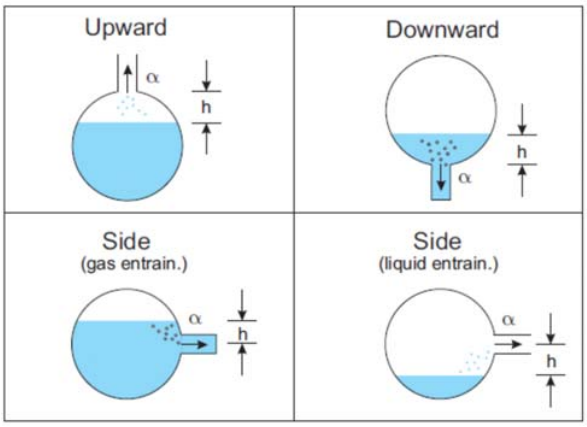

Figure 26: Possible offtake configurations and determination of critical height, h (TRACE Theory manual).

5.1.2 Limitations on use of TRACE code

As the developers of the TRACE code emphasize, a general rule, concerning computational codes like TRACE, is that the codes should only be applied within their assessment range. TRACE has been qualified to analyse the ESBWR design as well as conventional PWR and BWR large and small break LOCAs (excluding B&W designs). At this point, assessment has not been officially performed for the BWR stability analysis or other operational transients.

The TRACE code is not appropriate for modelling situations in which the transfer of momentum plays an important role at a localized level. For example, TRACE makes no attempt to capture in detail the fluid dynamics in a pipe branch or plenum or flows in which the radial velocity profile across the pipe is not flat. The typical system model cannot be applied directly to those transients, in which the thermal stratification of the liquid phase in the 1D-components is expected to be observed.

Approximations in the wall and interface heat flux terms prevent accurate calculations of such phenomena as the collapse of a steam bubble blocking natural circulation through a B&W candy cane like TMI-2 had or of the details of steam condensation at the water surface in an AP1000 core makeup tank (TRACE Theory Manual, 2013).

5.1.3 Uncertainty quantification in TRACE

The TRACE code has been equipped with Uncertainty Quantification (UQ) possibility for certain parameters. Any variable that a user can enter in the TRACE input model can be used in an uncertainty quantification (UQ) or sensitivity value (SV) analysis; the UQ input specified in this section of input refers specifically to the normally unseen and

unchangeable values present in the TRACE code itself. The TRACE code does not perform any UQ or SV functions itself. The term "Uncertainty Quantification" is used here only to denote the intended use of internal TRACE parameters that are exposed by this input. Currently, there are 38 sensitivity coefficients available in the TRACE modelling, for example liquid to interface bubbly-slug heat transfer and liquid to interface annular-mist heat transfer coefficient. This feature is limited to parametric uncertainty, and it has not been used in this work.

5.2 TRACE model of the PACTEL facility

The TRACE model of the PACTEL facility has been developed at Lappeenranta University of Technology. There was no particular experience of using the code previously. The model was constructed from scratch with the aim to cover finally all the main parts of the primary and secondary sides of the facility. The input model development and the main part of the validation work were carried out in the frame of the PACSIM project in the SAFIR research programmes. The modelling of the PACTEL facility with the TRACE code resembles the guidelines adopted in the RELAP5 modelling for PACTEL. At first, the used version of TRACE was 4.06. New versions have been adopted as they have become available. The latest version in use has been TRACE 5.0 patch 3. The TRACE modelling was conducted using Symbolic Nuclear Analysis Package (SNAP), which consists of a set of integrated applications designed to simplify the process of performing the thermal-hydraulic analysis. The model editor and animation tool of the SNAP applications were used to help in the TRACE model preparation.

The modelling work and validation calculations were carried out according to the novel V-model validation procedure presented in Chapter 2.

The construction of the PACTEL facility input model was started by creating the different parts of the facility and testing them separately. All main parts of PACTEL; the pressure vessel part, main circulation loops, steam generators and the pressurizer; were created and tested separately. The input creating procedure contains geometry definitions, the decision of nodalization formulation (density, location) and the degree of lumping needed.

The nodalization of the TRACE model was largely derived according to the guidelines approved for the RELAP5 input deck of the PACTEL facility (Riikonen et al., 1995; Virtanen et al., 1997). In some cases, exceptions in the TRACE nodalization following the RELAP5 nodalization had to be made. For example, the different approach between RELAP5 and TRACE in the handling of bending pipelines causes a totally different nodalization. The basic rule in the nodalization is that it should be in balance between coarse and fine nodalization. The nodalization has to be fine enough to be able to describe the essential changes throughout the system and coarse enough to perform the simulation calculation within a reasonable time frame.

At first, a stand-alone horizontal steam generator model was prepared. In this phase, different modelling options were tested against the loss-of-feedwater (LOF-10) PACTEL experiment. The main parameter defining the applicability of the model was the propagation of the collapsed level on the steam generator secondary side. The main used modelling options were the number of layers of the heat exchange tubes (14 in the facility). The first attempt was implemented with four rows to model the heat exchanger tube bank. The second phase was to increase the row number to five. The calculation results indicated that the proper modelling of the tube packages requires eight layers at the minimum to bring out the level behaviour similar to the experiment result. The stand-alone TRACE model of the PACTEL horizontal steam generator is presented in Figure 27.

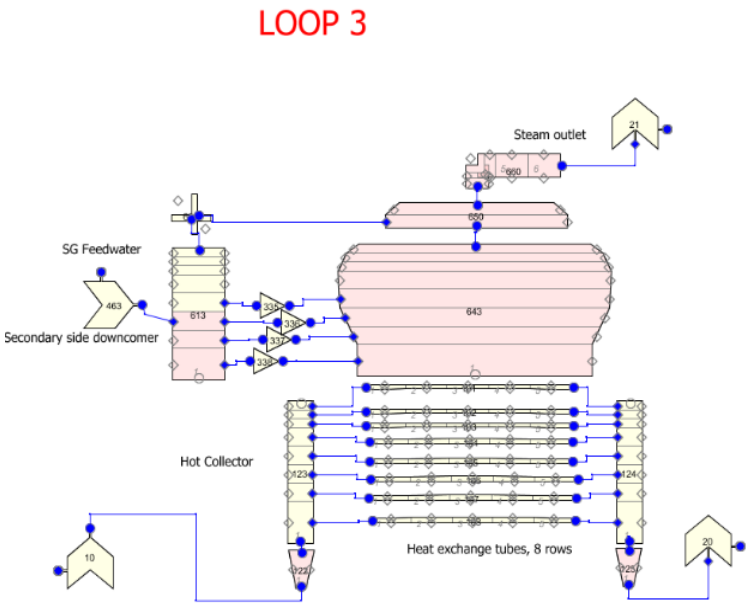

TRACE tubes vs. PACTEL

TRACE	PACTEL
Tube 1	Row 1
Tube 2	Row 2
Tube 3	Row 3
Tube 4	Row 4
	Row 5
Tube 5	Row 6
	Row 7
Tube 6	Row 8
	Row 9
Tube 7	Row 10
	Row 11
Tube 8	Row 12
	Row 13
	Row 14

Figure 27: Stand-alone TRACE/SNAP model of the PACTEL HSG. The model contains eight tube rows. Note TRACE tubing correspondence to PACTEL HSG (right).

The full model with all three loops was then constructed and modelled. The functionality of the model was tested with calculations of pressure and heat loss experiments. During the development process of the model, it was modified and expanded due to the needs of different validation cases. The model was also updated step by step according to the recommendations of the code developers.

The upper plenum part of the PACTEL facility has a diffuser structure, which consists of two nested concentric pipes preventing the direct flow of the ECC water from the hydro-accumulators (HA) or from the HPI system to the loops. For the TRACE

simulation model, a similar structure was built using two parallel pipes, which were connected together with single components. This modelling structure clearly improved the upper plenum behaviour especially during events with decreasing level. The similar structure exists also on the downcomer side of the PACTEL facility. This structure was modelled to the input. The pressurizer was modelled using a standard pipe component. The core section was divided into three parallel lines, and the heat production in the core as well as in the pressurizer heaters was implemented with POWER components, which can be controlled with time dependent functions and trips. As the primary tube bank in each horizontal steam generator is divided into eight rows, the three top rows represent one tube row of the real PACTEL facility. Other tube rows represent two rows of the real facility. The secondary side is divided into the riser and downcomer sections. It was found out in the modelling of the PSL experiment that the inner circulation in the steam generators seemed to be too strong. Hence, the amount of flow paths connecting the downcomer and riser parts was restricted, and the flow friction factors were increased to reach better behaviour on the secondary side. The final stage of the model is shown in Figure 28 representing the layout of the main parts of the PACTEL facility containing Loop 1 (SNAP, Model Editor). The other two loops and auxiliary systems are drawn in separate windows.

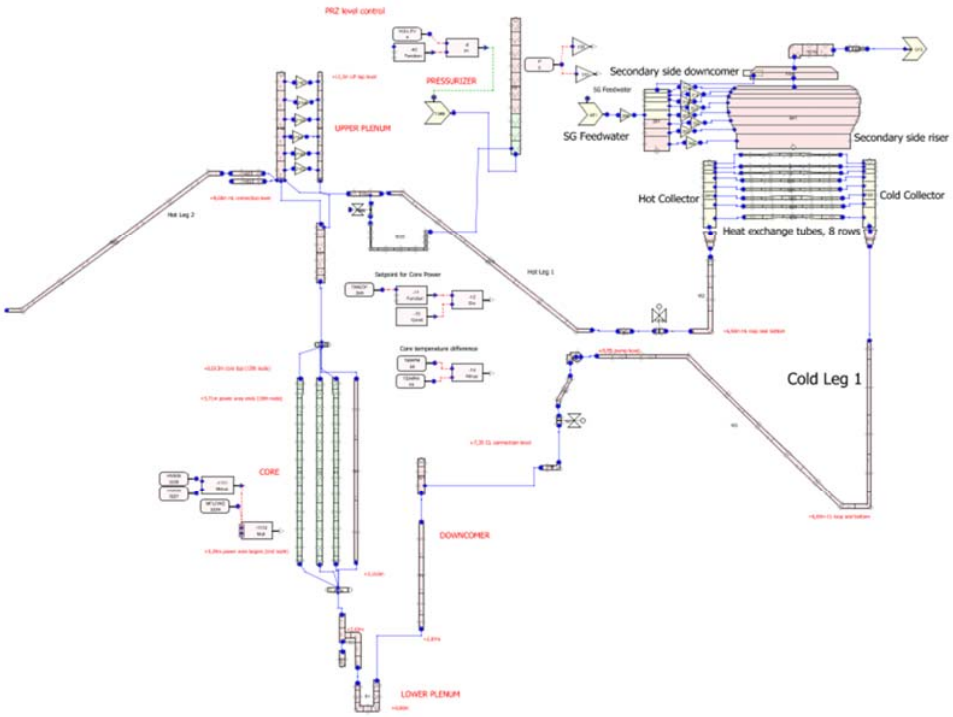

Figure 28: TRACE code model of the PACTEL facility. One of three loops visible.

In the SBLOCA experiments, the break flow was set to Cold leg 2 near the downcomer. The break orifice set-up was realized with a single junction component connected with a cross-flow junction to the cold leg. The break valve takes care of the break initiation and leads the flow to the break component, which acts as a pressure boundary (see Figure 29, left).

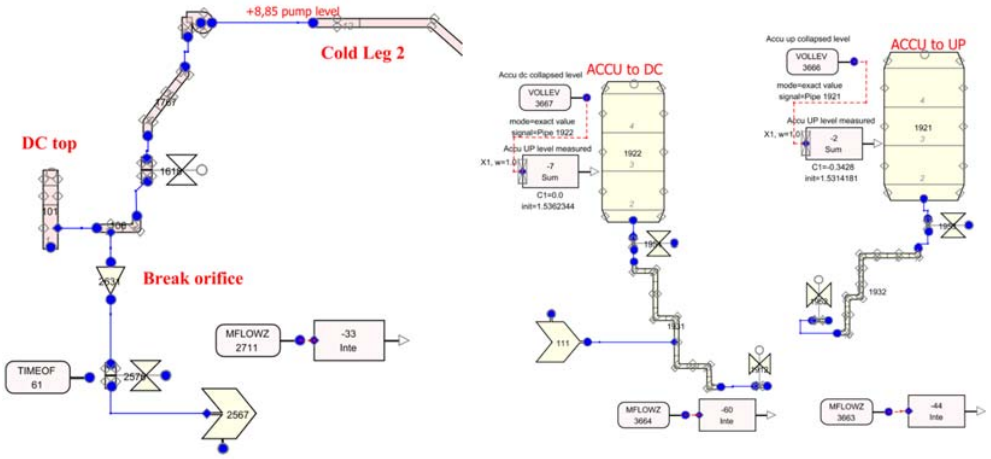

Figure 29: Break setup (left) and hydro-accumulators (right) presented by SNAP editor. LPIS (No.111) is connected to the downcomer injection line.

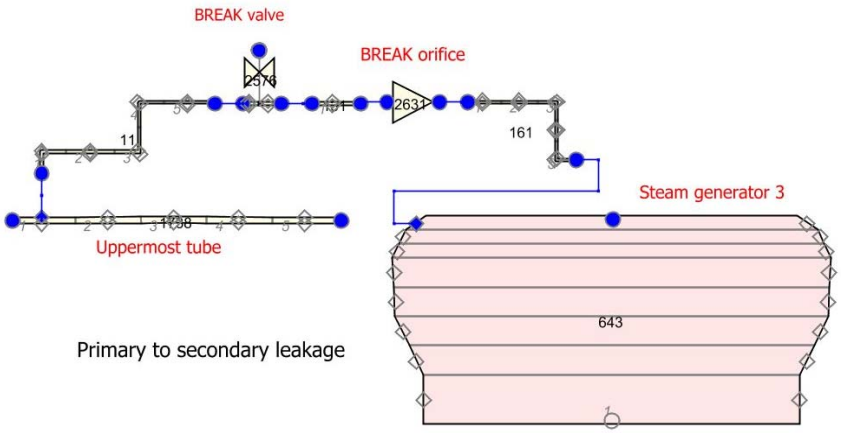

Figure 30: TRACE/SNAP break model set-up for primary-to-secondary leakage experiments.

The PACTEL facility has two hydro-accumulators, which were also modelled in the input (see Figure 29, right). The larger accumulator is injecting to the upper plenum and the smaller one to the downcomer. The TRACE code contains a special option in the PIPE component for introducing the hydro-accumulator. With this option, the water level and water discharge can be defined. It has also the implementation of an interface sharpener. The initial level is set using the partial pressure of non-condensable gas fraction.

The break in the simulation of PRISE experiments was implemented with a single junction component, which simulated the break orifice. A break valve was also modelled to initiate the break correctly. In the primary-to-secondary leakage (PSL) experiments, there was not any other indicator than pressure to check the break flow correctness since the break flow rate was not recorded in the experiments. The break setup used for the modelling of PSL-experiments is presented in Figure 30.

5.3 Validation case results

During the model construction and validation processes, all 15 experiments in the PACTEL validation matrix were calculated. In this section, all validation case results are presented generally, and more specific issues and finding are discussed separately.

5.3.1 General trends

In the following sub-sections, the validation case results are presented generally. The comparison of calculated and experiment results are presented and discussed.

5.3.2 Pressure loss simulations

The pressure losses were defined separately for the different parts of the full TRACE model. At this phase, the model nodalization was rechecked to correspond to the locations of the pressure difference measurement taps. As stated in the staggered grid method, the pressure is implemented into the centre elevation of the node. The exact match of the locations of the measurement in the facility and in the calculation model was not possible in all cases since the node length would have become too short and caused time step problems. In most cases, the correspondence of the locations in the facility and in the model was accurate.

The actual procedure with the code model was similar to the procedures that were carried out with the experiments. Similarly, all main parts in the input model were calculated separately. The basic adjustment was done according to the highest mass flow rate in the experiment. The local form loss factor was changed in the location where pressure losses naturally appear, that is, in valves, flow area change points or pipe bends. In the TRACE code it is possible to set loss factors to both normal and reverse flow directions separately. When the necessary accuracy of the adjustment in one measurement point was achieved, the mass flow rate was changed according to the

measurement data point. All the measured pressure differences were adjusted to the TRACE code model, where they were applicable.

An example of the pressure difference adjustment in both normal and reverse flow directions over the core region is presented in Figure 31. Generally, the calculated form loss adjustments agreed well with the experiment results as found in the normal flow direction case of Figure 31, left. However, it was found out that the curve shapes were not matching each other like in the reverse flow case (see Figure 31, right). The core region of PACTEL has multiple flow paths, and it has a more challenging geometry than the normal pipeline. In cases similar to Figure 31 (right) presented with a large deviation between the experiment and calculation, the adjustment procedure was changed. To achieve a better correspondence in the normal experiment conditions, where the flow rates are usually below 10 kg/s, the normal flow direction adjustment was carried out according to the mass flow point at the halfway of the total range. Thus, the calculated pressure loss was less deviated from the experiment result at the low flow rates.

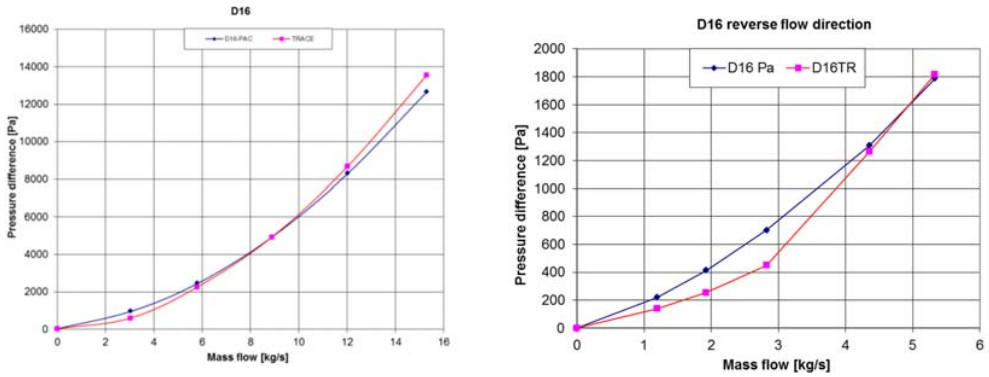

Figure 31. Pressure losses versus mass flow rate over the core (D16) in the PACTEL facility measurements and in the TRACE model calculations in normal (left side) and in reverse flow (right side) directions.

5.3.3 Heat loss simulations

The heat losses for the PACTEL facility were defined using the heat-up and cool-down method. The heat losses for the TRACE model of the PACTEL facility were defined using the cool-down method only. The heat-up procedure contained operator actions that could not be reproduced in the calculation without having very large uncertainties in the procedure. The pressurizer heat losses were defined with separate test calculations. The singular heat losses were adjusted according to the data from ISP-33, and the pump heat losses from a separate data. The overall heat losses were verified against the data from PACTEL experiment HL-22. The main varied parameter used for the adjustments was the thermal conductivity of the insulation material. Several user

defined materials were created to set the heat loss distribution in detail. The heat losses of the primary circulation pumps are large, almost one third of the total heat losses at the nominal PACTEL conditions. The pumps are not insulated, and thus the casing material was used for heat loss adjustment.

The calculated results deviated from the experiment results to some extent. A probable explanation for the differing results could be as follows. In the experiment, the heat transfer from the primary to the secondary side was minimized by filling the secondary side with air. In the calculation, the heat transfer from the primary to the secondary side during the steady state was about 300 W. This could not be verified in the experiment since the temperature difference between the inlet and outlet varied within 2 ºC being the accuracy limit of the measurements. Also, the magnitude of inner circulation at upper plenum was one unknown factor. Despite the problems and quite large uncertainties, the overall heat losses could be defined with agreeable accuracy. Figure 32 presents the measured and calculated temperature in the core during the cooling down of the facility. The temperatures indicate that in the TRACE code calculation, the cooling rate is too fast compared to the experiment.

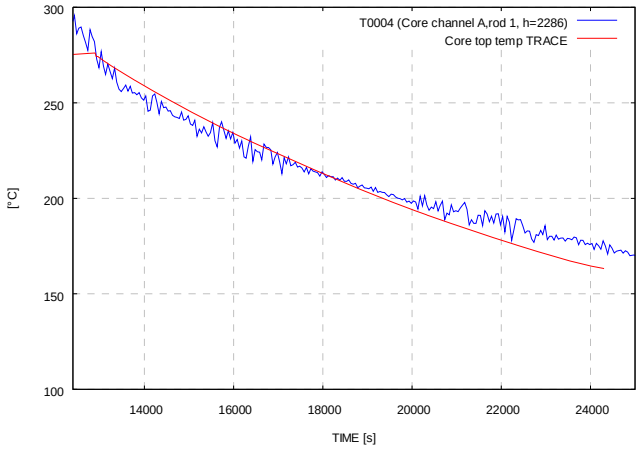

Figure 32: Core temperature propagation in the experiment HL22 and in the calculation of the TRACE code presenting the facility cool-down.

5.3.4 **Loss-of-Feedwater simulation**

The Loss-of-feedwater experiment, LOF-10, was chosen to give information for the TRACE model preparation of the PACTEL horizontal steam generator. The actual transient calculation was a restart calculation from the stabilizing calculation. The transient calculation followed the experiment procedure. After the 1000 s steady state period, the primary flow was changed simulating the pump stopping and the beginning of natural circulation in the experiment. Hence, at this point, the primary inlet flow in the calculation was changed from 5 kg/s to 0.63 kg/s through a short, almost stagnated,

period. The primary side inlet temperature was also let to change at this moment according to the experiment data. These moments expressed the initiation of natural circulation flow. In the four pipe model, constant boundary conditions for pressures were used. In the eight pipe model, the variation of both primary and secondary side pressures were implied to the boundary condition components and taken from the exact experiment data. Since no feedwater was injected after 1000 s from the beginning, the water on the secondary side started to boil-off, and the level started to decrease as in the experiment. Figure 33 presents a comparison between the evolutions of the secondary side collapsed levels in the calculation cases with four and eight tube layers and in the experiment. The node boundaries in the riser part of the steam generator model both in the four and eight pipe layer models are illustrated in the graph. The calculated levels agreed well with the experiment until 5000 s. Thereafter, the four pipe case differed from the experiment more than the eight pipe case that remained quite close to the experiment. In the four tube layer model, the uppermost pipe corresponded to three layers of tubes in the PACTEL steam generator. At the end of the transient, the discrepancy of the collapsed levels from the experiment was approximately 7 cm in the four pipe case and almost equivalent with the experiment in the eight pipe case. Similar level behaviour in the eight tube layers model suggests that heat transfer is correctly modelled.

The two-phase level tracking model was introduced and set on for the secondary side riser component and tested in the eight pipe model, but it did not bring any significant improvement to the calculations results.

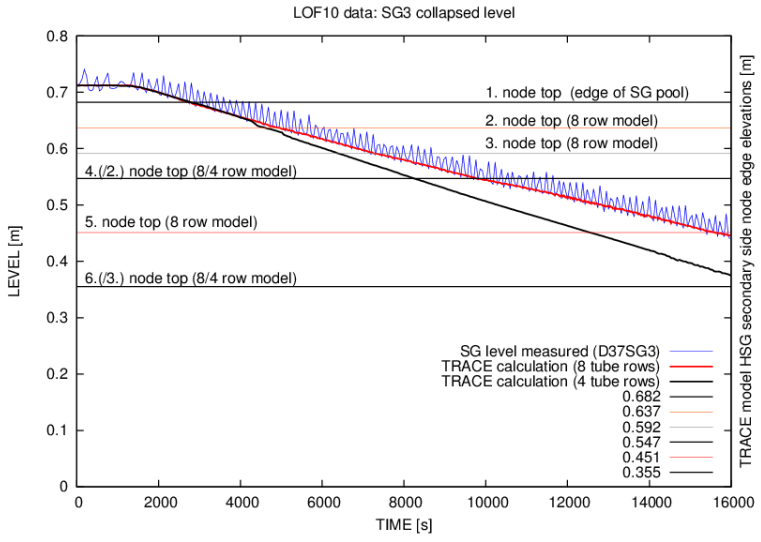

Figure 33. Measured and calculated collapsed level in steam generator. Experiment LOF-10 vs. TRACE calculation. Four and eight tube layers. The secondary side node top edge elevations are also indicated here.

When the steam generator level depletion continued, the primary to secondary heat transfer degraded further. Thus, this was indicated in the rising trend of the primary side outlet temperature. The calculation showed stepwise behaviour when the temperature jumped up after the node dry out. The calculated outlet temperature (cold leg) was overestimated more than 1 ºC resulting in lower heat transfer (~5 % difference) than in the experiment (Figure 34). This contradicts the previous observation concerning heat transfer accuracy and level behaviour.

The calculated primary side temperature at the uppermost tube layer was almost similar to the experiment (see Figure 35). At 5000 s the calculated temperature jump was observed almost at the same time as in the experiment. The calculated temperature increased more rapidly, and the jump was higher than in experiment. Therefore, the temperature rise was merely a sign of the local heat transfer degradation from the primary to the secondary side.

When the uppermost tube layer started to uncover in the experiment, the heat transfer started to degrade simultaneously at 5000 s and was uncovered at 5500 s. When the uppermost layer of tubes in the steam generator secondary side was no longer covered by water in the experiment, steam on the secondary side started to superheat (see Figure 36). In the calculations, the superheating of the steam was possible only after the uppermost cell on the secondary side had voided thoroughly. In the eight pipe case, the superheating of the steam started almost simultaneously with the experiment, but with stepwise manner, and it was even slightly overestimated.

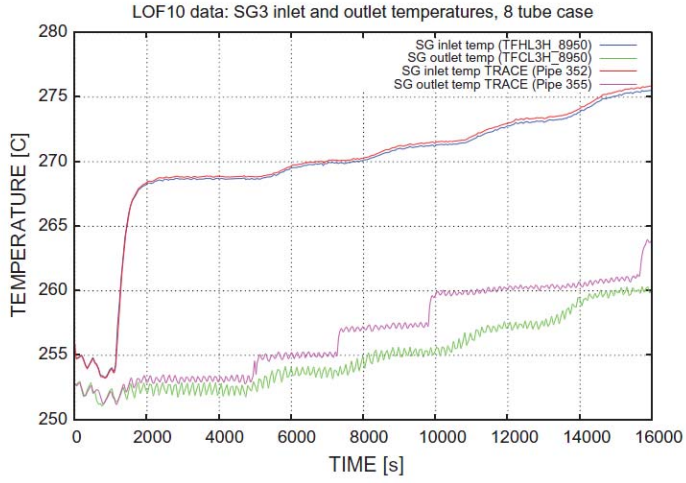

Figure 34: Primary side inlet and outlet temperatures in the experiment and in the TRACE calculation with the eight pipe layer model.

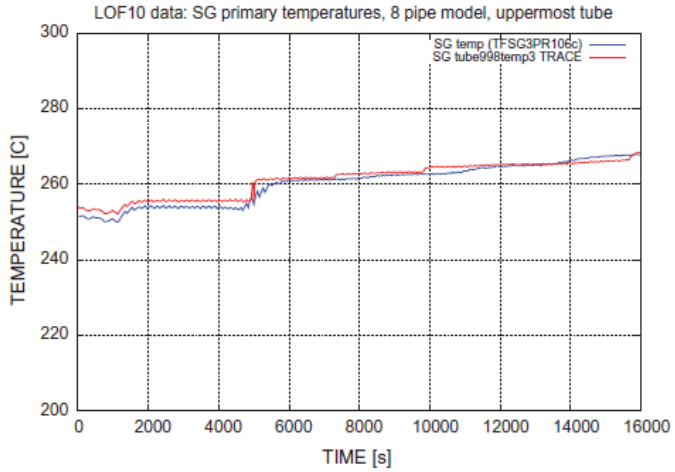

Figure 35: Primary side temperature at uppermost tube layer (location c in Figure 23) in the experiment and in the TRACE calculation with the eight pipe layer model.

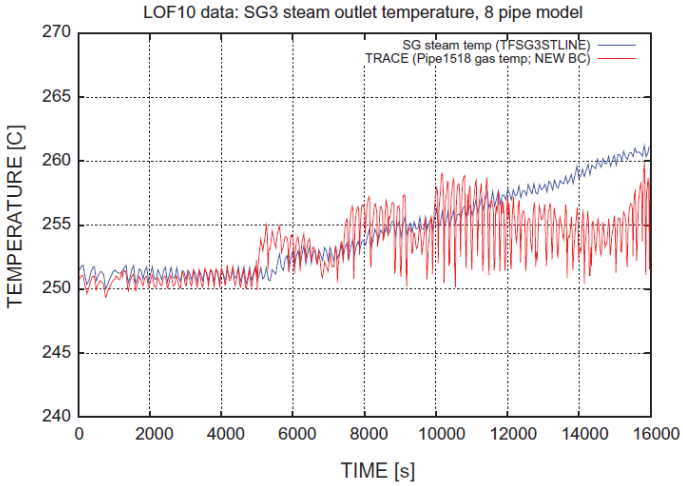

Figure 36: Steam outlet temperature in the experiment and in the TRACE calculation with the eight pipe layer model.

The temperature profile in the heat exchange tubes as a function of wet tube layers clarifies how the internal circulation was changing when the secondary inventory was depleted. Consecutive figure series (see Figure 37a, Figure 37b, Figure 37c, and Figure 37d) present the fluid temperature evolution in four heat exchange tubes both in the

LOF-10 experiment (left side graphs) and the TRACE calculation results (right side graphs). The coding R1C2 in the experiment refers to the uppermost tube row (R1) and to tube column 2. Tube 1 in the calculation corresponds directly to row 1 (R1) in the experiment. Other rows, 6, 10 and 14, in experiment have no individually correspondent tube layer in the calculation. Tube 5 in calculation represent row 6 and 7 in the experiment and Tube 7 represent rows 10 and 11 in the experiment. Tube 8 represents the three lowest rows (12, 13 and 14) in the experiment. Hence, the calculated temperature distributions are not quantitatively comparable with the experiment.

When all tubes are wetted, the flow direction was from the hot to the cold collector in Row 1 and Row 6 in the experiment. The measurements in Row 10 and Row 14 indicated reverse flow as well as the calculation result with Tube 7 and Tube 8. The calculated temperatures in the lowest tube layer (Tube 8) were slightly higher than above, in Tube 7. As the first row of tubes uncovered, the heat transfer was lost in the topmost tubes. The temperatures suggested flow reversal succession in the lowest tubes. This observation is identical both in the experiment and in calculation.

When two layers were uncovered, the loop temperature was higher, but the flow distribution remained almost the same both in the experiment and calculation. The uncovery of Tube layer 12 transformed the temperature profile in Layer 10 in the experiment, which suggested a drastic change in the tube flow rate and flow direction. The flow direction became from the hot to the cold collector. The calculation could not produce this phenomenon at this point.

This analysis reveals the influence of nodalization. Because all tube layers are not individually modelled, the flow reversal phenomenon is not appearing as in the experiment.

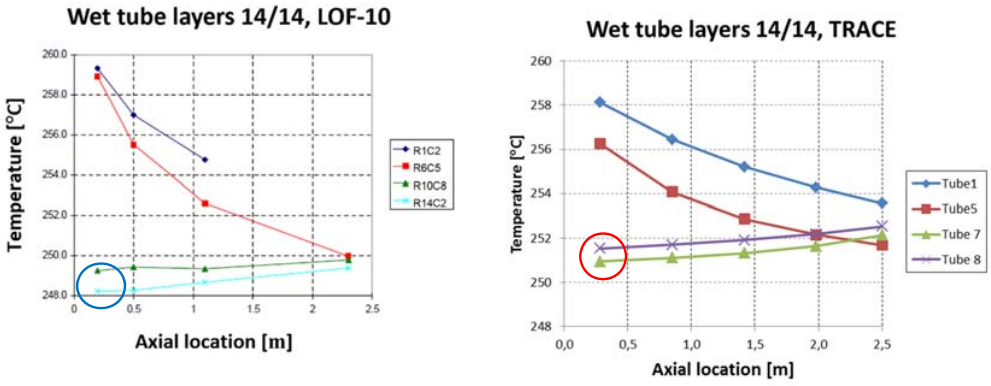

Figure 37a: Temperature profiles in heat exchanger tubes; 14 of the 14 wetted tube rows. Left: LOF-10 experiment; right TRACE calculation. Note that calculated temperatures (inside red circle) in reversed flow tubes are ~3 ºC higher than in experiment (blue circle).

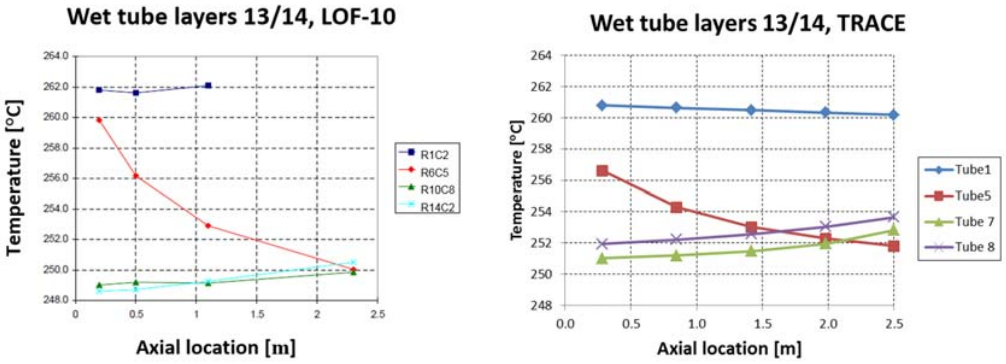

Figure 37b: Temperature profiles in heat exchanger tubes; 13 of the 14 wetted tube rows. Left: LOF-10 experiment; right TRACE calculation.

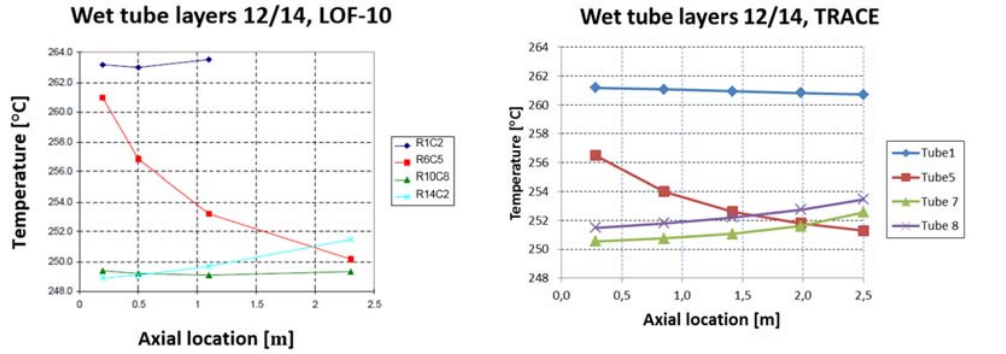

Figure 37c: Temperature profiles in heat exchanger tubes; 13 of the 14 wetted tube rows. Left: LOF-10 experiment; right TRACE calculation.

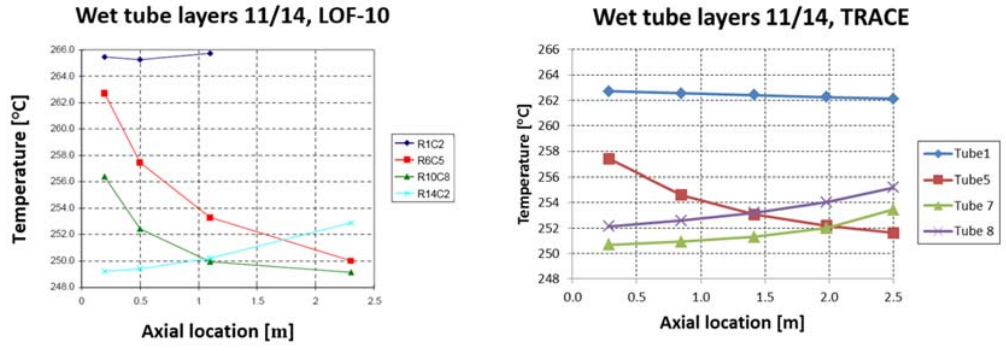

Figure 37d: Temperature profiles in heat exchanger tubes; 11 of the 14 wetted tube rows. Left: LOF-10 experiment; right TRACE calculation.

The earlier research with PACTEL experiments and the previous temperature curve analysis suggest clearly flow reversal phenomenon. Thus, the flow behaviour in the lowest tube rows was investigated in more detail also with the TRACE code. Hence, the mass flows in different pipes representing the tube rows as well as pressure differences between hot and cold collectors were studied. The calculation results showed clearly that flow reversal in the steam generator tubes occurred also with the TRACE code modelling (see Figure 38). The change of pressure head between hot and cold collectors in the beginning of the natural circulation phase caused the flow reversal in the lowest two pipes. The calculated pressure differences between hot and cold collectors show clearly that the two lowest pressure differences are negative when the flow rate is changed to correspond to the natural circulation rate in the experiment. As the secondary side inventory is decreasing further, the pressure difference in these two lowest rows is stepwise fading towards zero.

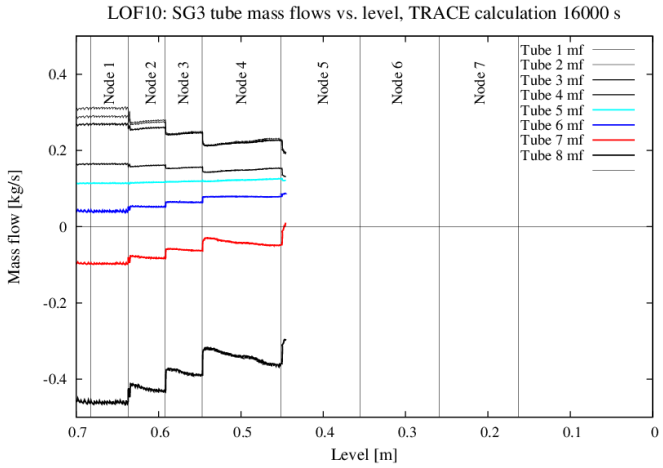

Figure 38: Calculated mass flow rates in the heat exchanger tubes versus collapsed level on the secondary side. Vertical lines illustrate node edges. TRACE calculation of LOF-10 experiment (16000 s) with the eight tube layer model.

5.3.5 Stepwise Inventory Reduction simulations

The main purpose of the Stepwise Inventory Reduction (SIR) experiment simulations was to find out the TRACE code capability to reproduce the natural circulation flow conditions at different primary side inventories and at different pressure ranges.

SIR-23

The SIR-23 experiment was operating at the nominal PACTEL pressure. Although most of the phenomena that took place in the experiment SIR-23 were also found in the TRACE calculations, some discrepancies occurred. The primary and secondary side

pressures describing the overall behaviour are presented in Figure 40. The calculation results agreed well with the experiment during the steady state period (first 1000 s).

When the primary circulation pump was halted, single phase natural circulation flow started. Because natural circulation flow rate here was only 10 % – 15 % of the forced flow rate, the temperature at the core outlet increased rapidly (see Figure 41). The calculated flow rate was smaller than in the experiment. The natural circulation continued in the single phase mode until the collapsed level decreased to the level of hot leg inlet elevation. Figure 42 presents the cold leg mass flow rate together with the facility collapsed level in the same graph. The collapsed level decrement clearly indicates the stepwise reductions of primary inventory. The steam and water mixture started to flow into the hot leg, and thus, the two-phase natural circulation mode was initiated. Almost at once, the primary flow rate decreased and finally stagnated totally due to the loop seal effect, and thus, the primary pressure started to rise. This phenomenon was observed and estimated precisely in the calculation.

The third draining was initiated earlier than intended to avoid the pressure rise over the design pressure limit of 80 bars. The primary pressure cut-off was assisted by switching off the heating power for a short period. These operations turned the primary pressure to decrease again. As the measured primary pressure dropped close to the secondary side pressure, the calculated pressure remained about 6 bars higher. After the next draining, the water connection to the hot leg broke, and only steam flowed through the hot leg to the steam generator. At this stage, natural circulation changed to the boiler-condenser mode. It seemed that from this point onwards, the flow rate was so small that it was out of the measurement range in the experiment.

In SIR-23 the upper plenum level behaviour was studied for the first time. The upper plenum part of the PACTEL facility has a diffuser structure, which consists of two nested concentric pipes preventing direct flow of the ECC water from the accumulators or from HPI system to the loops. For the TRACE simulation model, a similar structure was built using two parallel pipes, which were connected together with single components. This modelling structure clearly improved the upper plenum behaviour, especially during decreasing level. Figure 39 presents the original simple nodalization structure and modified nodalization with diffuser structure modelled.

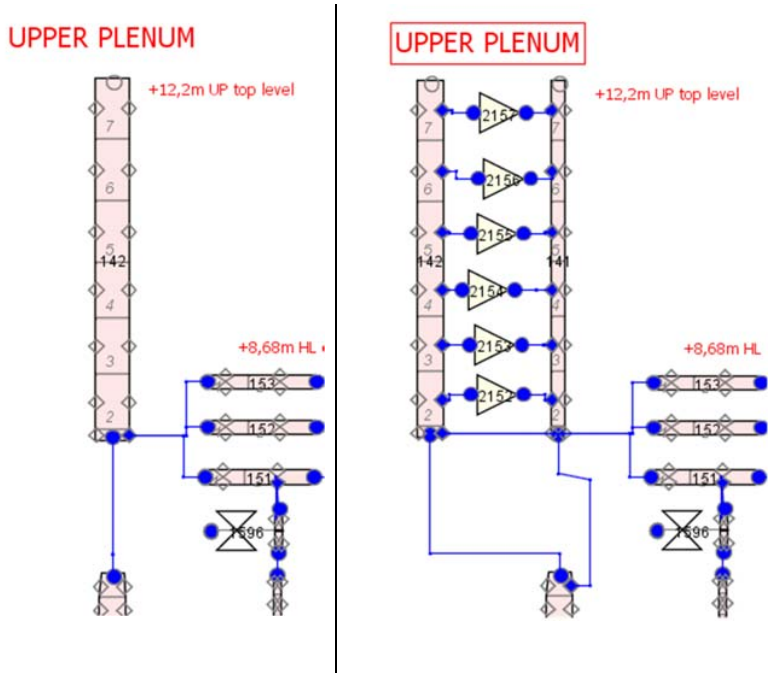

Figure 39: TRACE code modelling structures of upper plenum of PACTEL. Original simple nodalization (on left) and modified nodalization with diffuser structure (on right).

The calculated primary pressure increased slightly after each remaining draining. The explanation for the pressure and flow discrepancies between measured and calculated data is most probably due to the different distribution of heat losses in the experiment facility and calculation model. The heat losses affect the surface temperatures of upper plenum wall structures and thus directly the amount of water flashing to steam. Even though heat loss evaluation has been carried out earlier, more accurate comparison of heat losses was not possible since exact data of the heat loss distribution was not available. An additional uncertainty source was the heat loss to the pump cooling, the amount of which remained undefined.

The set point of the heating power in the SIR-23 experiment was 115 kW. However, the average heating power according to the measurement data was lower than intended, approximately 104 kW. Different power values between these values were tested. According to the test calculations, the case with 104 kW heating power gave results that resembled most the experiment pressure timing and temperature behaviour.

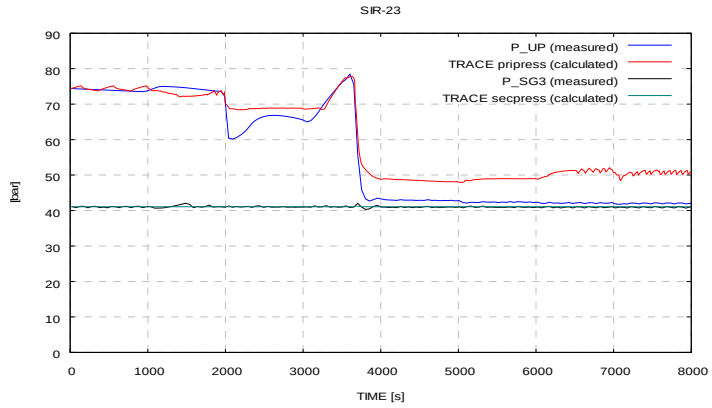

Figure 40: Primary and secondary side pressures in SIR-23 experiment vs. TRACE calculation.

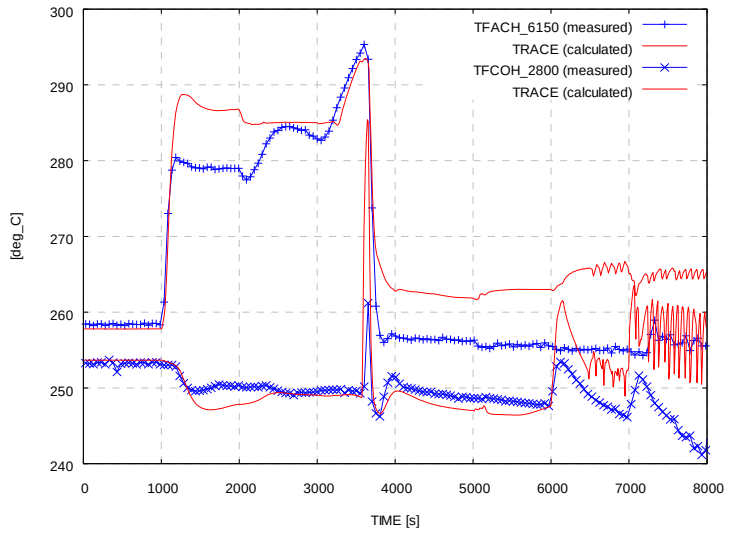

Figure 41: Temperatures below and above core region in PACTEL experiment SIR-23 (blue lines with markers) vs. TRACE calculation (red solid lines).

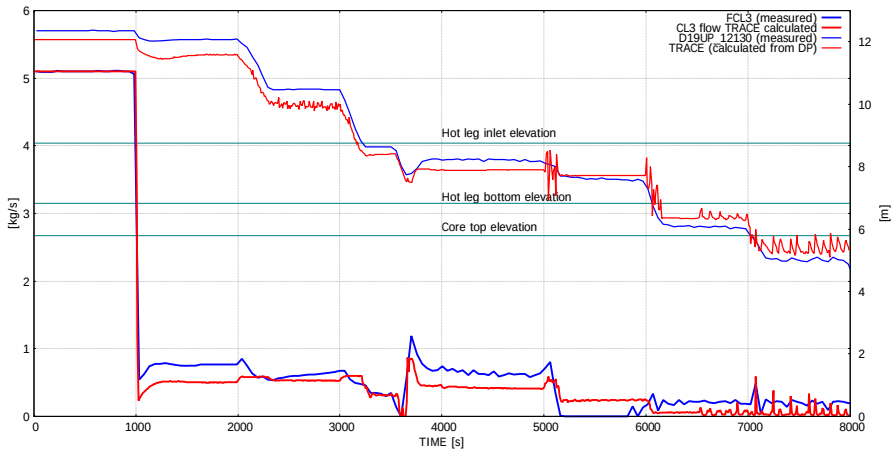

Figure 42: Cold leg mass flow rates and together with the collapsed levels in PACTEL experiment SIR-23 vs. TRACE calculation. The hot leg elevation and core top elevations are shown as well.

SIR-21

The SIR-21 experiment was set to operate at low pressure range (1.6 MPa). The core heating power in the calculation was set to 115 kW, which corresponded to the experiment value. The heating power was supplied continuously without any interruptions. The secondary side pressure and feedwater flow to the steam generator were boundary conditions in a similar way as in the calculation procedure of SIR-23.

At 1000 s, the pump was stopped and single phase natural circulation was initiated. The calculated natural circulation was less than in the experiment (see Figure 43). The first draining at 2000 s decreased the primary pressure (see Figure 44) and collapsed level promptly (see Figure 45). The calculated primary pressure did not decrease as low as in experiment. This corresponded to the findings in the calculation results of SIR-23.

After the second draining (at 3000 s), the flow changed from the single-phase to two-phase natural circulation. The primary pressure started to rise both in the experiment and calculation. The primary flow stagnated shortly after the third drain (at 4000 s), and a pressure peak took place. The calculated primary pressure followed nicely the experiment trend from this point till 6000 s. Although the flow rate modelling was good, it departed from 5000 s onwards. The calculated flow rate reached here the highest value. The differences in the collapsed levels are presented also on cold leg side (see Figure 46). The first level drop appears in the experiment already at 5000 s but in the calculation at 6000 s. A similar time difference is with the final depletion of the cold leg. This suggests that the flow oscillations between the downcomer and core are not occurring at a similar pace in the experiment and calculation. However, the difference between the experiment and calculated inventory at the time of the final stage was only 0.5 %.

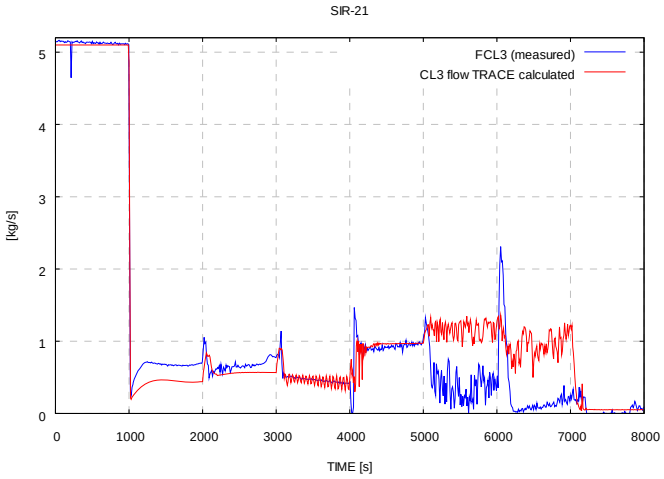

Figure 43: Cold leg mass flow in PACTEL experiment SIR-21 vs. TRACE calculation.

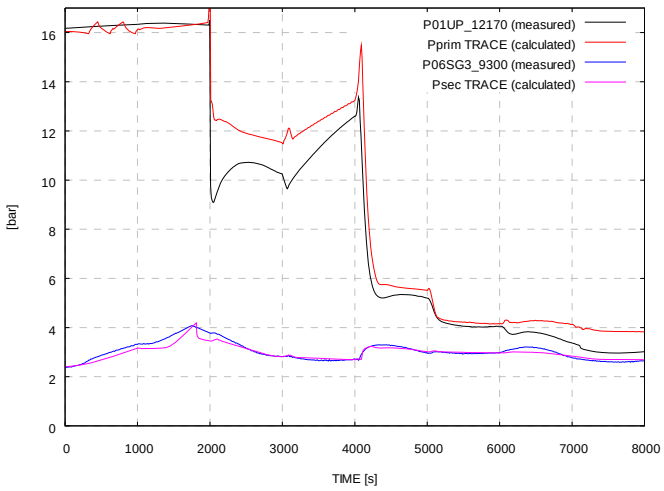

Figure 44: Primary and secondary side pressures in SIR-21 experiment vs. TRACE calculation.

Figure 45: Collapsed level in PACTEL experiment SIR-21 vs. TRACE calculation.

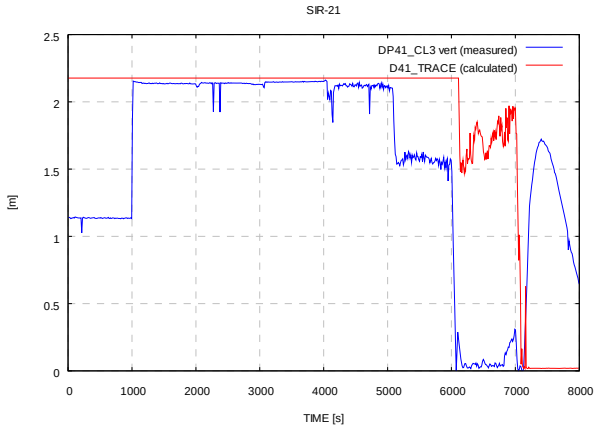

Figure 46: Collapsed level at vertical part of cold leg in PACTEL experiment SIR-21 vs. TRACE calculation. (Measured value was not valid when the main circulation pump was running (0 s–1000 s) due to the large dynamic pressure component.

5.3.6 **Small Break Loss-of-Coolant Accident simulations**

SBL-30

In Small Break Loss-of-Coolant experiment, SBL-30, a 1 mm continuous break was introduced. In this experiment, ECC was not introduced. The flow adjustment for the calculation model was carried out by testing different additive loss factors in the single junction component simulating the break orifice. Thus, the modelling of the break flow was quite accurate (see Figure 47). The purpose was to investigate the appearances of natural circulation modes and the hot leg loop seal effect in calculation. All the natural

circulation modes were present also in the calculation. The flow stagnations due to loop seal effect were also found in the calculation. In the primary pressure behaviour there was some discrepancy between the calculation and experiment. The overall tendency with several stagnations and resumes in natural circulation flow showed rather good agreement in timing, but the calculation underestimated the flow rate (see Figure 49). However, the calculation of SBL-30, with a continuous break and all three loops in operation, succeeded better than the calculations of SIR-experiments to estimate the pressure propagation.

Void at the top of the DC took place approximately 270 s earlier in the calculation, simultaneously with the break flow change from single-phase to two-phase flow.

Core heat-up was observed at the end of the experiment when the cladding temperature started to rise and finally exceeded 300 °C and the experiment was terminated. Core heat-up was not observed in the calculation. At the time of the termination, the topmost node of the core region was not the fully voided. In all other nodes below, the void fraction was approximately 0.6. Thus, the cladding surface was still wetted at the end of the calculation.

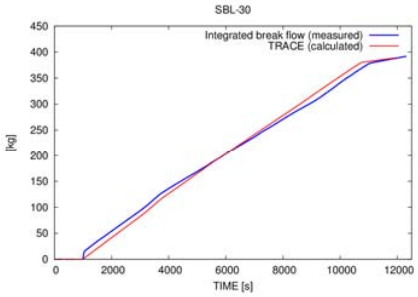

Figure 47: Break mass flow (integrated) SBL-30; Break size 1 mm.

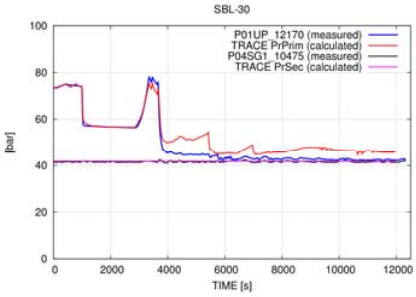

Figure 48. Primary and secondary side pressures SBL-30 vs. TRACE calculation.

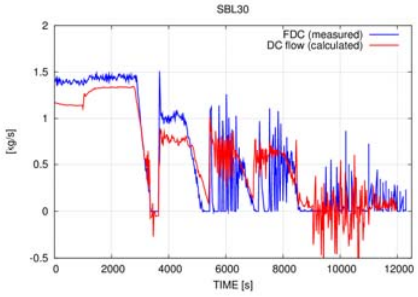

Figure 49: Downcomer mass flow rate in SBL-30 vs. TRACE calculation.

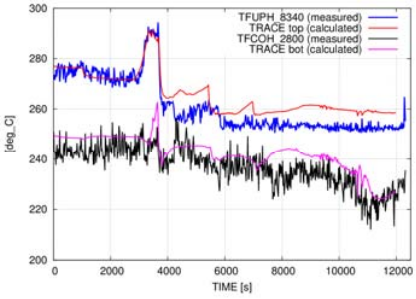

Figure 50: Temperatures above and below core region in SBL-30 vs. TRACE calculation.

SBL-31

The PACTEL experiment SBL-31 with the break diameter of 2.5 mm was calculated using the TRACE code model. The main intention of this calculation was to test the modelling of hydro-accumulators and the secondary side feed and bleed procedure. The two hydro-accumulators were in use and modelled. The main interest in the calculation was focused on the inventory distribution during depletion and recovery, break flow rate and the events related to hot leg loop seal.

The single-phase break flow was accurately modelled. At the moment (4400 s) when break flow changed to two-phase flow in the experiment, the calculated flow continued in single-phase. The calculated primary side pressure was in rather good agreement with the experiment result (see Figure 53). The secondary feed and bleed was successfully modelled; however, the calculated primary side pressure was slightly overestimated during the period from 2000 s to 3000 s.

The downcomer of the PACTEL facility has a diffuser structure with parallel nested pipes. This structure was modelled in nodalization to obtain a more realistic flow path structure in the input. This change in modelling improved the calculation behaviour significantly, because the injected ECC water was directed to the correct location in the primary circuit. See Figure 51 with original simple nodalization and modified nodalization with diffuser structure modelled.

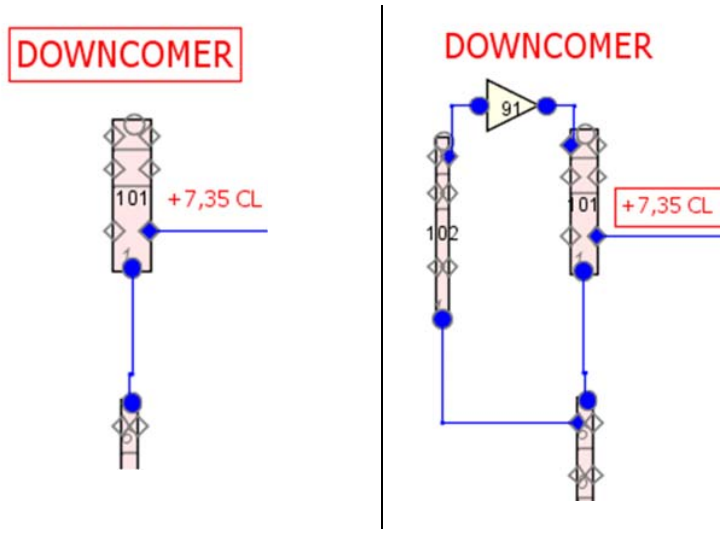

Figure 51: TRACE code modelling structures of downcomer of PACTEL. Original simple nodalization (on left) and modified nodalization with diffuser structure (on right).

The hydro-accumulator injections started at approximately 1700 s and were ceased at about 4000 s. The calculation estimations of the injections were almost precise. However, the integrated mass in the calculation deviated largely from this moment onwards. All these observations indicate that the inventory distribution was different in the calculation than in the experiment. This was confirmed also in the behaviour of the upper plenum collapsed level (see Figure 55), which was lower in the calculation than in the experiment. The natural circulation modes and timing of flow stagnations were modelled satisfactorily.

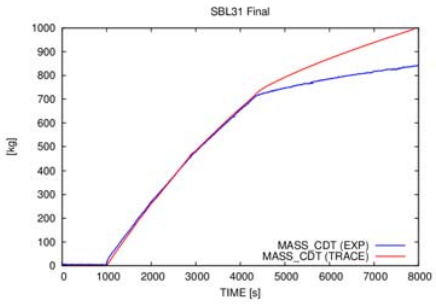

Figure 52. Break mass flow (integrated) in SBL-31 vs. TRACE calculation; break size 2.5 mm.

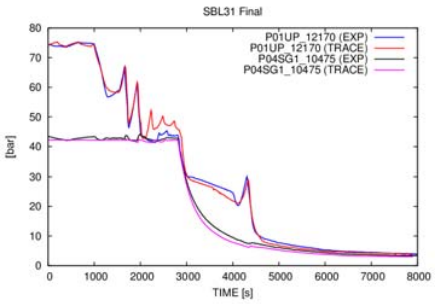

Figure 53: Primary and secondary side pressures in SBL-31 vs. TRACE calculation.

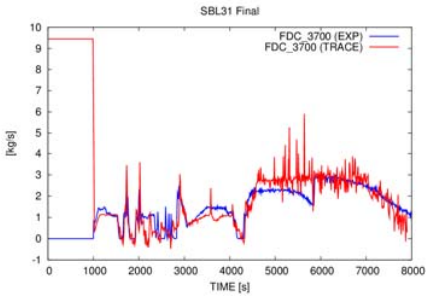

Figure 54: Downcomer mass flow rate in SBL-31 vs. TRACE calculation.

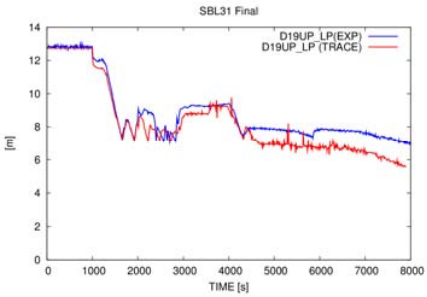

Figure 55: Collapsed level in upper plenum in SBL-31 vs. TRACE calculation.

SBL-33

The PACTEL experiment SBL-33 with the break diameter of 3.5 mm was calculated using the TRACE code model. The main intention of this calculation was to test the modelling of hydro-accumulators and the secondary side feed and bleed procedure. The duration of the boiler-condenser natural circulation mode was under consideration. The two hydro-accumulators and the high pressure injection (HPI) system were in use and modelled. The HPI was initiated from the low pressurizer level (2.8 m) injecting 0.08 kg/s constantly. The main interest in the calculation was focused on the inventory

distribution during depletion and recovery, break flow rate and the events related to hot leg loop seal.

The single-phase break flow was accurately modelled. The change to two-phase flow took place much later (+700 s) in the calculation. The integrated mass flow in the experiment hardly increased further indicating that break flow was almost pure steam. In the calculation the integrated mass flow kept on increasing, and at the time termination it was approximately 200 kg (+17 %) more than in the calculation (see Figure 56). The primary pressure propagation was quite accurately estimated in the calculation. The pressure peak due to flow stagnation occurred almost simultaneously. When hot leg loop seals cleared and the primary side pressure started to decrease, the hydro accumulators started to inject (see Figure 57).

When the primary pressure decreased further, it dropped below the secondary side pressure both in the experiment and calculation. This was possible since the secondary side pressure had remained almost constant from the start of the experiment. The direction of the heat transfer changed, and as a result, the secondary side was cooled down by the primary side. The calculated secondary side pressure decreased faster than pressure in the experiment during the period from 2000 s to 3000 s (see Figure 57). Hence, the calculation overestimated the reversed heat transfer. However, when bleeding was started through the secondary side valve, the secondary pressure decrease proceeded satisfactorily according to the experiment.

The injection of hydro accumulators was started simultaneously with the experiment. The calculated mass from the accumulator injecting to the upper plenum was much higher, and the total injected mass in the calculation was approximately 100 kg more than in the experiment. This was due to the ambiguity in the initial level value in the experiment. However, the calculated mass from the accumulator injecting to the downcomer was almost the same as in the experiment. The overestimated injection to the upper plenum caused a jump in the upper plenum inventory (see Figure 59). Despite these discrepancies, the mass flow rate was quite accurately calculated (see Figure 58).

The transition from single-phase natural circulation to two-phase flow took place at about 3200 s in the experiment and 100 s later in calculation.

Considering the boron dilution possibilities, the interesting period started at 3230 s in the experiment when the hot leg loop seals cleared. In calculation, Hot leg 1 emptied approximately 100 s later and Hot leg 2 about 800 s later than in the experiment. The emptying of Hot leg 3 occurred approximately 200 s earlier in calculation than in the experiment. Shortly after this event, the boiler-condenser heat transfer mode was established, and it existed until the end of the experiment. The primary pressure dropped below the LPIS head at 5825 s in the experiment. Thus, in the experiment, a period of about 2600 s existed when condensation could have taken place in the SGs and the generation of an unborated and unmixed water slug would have been possible. In the calculation, this period was estimated to be about 600 s shorter than in the experiment.

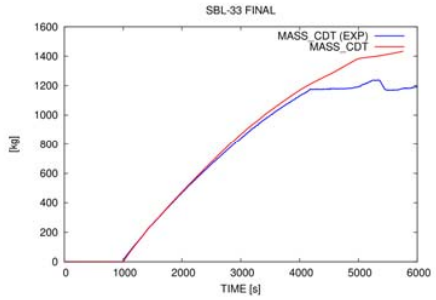

Figure 56: Break mass flow (integrated) in SBL-33 vs. TRACE calculation; Break size 3.5 mm.

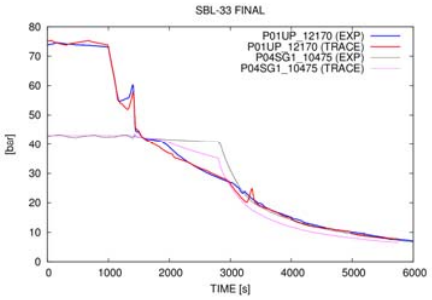

Figure 57. Primary and secondary side pressures in SBL-33 vs. TRACE calculation.

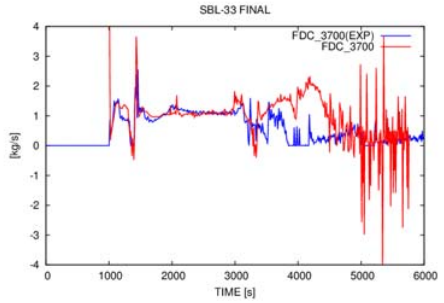

Figure 58: Downcomer mass flow rate in SBL-33 vs. TRACE calculation.

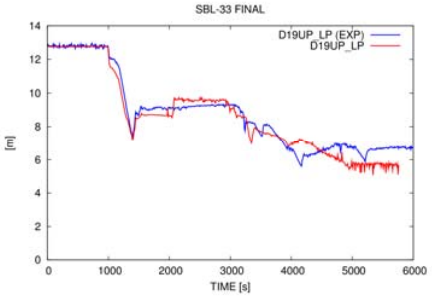

Figure 59: Collapsed level in upper plenum in SBL-33 vs. TRACE calculation.

IMP-06

The PACTEL experiment IMP-06 with the break diameter of 7.8 mm was calculated using the TRACE code model. The main intention of this calculation was to test the modelling of hydro-accumulators. The two hydro-accumulators, the high pressure injection (HPI) system and a low pressure injection system (LPI) were included and modelled. The hydro-accumulator pressure was reduced to 3.5 MPa, and the amount of water in the accumulators was increased. Special interest in this test was to determine whether the system pressure decreases to the head of the LPIS pumps of 0.7 MPa before the core overheating occurs.

The IMP06 experiment challenged the TRACE model in many ways: the steady state period was run with the full power rate of PACTEL, that is, 940 kW; the break size was largest so far (7.8 mm) and both hydro-accumulators contained cold water (25 °C). The

calculations of this experiment were not fully successful with these parameters. There was discrepancy especially in the modelling of the break flow.

In the calculation, the integrated break mass flow was similar to that in the experiment till 500 s (see Figure 60). However, the calculated primary side pressure decreased more rapidly than the experiment pressure (Figure 61). Thus, the hydro-accumulators in the calculation started to inject earlier than in the experiment, and the injection period in the calculation lasted longer; this caused discrepancies. The break flow in the calculation was less than in the experiment until time 1000 s when the break changed to vapour.

The natural circulation flow was in the boiler condenser mode at the very beginning because of the relatively large break size. The calculated flow showed largely oscillating behaviour while the measurement showed no flow (Figure 62).

The break flow in the experiment changed from liquid to vapour and back to liquid depending on the starts and stops of the accumulator and LPIS injections. For the first time the change took place when the accumulator injecting to DC had stopped injection. The break flow changed back to liquid flow when the LPIS started to inject. These changes were observed also in collapsed level behaviour (Figure 63).

This calculation case appeared to be quite difficult because the calculation was terminated due to a time step error. To pass over this problem it was necessary to use a relatively small maximum time step, which was 0.005 s in the beginning and 0.002 s after 600 s until the end of the transient. However, core overheating did not occur either in the experiment or in calculation. Table 10 presents the main events of the experiment IMP06 and remarks from the TRACE calculation.

Table 10: Timing of main events in experiment IMP06 (T2.3) and in TRACE calculation.

TIME [s]	**EVENT in experiment**	**Remarks from calculation**
0	Break initiated, pump coast down (150 s), power scram, FW stopped, PRZ heaters switched off	Simultaneous
410	HAs injection started (prim. pressure < 3.5 MPa)	−80 s
650	HA to UP injection terminated	+100 s
730	HA to DC injection terminated	+100 s
1490	LPIS started	−260 s
2464	Experiment terminated	Simultaneous

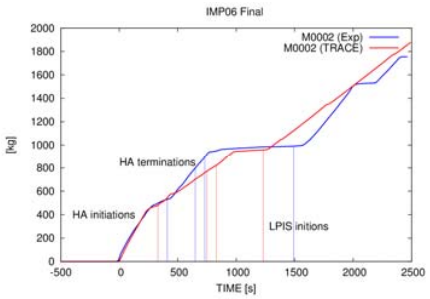

Figure 60: Integrated break mass flow in IMP06 vs. TRACE calculation.

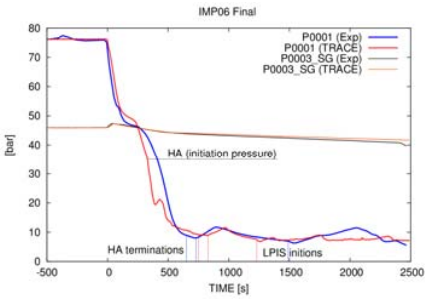

Figure 61: Primary and secondary side pressures in IMP06 vs. TRACE calculation.

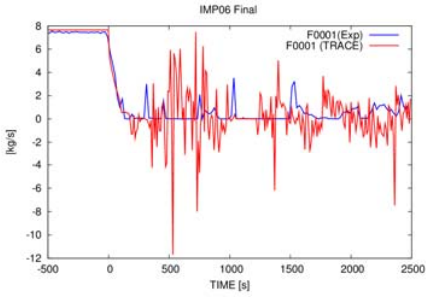

Figure 62: Downcomer mass flow rate in IMP06 vs. TRACE calculation.

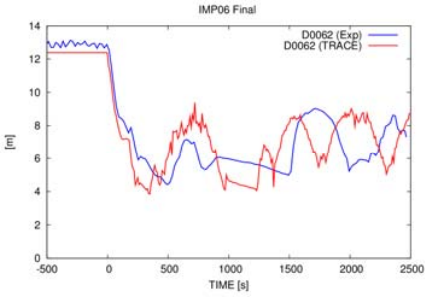

Figure 63: Collapsed level in upper plenum in IMP06 vs. TRACE calculation.

The overall behaviour could be modelled satisfactorily, even though some discrepancies appeared. There were also difficulties reaching the end of the transient time due to time step problems. The main reason for the unexpected termination remained unknown in many cases because the code output listing did not specify the actual problem point. Most likely, the reason was difficulties in nearby the break, where cold water met warm water and flows were oscillating heavily. Although a more thorough sensitivity analysis would have been necessary at least for assessing the effect of break setup, this need could not be fulfilled completely due to limited resources.

The first calculation of IMP-06 indicated that the nodalization had to be modified. There were 12 nodes in the core pipeline and three in the bypass. This caused an unintentional and sudden drop in the primary pressure during facility depletion. The bypass nodalization was changed to be consistent with the core nodalization. Both the bypass and core pipelines contained thereafter 12 nodes.

5.3.7 Primary-to-secondary leakage

The Primary-to-secondary leakage experiments, PSL-10 and PSL-11, were calculated using the TRACE code model. The break diameters were 5.5 mm and 2.5 mm. The pressurizer spray, the hydro-accumulators and high pressure injection system were in use and modelled. The experiments focused on reducing the primary pressure and temperature with fast cooling according to the regulations for operator actions so low that the primary pressure stays below the opening pressure of the steam generator safety valve.

The HPI was set to start immediately after the break initiation with a constant 0.2 kg/s mass flow rate. The spray was activated if the primary pressure exceeded 45 bars. In PSL-10, the spray was controlled to keep the pressurizer collapsed level between 2.5 m and 6 m. The operation of the safety valve in the broken steam generator (SG3) was also simulated, even though lack of exact operator parameters of the experiment caused quite large uncertainty.

Model changes and improvements were introduced concerning steam generator behaviour. It was necessary to restrict the inner circulation of the horizontal steam generator to model the pressure behaviour more precisely.

When the break valve was opened, the primary side pressure and pressurizer collapsed level started to decrease very rapidly. The calculation estimated this period very well (see Figure 64 and Figure 65). The secondary side pressures in all steam generators decreased simultaneously until the broken steam generator (SG3) was isolated. From this point onwards, the SG3 pressure started to rise. The calculated pressure rose much faster than in the experiment. The relief valve in SG3 cut off the rapid pressure rise in the calculation. The primary side and broken steam generator pressure were equalized almost simultaneously at approximately 1600 s.

The overall behaviour could be modelled satisfactorily, even though some discrepancies appeared. Especially in the experiment PSL-10, the valve operations concerning the broken steam generator had significant effect on the overall behaviour of the calculations. After several test calculations, appropriate valve operation settings were achieved.

In PSL-10, the calculated pressurizer spray started almost simultaneously with the experiment. The calculated pressurizer collapsed level started to rise earlier than in the experiment already before the spray initiation. This suggests that the primary side has too much inventory in the calculation. The criterion of 6 m of pressurizer collapsed maximum level was in use for the spray termination. The spray in calculation was stopped at 2300 s when the criterion was taking place (see Figure 65).

In the calculation, the break flow reversed few times during the period of 1700 s–2300 s. The reversed flow lasted 50 s at the most. Since a clear indication of flow reversal was not found in the experiment, this phenomenon was not investigated further.

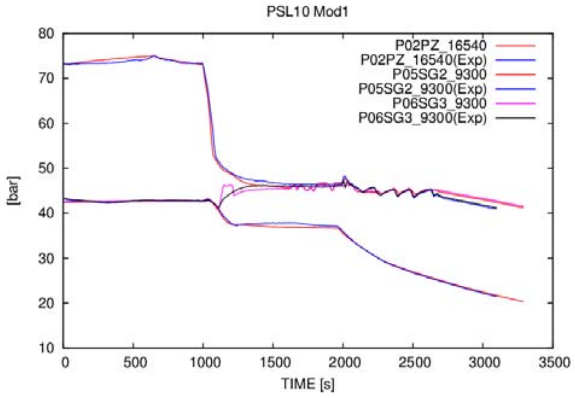

Figure 64: Primary and secondary side pressures in PSL-10 vs. TRACE calculation.

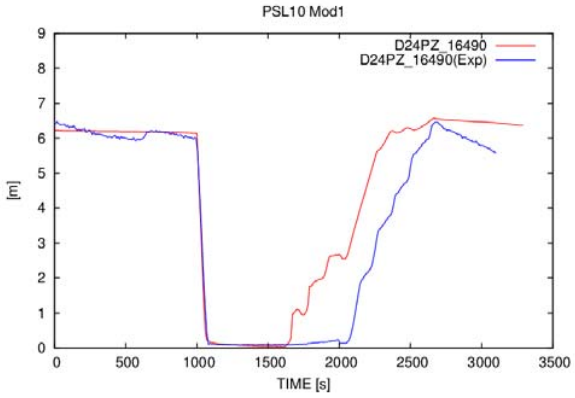

Figure 65: Pressurizer collapsed level in PSL-10 vs. TRACE calculation.

In the calculation of PSL-11, the primary side pressure was not decreased as expected. Some improvement could be implied by modifying the break loss coefficient. However, this modification could not make the calculated results good enough. Then, the HPI flow was decreased to achieve better results for the primary side pressure and pressurizer collapsed level. The changes that had to be made for the HPI mass flow fell even beyond the error margins, and thus, the mass flow rates were unrealistic. The pressure propagation in PSL-11 compared to the TRACE calculations results is presented in Figure 66 and Figure 67.

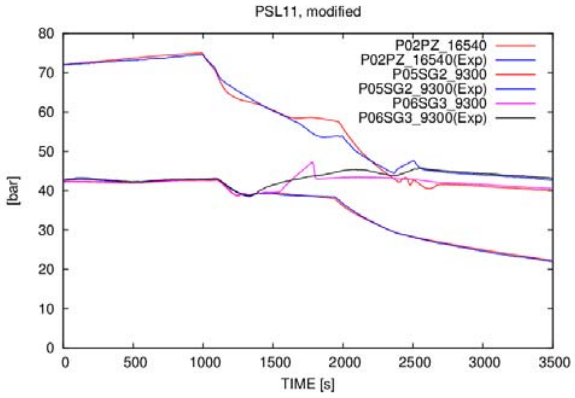

Figure 66: Primary and secondary side pressures in PSL-11 vs. TRACE calculation.

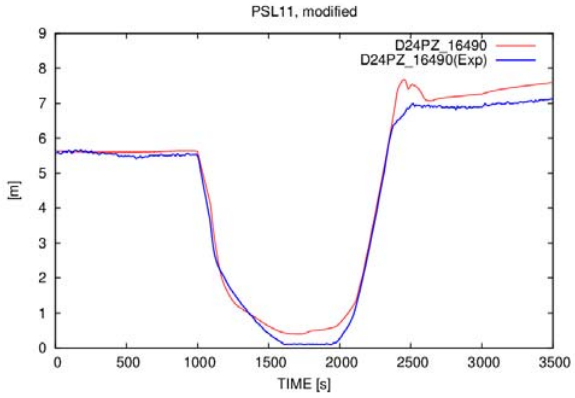

Figure 67: Pressurizer collapsed level in PSL-11 vs. TRACE calculation.

5.3.8 **Anticipated transient without scram**

The Anticipated transient without scram experiment, ATWS-32, was modelled and calculated using the TRACE code. The experiment was simulating the control rod withdrawal from the core, when the core was operating with almost zero power. A prompt power excursion to the maximum value was introduced, causing a pressure increase and intensifying the heat transfer to the secondary side and thus decreasing the collapsed level in the steam generators. According to the procedure, no emergency core cooling systems were in use. Only fixed rate feedwater in every steam generator was set in operation.

Some model changes and improvements were introduced to the TRACE calculation model. The additional pressure relief valves were modelled with a similar setup to the experiment. The core power in the calculation was set as a boundary condition according to the averaged measurement data values. The power feedback according to the core voiding was not coded in the calculation model (see Figure 72).

The overall behaviour was modelled satisfactorily until the moment when flow stagnation took place in Loop 1 in the experiment. The flow stagnation decreased the heat removal from the primary side system, causing the primary side pressure to remain high in the experiment (see Figure 68). Thus, the SG1 collapsed level stopped decreasing in the experiment (see Figure 73). The primary pressure in the calculation was decreased because the flow stagnation event did not occur in the TRACE calculation (see Figure 69).

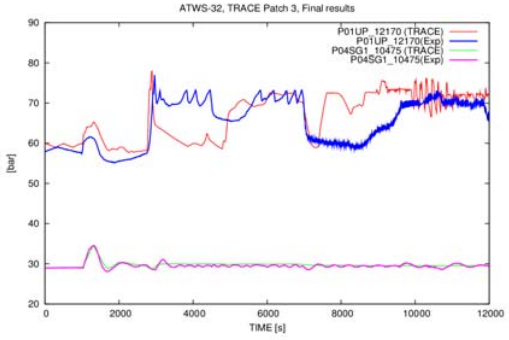

Figure 68. Primary and secondary side pressures in ATWS-32 vs. TRACE calculation.

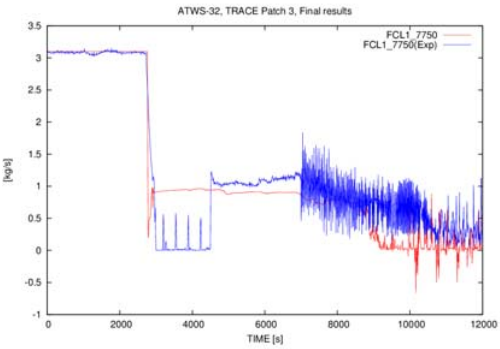

Figure 69. Mass flow rate of cold leg 1 in ATWS-32 vs. TRACE calculation. Note flow stagnation between 3000 and 4500 s. The code fails to reproduce the experiment.

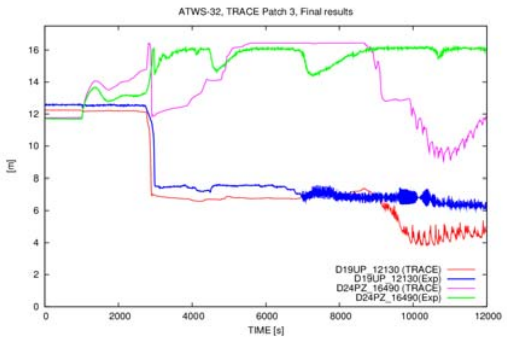

Figure 70. Pressurizer and upper plenum collapsed levels in ATWS-32 vs. TRACE calculation. Note how the pressurizer drains after ~9000 s in the calculation, not in the experiment.

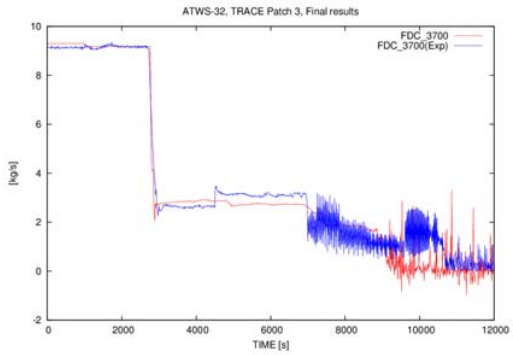

Figure 71. Mass flow rate in downcomer in ATWS-32 vs. TRACE calculation.

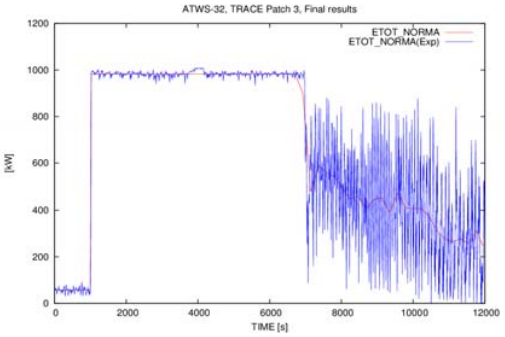

Figure 72: Core power in ATWS-32 vs. TRACE calculation.

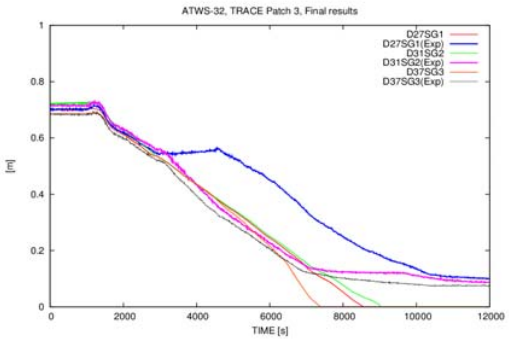

Figure 73: Collapsed level of steam generators in ATWS-32 vs. TRACE calculation. Note how the failure to predict flow stagnation in loop 1 results incorrect secondary side level.

The flows in Loop 2 and Loop 3 were continuing without interruption either in the experiment or in calculation. The calculated flow in Loop 2 was less than in the experiment, and the flow in Loop 3 agreed well with the experiment. Despite the differing behaviour in the loops, the total flow in the downcomer was almost equivalent in calculation and in the experiment (Figure 71). A probable effect on the flow stagnation in Loop 1 is that the pressurizer was connected to Loop 1. When the flow was stagnated in Loop 1, the liquid level in the pressurizer remained high, and no draining was observed from pressurizer in the experiment. In contrast, the calculation produced the pressurizer draining (see Figure 70).

This discrepancy caused that the rest of the calculation results were not fully comparable with the experiment. The pressurizer relief valve operations were significantly driving the events during the experiment. The actual reason for the flow stagnation taking place particularly in Loop 1 could not be confirmed. The timing of the events proved that the operation of pressurizer relief valves was not the initiating action for the flow stagnation, but it likely extended the duration of the flow stagnation. The precise opening procedure of the relief valves in the ATWS-32 experiment was not known. Although the pressure limits were recognized, the possible delays in valve opening and closing times and also flow area fractions between fully open and fully closed valves were not known. Thus, the valve operations in the calculation were not possible to be simulated accurately. Despite the anomalies the calculated overall natural circulation flow rate appeared to agree rather well with the experiment.

The similarity between the current TRACE modelling case and the earlier TMI-2 exercise is quite apparent. Both cases suffered from deficiencies in the modelling of the pressurizer liquid hold-up phenomenon.

5.4 Observation on the results

In the following sections, the validation case results are assessed and discussed in more detail. The discovered phenomenological main points include the flow reversal in steam generator tubing and flow stagnation during natural circulation, containing an additional analysis related to nodalization. Attention is also paid to some modelling options, and they are discussed here. The flow reversal phenomenon during natural circulation is discussed separately and in more detail in Chapter 7.

5.4.1 Flow stagnation during natural circulation

In the TRACE calculations of small break LOCA experiments, like SBL-30, the flow stagnations occurred when the inventory on the primary side decreased to the hot leg connection level. The flow to the steam generator then changed to two phase flow. The steam at the beginning section of the hot leg formed a block, and natural circulation stagnated. This caused essential degradation of heat transfer, and the primary pressure began to rise. The primary side pressurization continued until the loop seals (or only one or some of them) cleared and natural circulation was recovered. The loop seal clearance is due to the dual effect of inventory reduction and steam pushing the liquid forwards from the bottom of the loop seal. After the loop seal clearance, the steam flow towards the steam generators can continue in the cleared loops.

The calculated mass flow rates in the loops did not match with the experiment. However, the combined mass flow rate at the downcomer resembled better the experiment result (see Figure 74). The clearance of hot leg 1 in the calculation was similar to that of the experiment, but in hot leg 2, a difference appeared. The flows in Loop 2 and Loop 3 showed contrary behaviour to each other, that is, the calculated flow in Loop 3 resembled more the situation in Loop 2 in the experiment. Thus, the accurate modelling of the asymmetric loop flow behaviour is a very difficult task. There are many uncertainties in the experiment situation, which cannot be taken into account in the calculations. The initiation of a loop flow is very sensitive to the appearance of small pressure or temperature differences. Also, the reliability of the measurements during two-phase flow presence is lower than in the pure single-phase case.

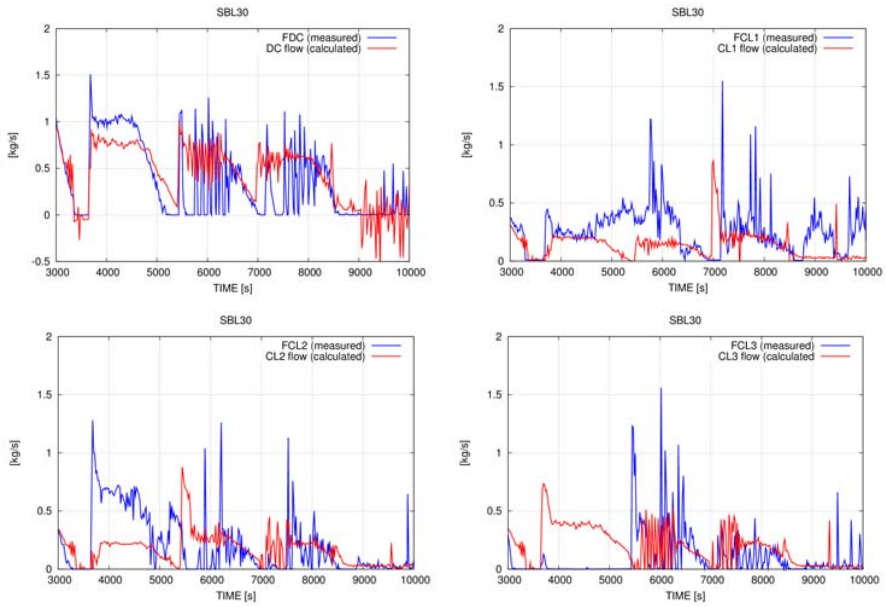

Figure 74: Loop (CL1, CL2 and CL3) and downcomer (DC) flows in SBL-30 experiment and in TRACE calculation.

The events in the hot legs clarify the stagnation phenomenon in the TRACE calculation of SBL-30. Flow stagnations and clearance took place asymmetrically between loops. The two-phase flow initiations took place in each loop after stagnations. The first stagnation occurred just before 3500 s. The flow recovered only in Loop 3, where the steam started to flow to the steam generator, and two-phase flow was then initiated. After the second stagnation at approximately 5500 s, the steam flow started in Loop 2. Finally, at about 7000 s, the two-phase flow started in Loop 1 (see Figure 75). Hence, the flow entering to the steam generator in Loop 1 was in single phase until 7000 s.

In the TRACE model, the hot leg inclined pipe section was divided into five nodes (see Figure 76a). Before the flow stagnation, the steam had reached Node 3 at the inclined part pipe of the hot legs. The stagnation event was ceased in the calculation when in Loop 3 the two-phase flow initiated vigorously at approximately 3700 s (Figure 76a). The other two loops remained stagnated and recovered slower with oscillating void fractions in Node 4 (Figure 76b). Three animation frames clarify the situation before, during and after the pressure peak related to the flow stagnation (see graphs in Figure 77a, Figure 77b and Figure 77c).

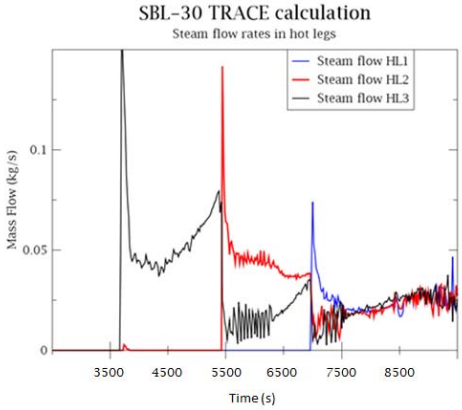

Figure 75: Steam mass flow rates at the end of Hot legs 1, 2 and 3. SBL-30 TRACE calculation.

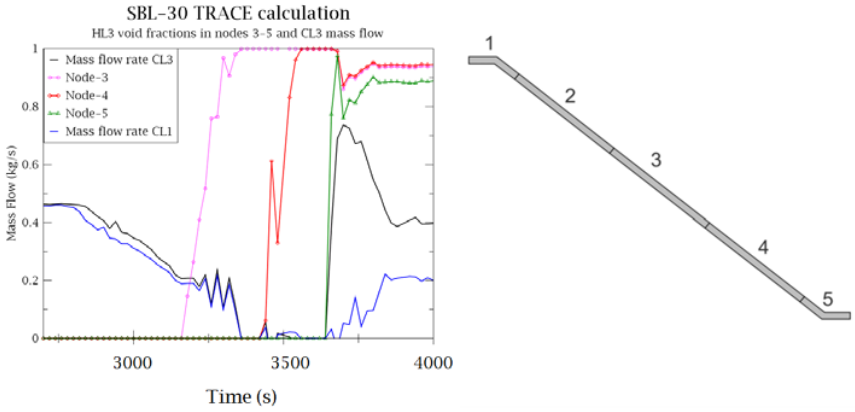

Figure 76a: Void fractions in Nodes 3–5 and CL3 and CL1 mass flow rates in the calculation of SBL-30 with the occurrence of flow stagnations. See node numbering on right.

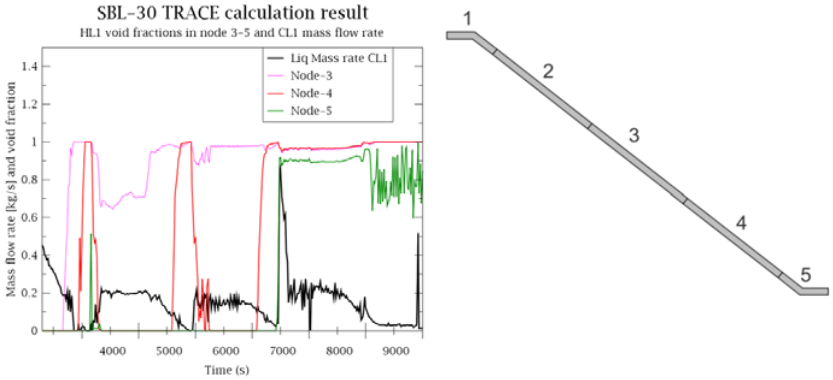

Figure 76b: Void fractions in Nodes 3–5 of hot leg inclined part and CL1 mass flow rate in the calculation of SBL-30 with the occurrence of flow stagnations (left). See node numbering on right.

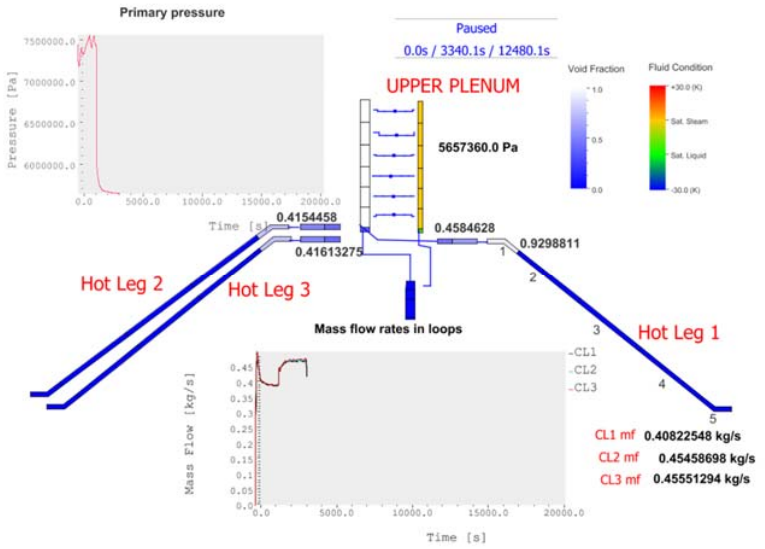

Figure 77a: Loop seal performance with flow stagnation and flow recovery in TRACE calculation results of SBL-30. Animation frame presenting situation before flow stagnation. The upper plenum is almost fully depleted and void fractions are rising at the beginning of hot legs.

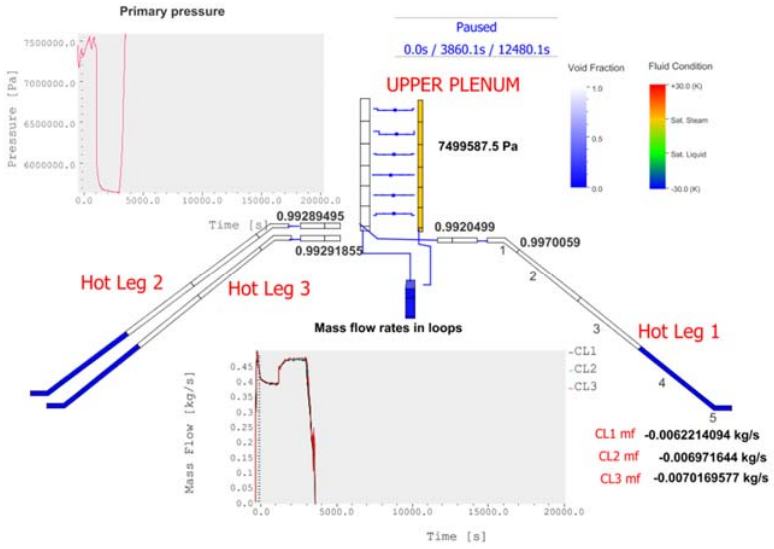

Figure 77b: Loop seal performance with flow stagnation and flow recovery in TRACE calculation results of SBL-30. Animation frame presenting situation during flow stagnation in all loops. Primary side pressure has promptly increased (graph at top left).

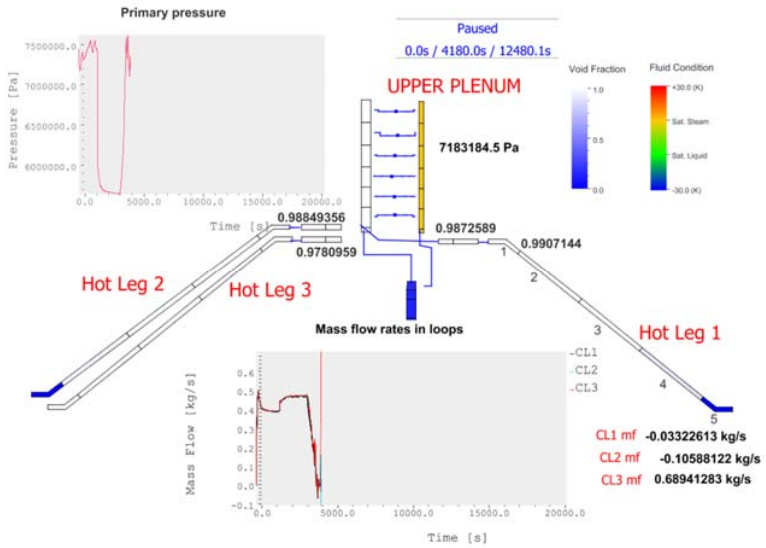

Figure 77c: Loop seal performance with flow stagnation and flow recovery in TRACE calculation results of SBL-30. Animation frame presenting situation after flow stagnation. The flow in Hot leg 3 has recovered (graph at bottom). Loop 1 and Loop 2 are still stagnated. Primary side pressure is decreasing (graph at top left).

The SBL-30 case was run also with alternative nodalization in the hot legs. The hot leg inclined part was renodalized by splitting the three straight nodes into two. However, there were hardly any changes observed between the original and the renodalized cases. The physical phenomenon taking place here was not dependent on the changes in nodalization. The main influence with the split nodes was that the calculation was terminated unexpectedly before the planned finish.

5.4.2 Break flow in the TRACE modelling of PACTEL experiments

In the modelling of PACTEL leakages, only the default choked flow option of the TRACE code in the break orifices and break valve components was used. User-specified multipliers were not used. As found already in the calculation results, the break flow propagation agreed reasonably well during the periods of single phase flow. Discrepancies appeared soon when the flow conditions turned into two phase flow conditions. In the smallest diameter case, SBL-30, the moment of two phase flow initiation and also the magnitude of the flow at the break was rather accurately estimated. When the break diameter was larger, like in the experiment SBL-31, the moment of the two phase flow initiation was precise, while the magnitude was largely overestimated. When the break diameter was even larger, like in SBL-33, the two phase initiation was delayed and the flow rate largely overestimated. However, in the case of

the largest break diameter, in the experiment IMP-06, the flow discrepancy of the calculation was not large compared to the experiment. The calculated break mass flow was momentarily larger and then also smaller than the experiment value. The general explanation for these discrepancies is that the inventory is not the same throughout the facility when comparing the contents of the experiment facility and simulation model. In other words, for example water in the calculation was not located similarly to the measurement.

The calculations were run also with setting on the TRACE offtake model. The model was set active in the cross-flow junction simulating the break in cold leg. The execution of the offtake model did not give any significant change to the calculation results.

5.4.3 **Modelling of valve operations**

All the valves of the real PACTEL facility are included in the TRACE model. Most of them are loop closing valves, which were usually not operated during experiments. Main operative valves were control valves, regulating pressure and safety valves. Typically, these valves were situated on the boundaries of the primary system and the atmosphere or the secondary side. The TRACE code has 11 valve types to choose from. The most often used type in the TRACE model of the PACTEL facility was the flow area as a function of pressure. This is the most practical way for representative pressure control. Detailed valve data from which the valve opening area could have been determined was not available; hence, the tabulated flow areas had to be fitted according to the pressure trend curve of the experiment.

5.4.4 **Modelling of heat losses**

The modelling of heat losses in the primary side loops is important for defining the efficiency of heat transfer from the primary to secondary side. However, heat losses are not the initiating force to drive natural circulation. The heat losses only restrict the efficiency of the heat transfer from the primary to secondary side. The heat losses in the hot leg affect the inlet temperature of the steam generator. The heat losses in the cold leg affect the temperature of the core inlet. The heat losses are not the same when the inventory is in the single phase state or in the two phase state. The difference between convective heat transfer coefficients can typically vary within decade if the surface is covered with pure water, two-phase mixture or pure steam.

Heat losses were defined for the TRACE model according to the PACTEL experiment data. Although overall heat losses were adjusted to match facility characterization tests, an accurate detailed distribution of heat losses could not be guaranteed because only the pressurizer and main circulation pump heat losses were known accurately. Moreover, the heat losses may vary in the different operating states of the facility. In some cases, the heat losses seemed to play a significant role, especially when the break size is very small and slow cooling is the dominating phenomenon in the transient. Due to the

facility geometry, the pressurizer and upper plenum or downcomer and upper plenum form a manometer system where level oscillations are driven by heat losses.

5.4.5 Time step management

The time step of a calculation is an essential parameter that regulates the progress of the calculation in time. The codes are usually equipped with time step management procedures. These procedures intend to run the calculation at the maximum allowed time step. The codes have also some criteria by which to reduce the time step when necessary. Also, some default values are pre-set with options for the user to change them. The default values of minimum and maximum time steps are usually giving the user a good starting point for the initiation of the simulations. However, in many transient simulation cases the default values have to be changed. If the initial status of the model to be simulated is unstable, it could be necessary to set either the minimum or maximum or perhaps both parameters to some smaller value to run the model to steady state.

The TRACE code has a special steady state option for the initiation of the case, which is recommended to be used before the actual transient simulation. The steady state option eliminates some controls and trips to simplify the solution.

In many PACTEL simulation cases, the use of the steady state option did not result in a proper steady state due to the exceedance of the convergence criterion on liquid or vapour velocities. This took place especially in the nodes related to the horizontal steam generator and pressurizer. These components were equipped with level control systems, by which the balance could be reached effectively. Thus, a long pre-transient steady state run was carried out. Also, some of the actual transient calculations were terminated unexpectedly due to a time step error with the message “cannot reduce time step further”. These problems were in many cases solvable by setting the maximum time step smaller manually. This change was set to an earlier point in time where the case had proceeded well, and in good time before the moment of termination. The case was then executed again with the new settings. This manually set time step management method worked very well in most cases.

5.5 Validation conclusions

The TRACE code input preparation and validation calculations for the PACTEL facility were implemented according to the validation procedure presented in Chapter 2. The key findings and remarks are presented as follows:

Phenomena related findings

- In many validation calculation cases, a part of the results, for example pressure behaviour, matched almost perfectly when break flow rate (valve area) was adjusted to achieve this.

- The asymmetric flow behaviour between the loops is difficult to predict accurately; minor (pressure) differences create major effects (different flows in parallel loops).
- Some observed phenomena did not occur at all in calculation: an example of this is the flow stagnation in ATWS-32.
- Over/under predictions of phenomena; heat transfer: primary to secondary and to ambient air, natural circulation flow rate.

For some parameters, mainly details of valve properties and operations, accurate data were not available from the experiment. This is not a code deficiency but could be seen as a validation process shortcoming.

Preparation of input

- A representative model of the PACTEL VVER-440 facility could be built, despite its many unique geometric features.
- All necessary components for the code input could be built.
- Some difficulties in setting up the nodalization; code warnings due to unavoidable violation of code guidelines could not all be eliminated, this pertains mainly to connections of multiple pipes especially in the core region and in the horizontal steam generator.
- This has an effect on the steady state achievement and on transient solution; this statement is based on output messages before the termination with “fatal error”.

Calculation management

- Manual time step management by the user is still necessary.
- Unexplained termination of calculation, difficulties to clarify the actual problem, hard evidence from code output listing at the final stage of calculation is missing.

In summary, it has proven possible to model VVER-440-like geometric features adequately in a generic thermal hydraulic code TRACE, but performing the calculations requires specific skills both in setting up the nodalization because a number of compromises have to be made between modelling detail and complexity, and some code use guidelines may need to be intentionally violated. Moreover, the calculations need to be managed manually to avoid the premature termination due to numerical issues. Therefore, a significant user skill set is required just to perform the calculation.

6 Uncertainty assessment

As stated already in Chapter 2, uncertainty assessment is essential when best estimate methodology is applied in thermal hydraulic system codes. For this purpose, many different kinds of uncertainty analysis methods have been developed. These uncertainty analysis methods are systematic, and today several methods can be considered well established. However, they concentrate on the evaluation of parametric uncertainties. This chapter presents some of the known methods for uncertainty evaluation.

6.1 Methods for parametric uncertainty evaluation

The internal assessment of uncertainty is a desirable capability for thermal hydraulic system codes. It could consist of the possibility of obtaining proper uncertainty bands each time a nuclear plant transient scenario is calculated.

For assessing parametric uncertainties, various methodologies have been developed for the quantification of the uncertainties. For example in the publications of OECD/NEA (2013) and Pourgol-Mohammad (2009), these methods have been reviewed widely. Statements concerned that the modelling with best estimate (BE) codes contains always simplifications, model approximations, round-off errors and numerical techniques, which cause uncertainties in the calculation. Thus, the uncertainty of the results obtained with the code (code output), which mainly depends on the uncertainty of the code inputs and the modelling itself, has to be quantified to give credit to the predictions obtained (Pourgol-Mohammad et al., 2011).

BEPU

The best estimate codes combined with the uncertainty analysis is known as the Best Estimate Plus Uncertainty (BEPU) approach (D'Auria and Mazzantini, 2011).

The structure of the BEPU is as follows: categorization of postulated initiating event (PIE), grouping of events, identification of analysis purposes, identification of applicable acceptance criteria, setting up of the "general scope" Evaluation Model (EM) and of related requirements starting from the identification of scenario-related phenomena, selection of qualified computational tools including assumed initial and boundary conditions, characterization of assumptions for the Design Basis Spectrum, performing the analyses and adopting a suitable uncertainty method.

In input-driven methods, the perturbations of uncertainty sources in inputs are propagated through code model inaccuracies, resulting in the range/distribution of the figure of the merit. In output-driven methods, inaccuracies of calculations are characterized by comparing measured and calculated output in scaled-down facilities to obtain the uncertainty range in the actual nuclear facility by extrapolation (Pourgol-Mohammad, 2009).

Methods for uncertainty assessment have been proposed and developed for the calculations of the LOCA analysis. The GRS, CSAU, UMAE (CIAU) and IMTHUA methodologies are briefly presented below.

GRS methodology

The GRS methodology (Glaeser et al., 1998) considers the effect of the uncertainty of input parameters like code models coefficients, initial and boundary conditions and other application specific input data and solution algorithm on the calculation results. The GRS method is a probabilistic method based on the concept of propagating the input uncertainties. All relevant uncertain parameters including the code, representation, and plant uncertainties are identified, any dependencies between uncertain parameters are quantified and ranges and/or probability density functions for each uncertain parameter are determined. This method relies on expert judgment and experience from code applications. Separate and integral test and full plant applications are the principal sources of information for uncertain parameters identification and quantification (Petruzzi and D'Auria, 2008).

The GRS methodology has been considered as a powerful statistical framework for uncertainty propagation through code calculation. The Wilks formula (Wilks, 1941) is used to determine the number of calculations needed for deriving the uncertainty bands. A total number of 100 runs is a typical amount for the application of the GRS method. The margin of licensing criteria of 95th/95th percentile would require 59 calculations (Petruzzi and D'Auria, 2008).

CSAU (Code Scaling, Applicability and Uncertainty) methodology

The CSAU method was developed to investigate the uncertainty of single-valued output parameters (Technical Program Group, 1989). The procedure is proposed to evaluate the code applicability to a selected plant scenario. Experts identify and rank phenomena, examining experimental data and code predictions of the studied scenario. In the resulting phenomena identification and ranking table (PIRT), ranking is accomplished by expert judgment, in a systematic way. The PIRT and code documentation is compared, and it is decided whether the code is applicable to the plant scenario. One-dimensional models, time and space averaging (use of relatively large nodes dominating some microscopic scale phenomena) and input level of uncertainty were treated in the original CSAU. Uncertainty is treated qualitatively as well as quantitatively, to consider all sources of information more through code assessment processes. The applicability of the TH code for a specific safety study of a particular scenario was also evaluated through code assessment steps.

UMAE (CIAU, Code with capability of Internal Assessment of Uncertainty)

UMAE (Uncertainty Method based upon Accuracy Extrapolation) is the coupled uncertainty methodology. The UMAE is the prototype method for the consideration of

"the propagation of code output errors" approach for uncertainty evaluation. The CIAU method has been developed with the objective of eliminating/reducing the limitations. The basic idea of the CIAU can be summarized as follows (Petruzzi and D'Auria, 2008):

1. Consideration of plant status: each status is characterized by the value of six relevant quantities and by the value of the time since the transient start.
2. Association of an "extrapolated error" or uncertainty with each plant status.

The method focuses not on the evaluation of individual parameter uncertainties but on the propagation of errors from a suitable database calculating the final uncertainty by extrapolating the accuracy from relevant integral experiments to full-scale NPP. The methodology has been founded on several assumptions (e.g. closeness of phenomena and transient scenarios in larger scale facilities to plant conditions), which cannot be verified methodically. The method utilizes a database from similar tests and counterpart tests performed in ITF, which are representative of plant conditions. The quantification of code accuracy is carried out by using a procedure based on the Fast Fourier Transform based method (FFTBM) (Prosek et al., 2008), characterizing the discrepancies between code calculations and experimental data in the frequency domain and defining figures of merit for the accuracy of each calculation. Different requirements have to be fulfilled to extrapolate the accuracy (D'Auria et al., 2007).

Some levels of qualifications are considered for the implicit consideration of code structure model uncertainty. These include the user and nodalization and test data qualifications. The code is treated as a black box in this methodology, and only code output is compared with the results from the experiments in qualified scaled-down test facilities. The accuracy-based calculations are extrapolated to calculate uncertainties in a full-scale plant. If considering differences in the results of model and reality as model uncertainties, the accuracy calculation stands for the code structural model uncertainty. It cannot be assumed that experimental data are the same as reality, considering measurement errors, applicability and scaling distortions. It gives an overall code uncertainty value and includes uncertainties in all of the uncertainty sources, including code structure sub-model uncertainties. There is no explicit, direct quantification for parameters and models in this methodology. Some levels of qualifications are considered for the code structure model uncertainty. This will help with the accurate quantification as a way to reduce uncertainties in those sources, based on available information and data. The main advantage of this methodology is its automated uncertainty quantification (D'Auria et al., 2007).

IMTHUA

The previously described methodologies are either input-driven or output-driven. The IMTHUA methodology (Integrated Methodology for Thermal–Hydraulics Uncertainty Analysis), developed by the Pourgol-Mohammad (2009), is a hybrid approach where an input-driven "white box" method is enlarged with output correction based on

experimental results relevant to the code output. The "white box" test uncertainty assessment allows the user to peek inside the "box," focusing specifically on internal knowledge of the code to guide the use of data and knowledge.

The IMTHUA methodology has a two-step uncertainty quantification (Pourgol-Mohammad et al., 2011). The first step quantifies the code output uncertainties associated with identified structural and parametric uncertainties at the input and sub-model levels. The second stage updates this uncertainty distribution with any available integrated experimental data and validation information. This "output uncertainty correction" phase is intended to account for the code user choices (user effects), numerical approximations and other unknown sources of uncertainties (model and parameter) that were not considered in the first phase.

The methodology is probabilistic, using the Bayesian approach for incorporating available evidence in quantifying uncertainties in the TH code predictions. The types of information considered include experimental data, expert opinion and limited field data in treating both the model and input parameter uncertainties. The code output is further updated through an additional Bayesian updating with available experimental data from the integrated test facilities. The methodology uses an efficient Monte Carlo sampling technique for the propagation of uncertainty, in which modified Wilks' sampling criteria of tolerance limits are used to significantly reduce the number of simulations.

6.2 User effect uncertainty

Compared to the presentation in Chapter 2, the uncertainty evaluation methods described above are taking care of parametric uncertainties well, but not at all the other types of uncertainty. Uncertainty assessment should cover all possible sources and types of uncertainties.

The user induced uncertainty or more commonly used term "user effect" is another type of uncertainty. In many ISP exercises the significance and importance of the user effect has been recognized (Aksan et al., 1995). The user influence has been particularly noticeable on those blind type cases when different participants using even the same code version produced remarkably different results. The ISP-33 showed that a large variety of results was obtained. Figure 78 presents the variation of the primary pressure. The ISP-33 proved to be a successful and valuable exercise. The observed discrepancies were easier to investigate than in most ISPs because the experiment was not excessively complicated. The reasons for these differences are that the codes still contain large amounts of options that the user can select from. There are possibilities for the user to make decisions between appropriate models, correlations and specific multipliers.

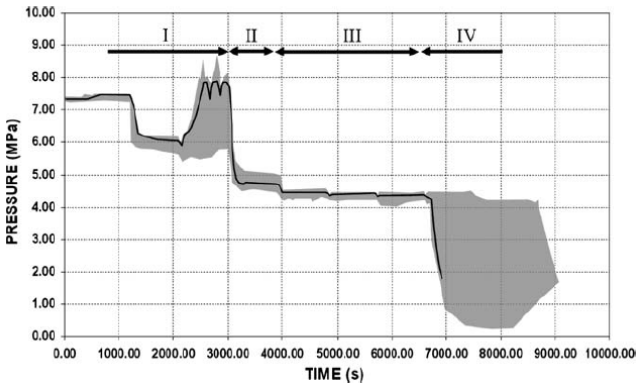

Figure 78: Primary pressure in the experiment (solid line) and variation in ISP-33 post-test calculations (grey area). Flow conditions: (I) one-phase flow, (II) flow stagnations, (III) two-phase flow and (IV) boiler-condenser mode.

User effects of different types have been identified in ISPs. Selected examples (Aksan, 1995) are as follows:

1. Lack of true steady state before the actual transient initiation can affect significantly the overall system balance and thus the final results.
2. System nodalization should be well established considering the anticipated important phenomena.
3. Misinterpretation of the experiment data used in validation.
4. User has not recognized that there is no specific model in the code to simulate the phenomenon in concern.
5. Approximations have to be made, for example defining material structures, masses etc.
6. Choices of physical and numerical options, for instance in break flow calculation.

The uncertainties recognized in the PACTEL validation experiments and uncertainties presented in ISPs by Aksan (1995) along with the TMI-2 modelling exercise were gathered together for comparison. Different uncertainty types are presented here according to the earlier classification proposal. They are divided into three main categories: physical, nodalization and parametric uncertainties. Table 11 presents the summary of all these cases and their uncertainty relations. This simple categorizing shows that parametric uncertainties form only a minor portion of the total spectrum of uncertainties. The assessment of parametric uncertainties is the most straightforward methodology in the quantification of overall uncertainties.

Table 11: Different uncertainty type classification proposed for ISPs with observed uncertainties in TMI-2 modelling exercise and selected PACTEL experiment calculation cases.

Uncertainty type	ISP effects	TMI-2	PACTEL
Physical	3, 4, 6		SIRs, SBLs, IMP-06, PSLs
Nodalization	1, 2, 3	X	LOF-10, PSLs, ATWS-32
Parametric	3		FLTs, HLs, SBLs

There are still many other types of identified acts in the modelling that can be considered as user effects. To reduce the user effect, some suggestions have been introduced (Aksan et al., 1995):

- The new code user should be trained and qualified by experienced user.
- The user guidelines and instructions should be well established.
- User discipline should also be considered. The extreme "tuning" to achieve identical calculation results with the experiment by using completely unrealistic input parameters is not desirable. This approach in modelling concludes confusion on true code capabilities and deficiencies and should be avoided.
- Clear quality assurance in preparation and testing of input model should be acquired.
- Also, code improvement should be focused on reduction of user effect. This means that the code would automatically define the mesh refinement based on local flow conditions and user should avoid deciding minimum cell or node sizes for specific components.

Despite the wide experience in ISPs and code developers' intention to decrease the number of options and parameters that the user has to choose obligatorily, no substantial reduction in the user effect has been achieved thus far.

The complete accuracy and acceptability of the thermal hydraulic analysis is defined by the success of the overall uncertainty evaluation. The user effect part of the uncertainties is very difficult to quantify. Thus, user training and experience have an important role in minimizing errors in analyses.

6.3 Uncertainty assessment for PACTEL simulations

The PACTEL experiment calculations with TRACE were performed to reach the best correspondence with the experiments.

The nodalization structure of the input was qualified after many test cases to reach the optimum structure. The best accuracy was reached with numerous parametric sensitivity

calculations. Due to the limited scope of the validation, the procedure did not include any possibilities to evaluate parametric uncertainties with the uncertainty assessment methods described before.

Various choices were made during the input model development process and during the preparation of the model for different validation cases. In the TRACE code, there are a number of parameters that the user has to choose from and optional parameters that the user can change when necessary. The main goal was to validate the input to such a stage that it would be the best estimate input for the purpose in question. In some cases, a large variety of parameters was tested since there was no background data by which the magnitude of the parameter could have been estimated. Some valve properties were tested by a large range of parameter variations due to lack of data from the manufacturer.

The code user induced uncertainties are based on the choices that the code user makes. This also contains the uncertainty type, which is usually called the "user effect". At first the decision has to be made what is the necessary amount of nodes that should describe the desired phenomenon.

An example of simplified horizontal steam generator modelling shows how the user choices can prevent gaining necessary information. In this model (see Figure 79), with the TRACE implementation, the main parts and components of the steam generator are taken into account and modelled. However, each component is created using only a minimized number of nodes. This leads to a situation in which the most essential phenomena cannot be observed at all due to the rough nodalization. Even if the nominal operating values could be reached, that is, the amount of heat is correctly transferred and the primary and secondary side flows are correct, there is no guarantee of truthful operation in transient situations. For example, the loss-of-feedwater transient is almost non-recognizable and beyond accurate modelling approach. The revealing of different tube rows and boil-off on the secondary side are not possible to be modelled correctly because heat exchanger tubes are modelled with only one tube layer. Apparently, steam superheating on the secondary side cannot occur either.

The adequacy of physics modelling in a code is one uncertainty category. The PACTEL facility and PACTEL experiments did not bring out phenomena that the two-fluid model in the TRACE code would not cover. The hot leg loop seal design in VVER resembles to some extent the B&W candy cane like piping (TMI-2), where axial thermal conductivity in the fluid has considerable effect on the progress of loss of coolant transients; fluid axial conductivity is not modelled in the TRACE energy equations. However, no evidence of this effect was found in any of the PACTEL experiments. Thus it can be concluded that the TRACE physics modelling is sufficient to represent all the PACTEL tests analysed in this work. Adequacy of physics modelling can be evaluated only if the user has the understanding of the phenomena taking place and Integrals Effect Tests (IET) data is available representing the whole accident sequence of interest.

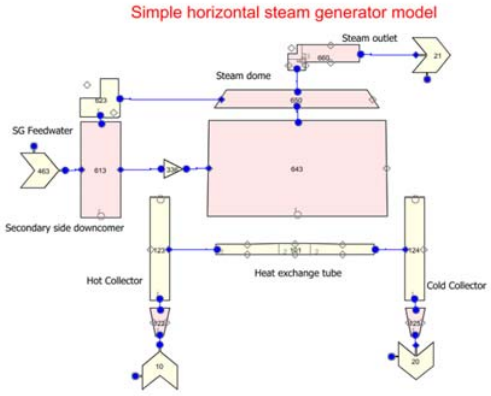

Figure 79: Simple standalone model of horizontal steam generator. TRACE code formulation.

6.3.1 Uncertainty factors observed in calculations of PACTEL experiments

The preparation of PACTEL input modelling and simulation calculation work with the TRACE code provided important information concerning different kinds of uncertainties.

The modelling of PACTEL experiments with the TRACE code introduced several uncertainty factors. These factors are gathered in Table 12. The most significant uncertainty factors are presented. The evaluation of the uncertainty factor is categorized taking into account the nature or source of uncertainty. Five different categories are presented here.

1) Experimental / Data uncertainty. Some properties were only vaguely on record or simply not known at all. Even if some properties were recorded, there were contradictions with data that was derived indirectly or with another method.
2) Physical uncertainty. Doubt in lack of modelling capabilities of physics.
3) Nodalization uncertainty.
4) Parameter uncertainty.

The presented uncertainties are qualitatively assessed. The comprehensive quantitative analysis is difficult especially concerning the uncertainties that stemmed from the nodalization.

The factors in Table 12 contain the following observations:

- Form loss definitions (FLT experiments) contain a parameter set of form loss coefficients.
- Heat loss definitions (HL experiments) contain a parameter set of material thermal properties.
- Number of tube rows (LOF-10) in steam generator. Rate of lumping to achieve optimized nodalization.
- Data uncertainty (SIR-23) in core power.
- SIR-21 operation in low pressure range, physics.
- SBL-experiments contain a parameter set of loss coefficients and critical flow multipliers in break.
- Inventory distribution is relevant in all experiments containing break and systems to compensate inventory losses.
- Primary to secondary heat transfer is an essential modelling factor in all experiments.
- Specification of certain component details is an essential factor.

Table 12: Classification of uncertainties in the TRACE modelling of PACTEL experiments.

Experiment	Uncertainty factor	Nature or source of uncertainty			
		Exp	Phys	Nodal	Parameter
FLT-XX	Local pressure drop				Form loss coefficient
HL-XX	Material thermal properties Facility heat loss distribution				Insulation material therm. prop.
LOF-10	Number of tube rows in SG Primary to secondary heat transfer			Nr. of tube rows	
SIR-23	Core power value Inventory distribution	Pow. data		Upper plenum diffuser	
SIR-21	Operation on low pressure range Inventory distribution		Low press		
SBL-30	Break flow				Critical flow multiplier
SBL-31	Break flow Inventory distribution, ECC inj.			DC top diffuser	Critical flow multiplier
SBL-33	Break flow Inventory distribution, ECC inj.				Critical flow multiplier
IMP-06	Break flow Inventory distribution, ECC inj.			Core bypass	Critical flow multiplier
PSL-10	Break flow Inventory distribution Pri/sec Heat transfer	Break flow rate		SG recirc.	Form loss multiplier at break
PSL-11	Break flow Inventory distribution Pri/sec Heat transfer	Break flow rate		HPI flow	Form loss multiplier at break
ATWS-32	Valve openings Valve modelling ECC inj.	Flow rate in valves		Pressur. & Valves	Critical flow multiplier in valves and/or valve opening characteristic

6.4 Concluding remarks on uncertainties

ISPs and TMI-2 modelling exercise have pointed out important insights to the appearance of uncertainties in the thermal hydraulic code validation work.

The validation of the PACTEL facility modelling brought out similar aspects of uncertainties. They can be divided into three main categories: physical, nodalization and parametric uncertainties. The concluding remarks are:

1) One-dimensional two-phase flow representation with parallel (lumped) flow channels is adequate to represent the PACTEL facility and its behaviour. This is to be expected because PACTEL is a height conserving volumetrically down-scaled facility, where the flow path length over diameter ratios (L/D) are prototypic or higher.
2) Nodalizing the VVER-440 geometry is possible within code guidelines, except for the horizontal steam generator. Incorrectly timed pressurizer draining, similar to the old TMI-2 simulations, also occurred in ATWS-32 PACTEL calculation.
3) Parametric uncertainty affects boundary conditions; break flow, heat losses and local friction loss coefficients.
4) User effect in terms of option selection and time step management.

The user effect is an uncertainty category that is very difficult to analyse. The user effect is related to the decisions that the user makes when preparing the input nodalization and choosing the parameters and options.

The traditional approach contains the assessment of parametric uncertainties. This is the most straightforward methodology in the quantification of uncertainties. Parametric uncertainty is the only uncertainty category that is statistically quantifiable, as required in Guide YVL B.3 by STUK.

The representativeness of a component nodalization can be assessed against component-specific separate effect tests (SET).

The presentation of physics in a code is one uncertainty category. Physics can be evaluated only if the user has the understanding of the phenomena taking place and Integrals Effect Tests (IET) data is available representing the whole accident sequence of interest.

7 Comparison of flow reversal mechanisms in horizontal steam generator and vertical U-tube steam generator

Previous chapters have discussed the VVER-specific steam generator behaviour including the flow reversal in steam generator tubes on the primary side. The primary side tube flow reversal can occur also in vertical U-tube steam generators (De Santi and Mayinger, 1993; Jeong et al., 2004; Yonomoto, 2005; Yang et al., 2008). In this chapter, both cases are studied further by means of theoretical analysis and TRACE code calculation.

7.1 Flow reversal in horizontal steam generator

As the main recirculation pumps start to coast down after the reactor scram, forced circulation in the primary loops changes to natural circulation. All three different natural circulation flow modes; the single phase liquid flow, the two-phase mixture flow and the boiler-condenser mode; are found.

The tube flows at the bottom of the SG tube bundle are reversed soon after the primary loop flow changes to natural circulation. As stated, Hyvärinen (1996) has given the following explanation of the reasons leading to this kind of behaviour. The onset of internal circulation in the SG results because at low flows, the total frictional pressure drop through the tubes falls below the counteracting gravitational pressure difference of the collectors. As long as the primary side is hotter than the secondary side, the circulation will always tend to transport coolant from the hot to the cold collector through the topmost tubes and bring cold coolant back from the cold to the hot collector through the bottom tubes. Once the circulating flow pattern has emerged, most of the primary-to-secondary heat transfer takes place at the top of the tube bundle and near the hot collector. The internal circulation in the SG tube bundle is also present during the boiler–condenser mode as long as the secondary side is cooler than the primary side. This is apparent if we keep in mind that the reversed flow is essentially caused by the collector density difference. As a result of steam voiding, the density variations are even larger in the two-phase than in one-phase flow period. In two-phase natural circulation, the energy transport is primarily affected by condensation in the SG. Thus, hot collector phase separation plays an important role because it forces a large fraction of the steam into the top rows of the tube bundle.

Inspired by the findings in the research by Hyvärinen (1996) concerning the flow reversal phenomenon, the flow behaviour in the lowest tube rows was also investigated in more detail with the TRACE code. Hence, the mass flows in different pipes representing the tube rows as well as pressure differences between hot and cold collectors were studied. The calculation results showed clearly that flow reversal in the steam generator tubes occurred also with the TRACE code modelling as seen in previous chapters. The change of pressure head between hot and cold collectors in the beginning of the natural circulation phase caused the flow reversal in the lowest two

pipes. The calculated pressure differences between hot and cold collectors show clearly that the two lowest pressure differences are negative when the flow rate is changed to correspond to the natural circulation rate in the experiment.

During the boil-off of the horizontal steam generator, heat transfer was found from the tube temperature measurements along the axial direction. The calculation results verify this observation. An example of this is presented in Figure 80. The axial temperature distribution disappears at time 4500 s, and heat transfer degrades when the secondary side collapsed level decreases below the tube row. The heat transfer coefficient to the pure steam is significantly lower than the boiling heat transfer coefficient.

A conclusion can be drawn that in the horizontal steam generator modelling, the heat transfer degradation phenomenon during the decreasing secondary side level is strongly affected by nodalization. Especially, if the top part of the heat exchanger tubes is lumped together too much, for example one tube is modelling three tube rows, the heat transfer rate remains too high and too long. If the lumping of tube rows continues consecutively, the total heat transfer will be misrepresented. This can apparently lead to an overestimation of the success of heat transfer and primary pressure control.

Similarity to the TMI-accident scenario can be considered in this frame. The loss of secondary side feedwater was an initiating event, which led to severe consequences. The analysis of this kind of a transient scenario using inadequate nodalization choices can affect heat transfer estimation and also the primary side pressure propagation relating to safety and time margins.

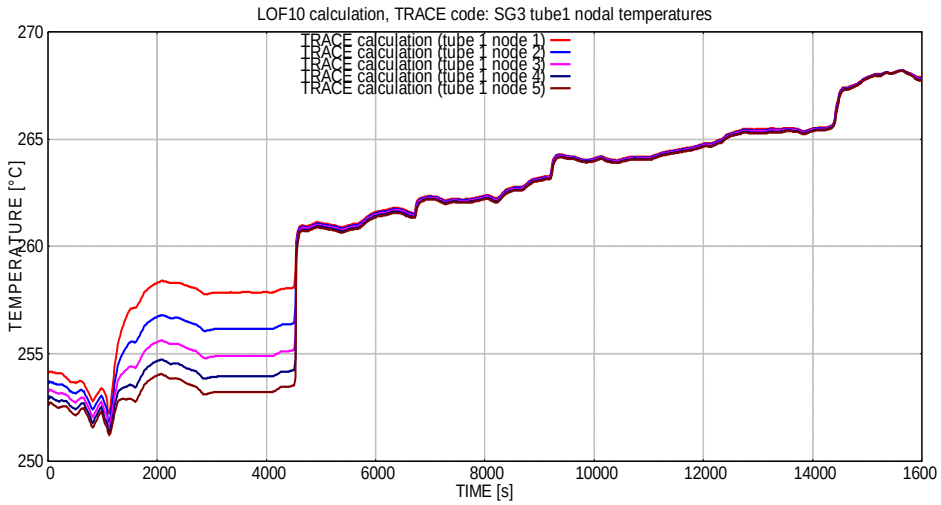

Figure 80: Calculated temperatures in the nodes of the top heat exchanger tube.

Flow directions in steam generator tubes during different natural circulation modes

Small flow rates are difficult to measure. Experiments are usually not able to present changes in flow directions. The calculations can produce this information easily. Following three animation frames (see Figure 81a, Figure 81b and Figure 81c) present the liquid flow directions in heat exchange tubes. The first frame indicates and confirms the previously presented result of flow reversal in three lowest tube rows during single phase natural circulation. The second frame is describing the two-phase flow situation when water level in steam generator collectors is decreasing and flow directions change. The third frame is captured from the boiler condenser mode. It is seen that liquid is flowing out from both ends of the middle node. This phenomenon is apparently due to slightly inclined tubes. The highest elevation is in the centre of the middle node, thus water can run naturally to both directions out from the node. The liquid in the hot leg side is highly oscillating while it cannot climb uphill in the hot leg and flow backwards towards the core.

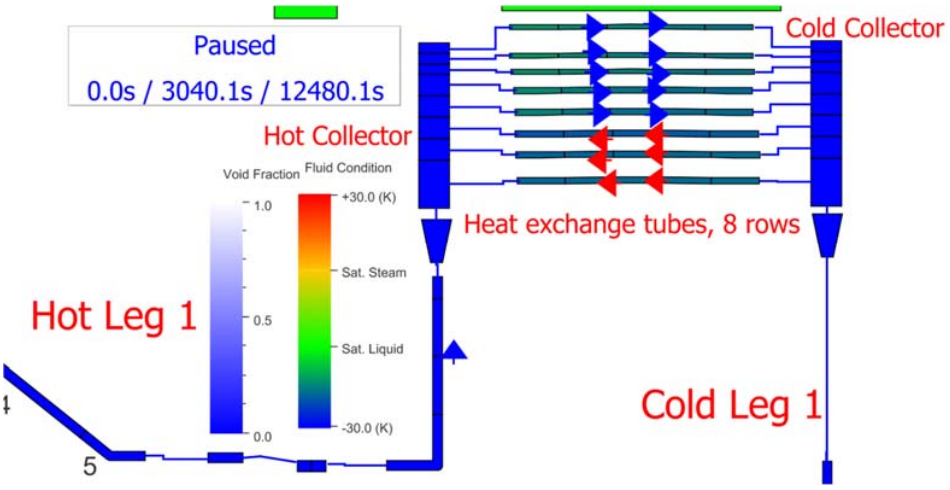

Figure 81a: Flow directions in heat exchanger tubes during single phase natural circulation flow mode. Animation illustration of TRACE calculation of SBL-30.

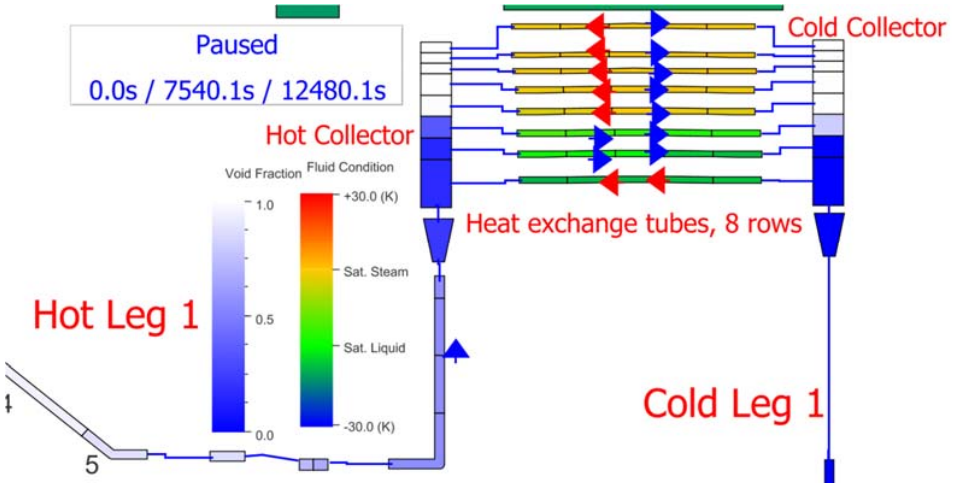

Figure 81b: Flow directions in heat exchanger tubes during two-phase natural circulation flow mode. Animation illustration of TRACE calculation of SBL-30.

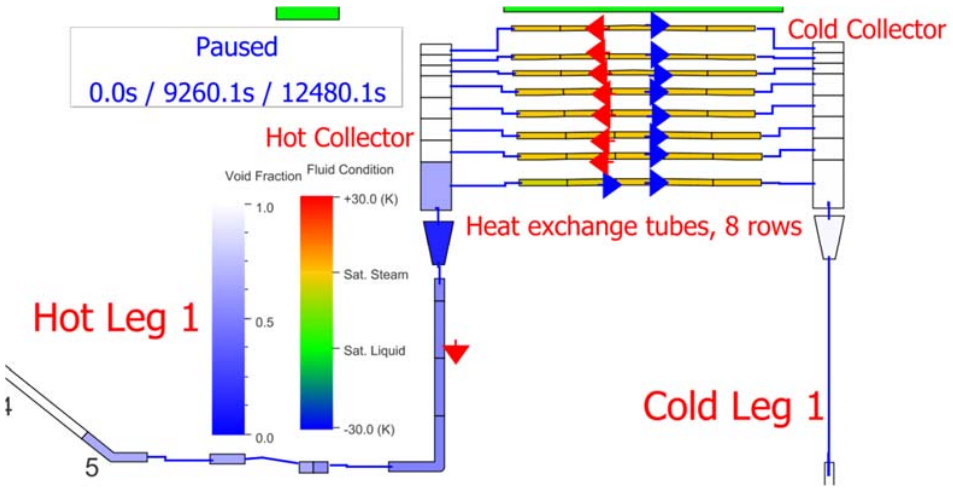

Figure 81c: Flow directions in heat exchanger tubes during boiler-condenser natural circulation flow mode. Animation illustration of TRACE calculation of SBL-30.

7.1.1 Calculation extension

The actual LOF-10 experiment was terminated at 16000 s. The eight tube layer nodalization produced rather good results compared to the experiment LOF10. Particularly, the early phase until the end of LOF-10 experiment data the horizontal steam generator level depletion was almost precisely modelled. However, the data gave only a situation when only four tube rows were dried out. Beyond this point, with the computer code model it was possible to continue the studies of the case and check the further propagation of the found phenomena. The boundary conditions were remained to the same values as in the final stage of the actual transient. The calculation was continued, and it was terminated at time 50000 s.

As the boil-off of the secondary side was continuing, the secondary side collapsed level also continued decreasing. The flow in the second lowest pipe row remained reversed until the level reached the corresponding node. The flow in the lowest pipe row also remained reversed and turned to the normal direction finally at 35000 s, when the lowest level had almost reached the bottom of the secondary side (Figure 82a and Figure 82b).

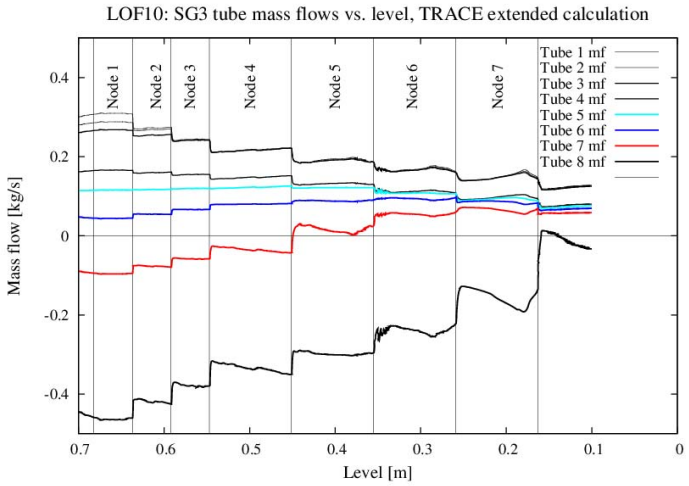

Figure 82a: Mass flow rates in heat exchanger tubes versus collapsed level on the secondary side. Vertical lines illustrate node edges. LOF-10 extended calculation.

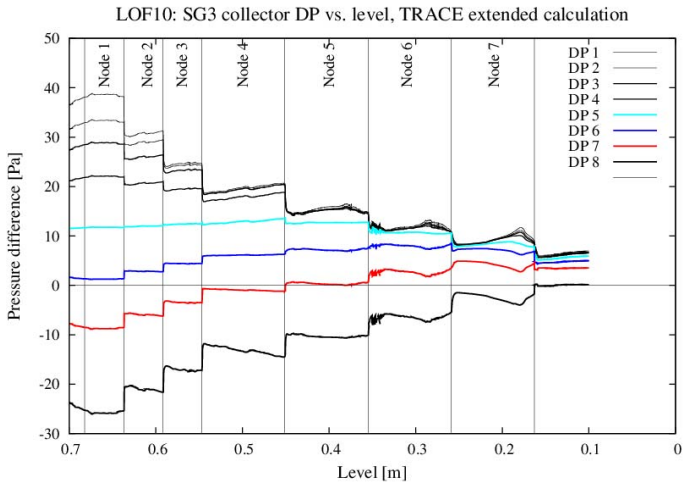

Figure 82b: Pressure differences between hot and cold collectors of steam generator vs. collapsed level. Vertical lines illustrate node edges. LOF-10 extended calculation.

Horizontal Steam Generator experiment HSG-1 (Hyvärinen and Kouhia, 1997) provided special data from the boil-off phenomenon. The main purpose of this experiment was to enlighten the heat transfer degradation as the secondary side depletes and complete boil-off takes place. This experiment was accomplished with multiple actions considering core power and secondary side pressure reductions. Thus, is not fully comparable to the LOF-10 experiment. Due to the complicated actions, the HSG-1 experiment was not simulated with the TRACE code. However, the extended LOF-10 calculation and HSG-1 experiment were compared. Dimensionless power as a function of wetted tube rows is presented in Figure 83. The HSG-1 curve and LOF-10 calculation curves are equal only when all tubes are wetted. Otherwise the difference is remarkable. In the HSG-1 experiment procedure the secondary pressure was reduced in several steps in order to maintain the absolute heat transfer reasonable even though the dimensionless transferred power degraded as the secondary side depleted. These actions in HSG-1 deviate largely from the LOF-10 calculation procedure explaining the most of the disagreed results. The discrepancy is partly due to the fact that nodalization is coarser at the lower part than at the upper part of the steam generator pool.

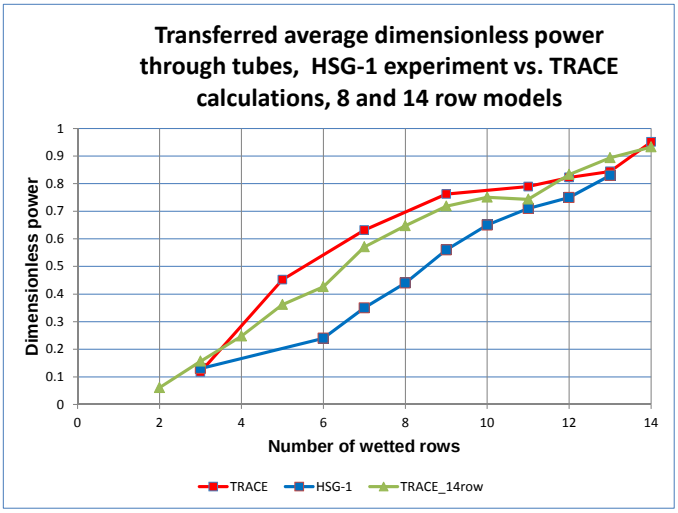

Figure 83: Transferred average dimensionless power through horizontal steam generator tubes as a function of number of wetted tubes in HSG-1 experiment vs. TRACE calculation, 8 and 14 tube layer models.

7.1.2 Detailed nodalization case with 14 tube layers

Additional and more detailed nodalization study was carried out. The purpose of this study was to find out how large dependency on the nodalization the calculated steam generator behaviour has. All the 14 tube rows of the PACTEL horizontal steam generator were modelled to check whether any improvement could be achieved. The model was modified on the secondary side as well. Each tube row on the primary side had a corresponding node on the secondary side pipe component. The downcomer part of the secondary side was also split to 14 nodes. Thus, the modelling modifications compared to the eight row model were targeted to the low part of the steam generator.

Although preliminary calculations were run, only a slight improvement was observed in the steam generator behaviour. During steam generator depletion the dimensionless power as a function of wetted tube rows showed some improvement compared to the eight tube row model (see Figure 83). However, the result of the 14 row model diverged still from the experiment HSG-1 considerably. The calculated dimensionless power behaviour was noisy, and it was not continuously decreasing. When ten tube rows were wetted, the calculated dimensionless power was increased compared to the conditions at 11 wetted tube rows. This occurred because the power throughput of the tube rows at the low part was increased significantly; the result is questionable because all experiments consistently show that the power transferred decreases with the decreasing number of wetted tube rows (secondary level).

This analysis shows that simply adding detail to the nodalization could not produce the full agreement with experiments. Future work should represent the experimental

conditions more closely, in order to see if the discrepancy between measurement and calculation prevails. If it does, then more detailed analysis of axial tube temperature distributions, indicating flow rates and heat transfer efficiencies at various elevations, are justified.

7.2 Flow reversal in UTSG

The preferential flow reversal in the long U-tubes has been observed in several experiments performed with the LOBI, SEMISCALE, BETHSY, PKL and ROSA/LSTF facilities (Yonomoto, 2005; Jeong et al., 2004). Hence, a good understanding of the flow behaviour is important. In vertical steam generators the pressure difference between the inlet and outlet plenum decreases with an increasing mass flow rate under low flow conditions. In this region, the mass flow rate is not a single valued function of the pressure drop, and flow excursions can occur (Figure 84). The primary side flow is stable only if the flow rate is higher than a specific threshold value (Yonomoto, 2005). For a negative pressure difference between the inlet and outlet plenum (the pressure at the inlet plenum of steam generator is lower than at the outlet plenum), three solutions exist for the U-tube flow rate corresponding to stable positive, unstable positive and stable negative (reverse) flow rates. When the flow rate in the U-tube falls into the unstable region, the flow inside the U-tube changes into either the positive (point D) or negative (point B) stable flow so that the unstable flow (points A and C) can be avoided.

Therefore, during natural circulation under a low flow condition, the outlet plenum pressure is higher than the inlet plenum pressure because of the global density differences between the up flow and down flow sides of the U-tubes, that is, lower densities on the up flow side and higher densities on the down flow side. That can drive the reverse flow in some U-tubes. The flow reversal tends to occur preferentially in the longer tubes (Yonomoto, 2005; Jeong et al., 2004). Because of the longer flow path, there is less flow in the long U-tubes. Thus, the fluid in these long tubes rapidly cools to the secondary side temperature. Because of the uniform fluid temperature distribution along the long U-tubes the gravitational head difference in the long U-tubes tends to be zero. Since all U-tubes in a steam generator are connected in parallel into the same inlet and outlet plenums, the same pressure difference exists in all the U-tubes. Because of the negative pressure difference between the inlet and outlet plenums the fluid moves from the outlet plenum to the inlet plenum through the long U-tubes. When the reverse flow occurs, the cold fluid flows back from the outlet plenum to the inlet plenum and mixes with the hot fluid from the hot leg. That causes a sharp drop in fluid temperature in the inlet plenum of steam generators (Yang et al., 2008).

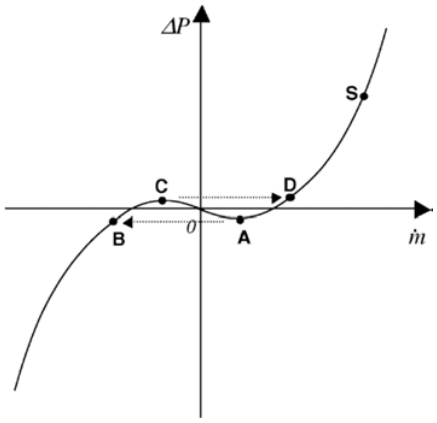

Figure 84: Flow excursions in the unstable flow region (Jeong et al., 2004).

7.2.1 **PWR PACTEL studies**

Three PWR PACTEL experiments (RF-02, RF-03 and RF-04) were carried out to experimentally verify the flow reversal in the vertical steam generator tubes for single phase liquid flow (Riikonen et al., 2011). The RF-02 and -03 were single loop experiments, and both the loops were used in the RF-04 experiment. All the experiments were carried out in steady state natural circulation. The primary side pressure was 7.5 MPa in all experiments and the secondary side pressure and core power was varied between different experiments. The total mass flow rate in the experiments varied between 1.1 kg/s and 1.3 kg/s. With the new differential pressure measurements between the inlet and outlet plenum and with the new temperature measurements in the steam generator plenums the non-uniform flow characterized by the coexistence of the normal and reversed flow was observed directly in the experiments for single phase liquid flow. The hot plenum temperature in the steam generator was significantly lower (e.g. 240 °C in RF-02) than the hot leg temperature (e.g. 277 °C in RF-02). Similar phenomenon was observed in all of these experiments.

These results indicated that intensive flow reversal occurred in the steam generators tubes. Further analyses showed that approximately in one third of the heat exchange tubes the flow was reversed. The analyses showed that most of the tubes, where reversed flow occurred, were located nearby the hot plenum inlet. It was also found that the amount of tubes where flow reversed was independent of the secondary side conditions.

The flow reversal phenomenon in the U-tubes of vertical steam generators was studied also with the TRACE code. Three different cases were introduced. The first two cases were carried out with a simple model of two tubes with different lengths transferring heat to the secondary side modelled as one pipe. The third case was an extraction of the PWR PACTEL steam generator as a stand-alone model with the primary flow boundary condition. In all the cases the primary side conditions at the inlet were 75 bars and 270 °C while the secondary side pressure was set to 43 bars.

Case 1: Stand-alone model, two tubes and pressure difference boundary condition
To test the TRACE code performance, the similar approach to the reference (Jeong et al., 2004) was adopted. However, the PWR PACTEL U-tube geometry and the thermal parameters used here differed from the reference case. The objective was to see how the flow reversal will occur when the pressure difference between the hot and cold collectors is introduced. Two tube lengths, the longest and the shortest tubes of the PWR PACTEL model, were used.

Case 2: Stand-alone model, two tubes and mass flow boundary condition
The second case was almost similar to the first case. In this case the inlet boundary condition was introduced using a FILL component by changing mass flow rate. Inlet flow was decreased linearly from 1 kg/s to zero and then back to 1 kg/s during 2000 s. A sudden change occurred when the inlet mass flow rate decreased below 0.26 kg/s. The flow in the longer tube reversed suddenly, and flow in the shorter tube increased to compensate the reversed flow. When the inlet mass flow started to increase, the flow in the longer tube did not change back to the normal direction similarly as during the decreasing mass flow period. Neither correspondence of timing nor mass flow rate was found between decreasing and increasing inlet flow periods.

Case 3: PWR PACTEL SG1 stand-alone model, mass flow boundary condition
The third case was an extraction of the PWR PACTEL steam generator as a stand-alone model with the primary flow boundary condition from the hot leg. This model contains five different tube lengths. The inlet mass flow was induced starting from 2 kg/s and decreasing linearly to zero in 1000 seconds. No flow was injected during 500 seconds. The flow was then increased back to 2 kg/s in 1000 seconds.

During the decreasing period the flow in the middle length tube reversed immediately after the inlet flow started to decrease. When the inlet flow rate decreased below approximately 0.6 kg/s, also the flow in the shortest tube reversed. During the no flow period the flow in the second shortest tube reversed. When the inlet flow started to increase, the flow directions were changed back to normal one by one. First the flow direction in the middle length tube was changed back, then the shortest tube and finally the flow in the second shortest tube. Additional changes between the directions of different tubes were observed. For example simultaneously with the flow recovery in the second shortest tube, the flow in the middle length tube reversed again for a short period. The results of the third case showed that the flow reversal is occurring but not the way that was expected on the basis of the results from Case 1 and Case 2. The flow did not reverse at all in the longest tubes.

A conclusion can be made of the TRACE code calculations that the flow reversal can take place in the U-tubes of the vertical steam generators. This phenomenon was investigated with a simple two tube flow model and a more detailed model with five tube lengths of the PWR PACTEL facility model. This investigation suggested that the flow reversal behaviour is dependent on whether the inlet flow to the steam generator is decreasing or increasing.

Apparently more studies are needed to map all affecting factors and reasons for the flow reversal phenomenon. In particular, in calculations the order of reversal (long, medium or short tube first) is different in the down and up ramps; this suggests that there is a history

effect, due to density distribution in the tubes. Tube density profile is driven by tube temperature profile, which is less steep at high flow than at low flow. During continuously changing inlet flow rate, the profile does not have time to settle into a steady-state value, but carries some memory of whether the flow is coming from the high rate downwards (less steep profile, smaller tendency to reverse) or low rate upwards (steeper profile, higher tendency to reverse). Occurrence of flow reversal is determined by a delicate balance of gravitational head and wall friction; careful modelling of these factors in an interconnected multi-tube system is needed.

8 The sense of "validated code"

Validated code and validated model are terms that have not been defined precisely in the literature. The minimum interpretation of the term "validated code" is, traditionally, that the code itself is considered as good enough for the analysis envisioned. In the frame of this work, the validation of thermal hydraulic code assumes a rather broader sense. Validated code should have the following definitions fulfilled:

- known to contain all necessary physics,
- known to be able to represent real geometry adequately and
- known ranges for parameters of experimental correlations and engineering factors.

The code validation is carried out against the experiment data. The general requirements for the data are that there should be appropriate, accurate and sufficient data available. Thus, the data conversions and transformations should have been made correctly.

There is no set of specific tests, algorithms, techniques or procedures that could be applied to determine the 'correctness' of a model. Some practical approaches have been developed for the verification and validation of the simulation models. Sargent (2013) has addressed general viewpoints to determine validated models. A model should be developed for a specific purpose and its validity determined with respect to that purpose. If the purpose of a model is to answer a variety of questions, the validity of the model needs to be determined with respect to each question. Numerous sets of experimental conditions are usually required to define the domain of a model's intended applicability. A model may be valid for one set of experimental conditions and invalid in another. A model is considered valid for a set of experimental conditions if the model's accuracy is within its acceptable range of accuracy, which is the accuracy required of the model for its intended purpose.

The intended purpose of thermal hydraulic codes is to predict the behaviour of nuclear power plants in abnormal conditions. The plant behaviour must stay within the envelope given by applicable design requirements and acceptance criteria of the analyses. Compliance with the acceptance criteria must happen with confidence.

It is often too costly and time-consuming to determine that a model is absolutely valid over the complete domain of its intended applicability. Instead, tests and evaluations are conducted until sufficient confidence is obtained that a model can be considered valid for its intended application (Sargent, 2013). Figure 85 shows a schematic presentation of this approach. This approach can be characterized as an optimization task between the cost and value of the model to the user. The cost curve is typically invariably increasing. The value of the model to the user curve has a decreasing derivative change rate when approaching to the maximum in confidence. The optimum can be found. Thus, it is not worth of putting cost effort beyond sufficient confidence level has been reached. The sufficient confidence means that some uncertainty is acceptable and is to be covered by safety margins.

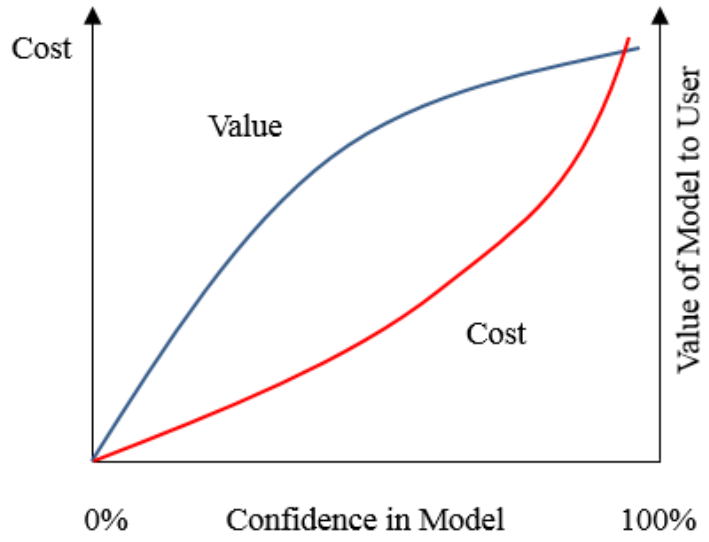

Figure 85: Schematic presentation of cost vs. value of model to the user.

Based on the compilation of earlier exercises and research work presented here, the definition for term “validated code” can be proposed. The Best Estimate approach has to be broadened from the code to incorporate the input as well. In even wider sense, the term “validated” has to be extended to the user or users of the code.

Validation of code input:

- General code input; applicable for all envisioned purposes. Tested against representative experiments and known to reproduce the observed *system behaviour* at acceptable (always imperfect) accuracy. Typical range of differences between main calculated and measured variables.
- Collection of separate inputs for various purposes. These would be used when high accuracy for one particular variable is desired; then dedicated input refinements are feasible at reasonable effort.

User validation:

- A user performing the validation work gains the experience of using the specific code.
- A group of users may get validated more efficiently than an individual if some group members are already experienced users. They can then speed up the learning curve of the inexperienced users.

Validation should result in uncertainty estimates that can be shown acceptable on all levels of Physical, Nodalization and Parametric uncertainties.

The term "validated" is extended here to cover the code itself, the input deck that describes the problem in question and also the user, who prepares the input model and runs the calculations. In the end, the scientific communities, plant operators and regulators, who represent the original problem field, and who set, assess and approve the acceptability criteria of the results, must be satisfied with the results.

9 Conclusions

This thesis deals with the validation of a generic thermal hydraulic computer code TRACE under the challenges of the VVER-440 type reactor. The code capability to model the VVER-440 geometry and thermal hydraulic phenomena specific to this reactor design has been checked and found acceptable.

The main challenge in the VVER-440 thermal hydraulics appeared in modelling of the horizontal steam generator. The major challenge here is not in the code physics or numerics but in the formulation of the representative nodalization structure. Another VVER-440 specialty, the hot leg loop seals, challenges the system codes functionally in general, but was proven readily representable.

It is important to define when validation is focused on the code itself and when on the input deck. In the frame of this thesis, a new input validation methodology was developed. A properly validated input model allows the identification and assessment of uncertainties of different characters at different levels of the modelling (selection of basic physics, discrete representation, input parameters).

It is important that parallel flow channels are described in sufficient detail. If boundary conditions are correctly set, the pressure behaviour and the total inventory modelling are quantitatively correct in all cases involving the loss of primary inventory. However, even correctly predicted total inventory in the primary circuit may be *incorrectly distributed* due to the nodalization characteristics. The timing of flow stagnation or core uncovery may differ from the experiment or, worse yet: the event may not be predicted at all.

Loop seal clearing taking place in correct succession is very difficult to calculate. In reality, the nature of this phenomenon is unstable, and thus the predictability in calculations is inherently poor. It is not reasonable to expect that the code would correctly predict the loop that clears when the clearing is triggered by an essentially random process.

Although the TRACE code has not been originally developed for the special geometry of the VVER-440 reactor type, it was proven that the code is capable for relatively accurate modelling on VVER-440 features if nodalization is implemented to properly represent the necessary details. Some code guidelines need to be violated to achieve this, though. Additional user effort is needed to steer the calculations over numerical instabilities that arise as a consequence of guideline violation.

The novel validation method presented in this thesis can be applied also to other thermal hydraulic system analysis codes similar to TRACE.

The presented simulations of PACTEL experiments indicate that no physical deficiencies appeared that could prevent the use of the TRACE code for the VVER-440 reactor type modelling. PACTEL, as a "thin" facility, is more one-dimensional than the real plants. Therefore, it is to be expected that the real plant prediction accuracy is not better than that achieved in PACTEL calculations.

In all practical applications, the system nodalization has to be optimized between lumping and detailing. The user must make sure that important information is not lost via excessive lumping when creating nodalization. Not only the node size is crucial but also the structure of the model, especially a representative number of parallel channels, is important to reach good calculation results.

Uncertainties have been classified into three main categories requiring dedicated means for uncertainty quantification:

1) Physical	- system Integral Effect Tests (IETs)
2) Nodalization	- component Separate Effect Tests (SETs)
3) Parametric	- statistic variation of input parameters

Statistical uncertainty quantification methods developed so far tackle usually well the parametric dependencies of the code models, but less or not at all the problematics of the nodalization structure or missing physics. Furthermore, some fraction uncertainties are likely to remain hidden when it comes to human errors in code developing and using them. The reduction of the user effects is possible only with systematic and mentored training and along with experience; confidence in code and user capability can only emerge if Separate Effects Tests and Integral Effects tests representative of the situation of interest are available for comparison.

This thesis presented a novel approach to the input model validation and uncertainty evaluation in the different stages of the computer code validation procedure. This new approach completes essentially the commonly used uncertainty assessment methods, which are usually conducted using only statistical methods. This thesis also showed that in the safety analysis, there are inevitably significant uncertainties that are not statistically quantifiable; they need to and can be addressed by other, less simplistic, means, ultimately relying on the competence of the analysts and the capability of the community to support the experimental verification of analytical assumptions.

References

Aksan, N., D'Auria, F., Glaeser. H., Pochard. R., Richards. C. and Sjöberg, A., (1994). Separate Effects Test Matrix for Thermal-Hydraulic Code Validation. Volume I&II, OECD/GD (94)82&83. OECD, Paris, France.

Aksan, S.N., D'Auria, F., Städke, H., 1995. User Effects on the Transient System Code Calculations, Final Report, NEA/CSNI/R (94)35, OECD, Paris, France.

Carlos, S., Sánchez, A., Ginestarc, D., Martorell, S., 2013. Using finite mixture models in thermal-hydraulics system code uncertainty analysis, Nuclear Engineering and Design, 262 (2013) 306–318.

D'Auria, F., Galassi, G.M., 1998. Code Validation and Uncertainties in System Thermalhydraulics, Progress in Nuclear Energy, Volume 33, No. 1/2, 1998, Pages 175–216.

D'Auria, F., Galassi, G.M., 2010. Scaling in nuclear reactor system thermal-hydraulics, Nuclear Engineering and Design, Volume 240, Issue 10, October 2010, Pages 3267–3293.

D'Auria, F., Mazzantini, O., 2011. The Best Estimate Plus Uncertainty Challenge in the Current Licensing Process of Present Reactors, Science and Technology of Nuclear Installations, Vol. 2011, Article ID 958218, 9 pages, [online document][retrieved 06.10.2014] Available at http://dx.doi.org/10.1155/2011/958218.

Degmova, J., Dekan, J., Slugen, V., Thees, C., Smiesko, I., Seliga, P., 2012, Analysis of Steam Generators Corrosion Products from Slovak NPP Bohunice, International Journal of Corrosion, Volume 2012, Article ID 643727, 6 pages, doi:10.1155/2012/643727.

De Santi, G.F., Mayinger, F., 1993. Steam generator and liquid holdup in steam generator U-tubes during oscillatory natural circulation, Experimental Heat Transfer, vol 6, pp. 367–387, 1993.

Ezsöl, G. Perneczky, L., Szabados, L., Toth, I., 2012. PMK-2, the First Integral Thermal-Hydraulics Tests for the Safety Evaluation of VVER-440/213 Nuclear Power Plants, Science and Technology of Nuclear Installations, Volume 2012, Article ID 780472, 22 pages, doi:10.1155/2012/780472.

FDA, 2002, [online document] [retrieved 06.10.2014], Available at http://www.fda.gov/RegulatoryInformation/Guidances/ucm126954.htm#_Toc517237938

Fortum, Loviisa power plant's most important safety systems, [online document] [retrieved 06.10.2014] Available at http://www.fortum.com/SiteCollectionDocuments/Energy%20production/Loviisa_power_plants_most_important_safety_systems.pdf

GE Hitachi, ESBWR_General Description Book, 2011. [online document] [retrieved 06.10.2014] Available at http://www.ge-energy.com/products_and_services/products-/nuclear_energy/esbwr_nuclear_reactor.jsp

GE Hitachi, Natural Circulation in ESBWR, factsheet, 2007. [online document] [retrieved 06.10.2014] Available at http://www.ge-energy.com/content/multimedia/-_files/downloads/ESBWR_General% 20Description %20Book.pdf

Gerrard, P., Thompson, N., 2002. Risk-based E-business Testing. Artech House.

Glaeser, H., et al., 1998. NEA-CSNI report; GRS Analyses for CSNI Uncertainty Methods Study (UMS). Nuclear Energy Agency-Committee on the Safety of Nuclear Installations.

Government Decree 733/2008 on the Safety of Nuclear Power Plants, Issued in Helsinki on 27 November 2008, [online document] [retrieved 06.10.2014] Available at http://www.finlex.fi/fi/laki/kaannokset/2008/en20080733.pdf

Heralecky, P., Blaha, M., 2010. Numerical Analysis of Mixing Factors in the RPV of VVER-440 Reactor Using the TRACE Code, International Agreement Report, NUREG/IA-0235, 2010.

Herzlich, P. 1993. "The Politics of Testing". Proceedings of 1st EuroSTAR conference, London, Oct. 25–28, 1993.

Hohorst, J.K., Polkinghorne, S.T., Siefken, L.J., Allison, C.M., Dobbe, C.A., 1994. TMI-2 Analysis using SCDAP/RELAP/Mod3.1, INEL-94/0157. Idaho National Engineering Laboratory, 1994.

Hyvärinen, J., 1993. An Inherent Boron Dilution Mechanism in Pressurized Water Reactors, Nuclear Engineering and Design, 145 (1993), pp. 227–240.

Hyvärinen, J., 1996a. On the fundamentals of nuclear reactor safety assessment: inherent threats and their implications, Dr. Tech. dissertation, STUK-A135, December 1996.

Hyvärinen, J., 1996b. Heat transfer characteristics of horizontal steam generators under natural circulation conditions, Nuclear Engineering and Design 166 (1996) 191–223.

Hyvärinen, J., Kouhia, J., 1997. Experiment Verification of the Horizontal Steam Generator Boil-off Heat Transfer Degradation at Natural Circulation, The Fourth International Seminar on Horizontal Steam Generators, Mar. 11–13, Lappeenranta, Finland (1997).

Hämäläinen, A., 2005. Applying thermal hydraulics modelling in coupled processes of nuclear power plants. Espoo 2005. VTT Publications 578. 103 p. + app. 99 p.

IAEA, 2002. Accident Analysis for Nuclear Power Plants, Safety Reports Series No. 23, IAEA, Vienna 2002.

IAEA, 2003. Accident Analysis for Nuclear Power Plants with Pressurized Water Reactors , Safety Reports Series No. 30, IAEA, Vienna 2003.

IAEA 2008. Best Estimate Safety Analysis for Nuclear Power Plants: Uncertainty Evaluation. IAEA Safety Reports Series No. 52. IAEA, Vienna 2008.

IAEA, 2009a. Safety Assessment for Facilities and Activities, IAEA Safety Standards Series No. GSR Part 4, IAEA, Vienna 2009.

IAEA, 2009b. Deterministic Safety Analysis for Nuclear Power Plants. IAEA Specific Safety Guide No. SSG-2. IAEA, Vienna 2009.

IAEA, 2012. Safety of nuclear power plants: Design. IAEA Safety Standard Series, Specific Safety Requirement SSR-2/1, International Atomic Energy Agency, Vienna, 2012.

IAEA Status report 108 - VVER-1200, 2011. [online document] [retrieved 06.10.2014] Available at http://www.iaea.org/NuclearPower/Downloadable/aris/2013/36.VVER-1200(V-491).pdf

IBM, 2013. [online document] [retrieved 06.10.2014] Available at http://www.ibm.com/developerworks/rational/library/compliant-agile-medical-device/index.html?ca=dat

Ishii, M., Revankar, S. T., Leonardi, T., et al., 1998. "The three-level scaling approach with application to the Purdue University Multi-Dimensional Integral Test Assembly (PUMA)," Nuclear Engineering and Design, vol. 186, no. 1–2, pp. 177–211, 1998.

Jeong, J.-J., Hwang, M., Lee, Y. J., Chung, B. D., 2004. Non-uniform flow distribution in the steam generator U-tubes of a pressurized water reactor plant during single- and two-phase natural circulations, Nuclear Engineering and Design 231 (2004) 303–314.

Kervinen, T., Jaakkola, S., Mattila, L., 1980. Reflooding Experiments in the REWET-I Single Pin. Proceedings of ANS/ENS Topical Meeting on Thermal Reactor Safety. Knoxville, Tennessee, USA, April 6-9, 1980, pp. 411–418.

Kervinen, T., Hämäläinen, A., Miettinen, J., 1983. Reflood Experiments in the REWET-II, Rod Bundle Facility Including Comparisons with Computer Calculations, Proceedings of Second International Topical Meeting on Thermohydraulics. Santa Barbara, California, USA, 11-14 January, 1983, pp. 638–645.

Kervinen, T., Tuunanen, J., 1987. Emergency cooling experiments with aqueous boric acid solution in the REWET-II facility. Transactions of the American Nuclear Society, Vol/Issue: 55; American Nuclear Society Winter Meeting, Los Angeles, CA, USA, 15 Nov 1987.

Kervinen, T., Purhonen, H., Kalli, H., 1987. Oscillations of the Natural Circulation Flow in Small Break Conditions in the REWET-III Facility, Proceedings of the ASME Winter Annual Meeting, Boston, Massachusetts, USA. December 13–18, 1987, pp. 83–89.

Kouhia, V., Purhonen, H., Riikonen, V., Puustinen, M., Kyrki-Rajamäki, R., Vihavainen, J., 2012. PACTEL and PWR PACTEL test facilities for versatile LWR applications, Science and Technology of Nuclear Installations, Volume 2012, p. 8, Article id 548513, doi:10.1155/2012/548513, ISSN 1687-6075.

Kukita, Y., Nakamura, H., Tasaka, K., Chauliac, C., 1988. Nonuniform Steam Generator U-Tube Flow Distribution During Natural Circulation Tests in ROSA-IV Large Scale Test Facility, Nuclear Science and Engineering, Volume 99, Number 4, August 1988, pp. 289–298.

Kyrki-Rajamäki, R., Talus, M., 2013. The 4th fundamental safety function for systematic evaluation of existing and new generation nuclear reactors: avoidance of fast exothermic chemical reactions, The 22nd international conference Nuclear Energy for New Europe in 2013, September 9–12, 2013, Bled, Slovenia.

Leyer, S., Wich, M., 2012. The Integral Test Facility Karlstein, Science and Technology of Nuclear Installations, Volume 2012, Article ID 439374, 12 pages, doi:10.1155/2012/439374.

Lomperski, S., Kouhia, J., 1994. Natural circulation experiments with a VVER reactor geometry. Nuclear Engineering and Design 147 (1994), 409–424.

Martinez-Quiroga, V., Reventos, F., 2014. The Use of System Codes in Scaling Studies: Relevant Techniques for Qualifying NPP Nodalizations for Particular Scenarios, Science and Technology of Nuclear Installations, Volume 2014, Article ID 138745, 13 pages, http://dx.doi.org/10.1155/2014/138745.

Navahandi, A.N., Castellana, S., Moradkhaniav, E.N., 1982. Scaling laws for modeling nuclear reactor systems. Nuclear Science and Engineering, 72.

Noël, B., Barbier, J.-C., Dumont, D., Weber, O., 1999. CATHARE simulations of the Loss of Residual Heat Removal System conducted at the BETHSY integral test facility, Proceedings of the 7th International Conference on Nuclear Engineering (ICONE-7), Tokyo, Japan, April 1999.

NUREG, 1993, Reactor Safety Issues Resolved by the 2D/3D Program (NUREG/IA-0127, GRS-101, MPR-1346 (July 1993). [online document] [retrieved 06.10.2014] Available at http://pbadupws.nrc.gov/docs/ML0625/ML062570376.pdf

Oberkampf, W.L., Trucano, T.G., 2007. Design of and Comparison with Verification and Validation Benchmarks. [online document] [retrieved 06.10.2014] Available at https://www.oecd-nea.org/nsd/reports/2007/nea6298/Invited_Papers/Oberkampf.pdf

OECD/NEA, 1991. TMI-2 Analysis Exercise Final Report, NEA/CSNI/R(91)8, 1991. [online document][retrieved 06.10.2014] Available at http://www.oecd-nea.org/nsd/docs/1991/csni-r91-8.pdf

OECD/CSNI, 1996. Integral Test Facility Validation Matrix for the Assessment of Thermal-Hydraulic Codes for LWR LOCA and Transients, OECD, Paris, France, 1996.

OECD/NEA, 2001. Validation matrix for the assessment of thermal-hydraulic code validation matrix, Tech. Rep. NEA/CSNI/R, OECD Support Group on the VVER Thermal-Hydraulic Code Validation Matrix, Paris, France, 2001.

OECD/CSNI, 2011. Workshop on Best Estimate Methods and Uncertainty Evaluations, Workshop Proceedings Part 2, Barcelona, Spain, 16–18 November 2011. [online document] [retrieved 06.10.2014]
Available at http://www.oecd-nea.org/nsd/docs/2013/csni-r2013-8-part2.pdf

Pourgol-Mohammad, M., 2009. Thermal-hydraulics system codes uncertainty assessment: A review of the methodologies, Annals of Nuclear Energy 36 (2009) 1774–1786.

Pourgol-Mohammad, M., Mosleh, A., Modarres, M., 2011. Structured treatment of model uncertainty in complex thermal-hydraulics codes: Technical challenges, prospective and characterization, Nuclear Engineering and Design, Vol. 241 (2011) pp. 285–295.

Prosek, A., Leskovar, M., Mavko, B., 2008. Quantitative assessment with improved fast Fourier transform based method by signal mirroring, Nuclear Engineering and Design Vol. 238 (2008) pp. 2668–2677.

Purhonen, H., Kouhia, J., Holmström, H., 1994. ISP-33, OECD/NEA-CSNI INTERNATIONAL STANDARD PROBLEM No. 33, PACTEL Natural Circulation Stepwise Coolant Inventory Reduction Experiment, Comparison Report, Vols 1 and 2, NEA/CSNI/R(94)24, Parts 1 and 2, December 1994.

Purhonen, H., 2004. PACTEL Experiments. Summary report. EU Project IMPAM-VVER, Improved Accident Management of VVER Nuclear Power Plants, Project No. FIS-2001-00117, 30p +app. 40p.

Purhonen, H., 2007. Experimental thermal hydraulic studies on the enhancement of safety of LWRs, Acta Universitatis Lappeenrantaensis, 293, Lappeenranta University of Technology, Digipaino 2007, Lappeenranta, 2007, 73+apps.

Purhonen, H., Puustinen, M., Riikonen, V., Kyrki-Rajamäki, R., Vihavainen, J., 2005. PACTEL—a versatile facility for research of thermal hydraulics, the 11th international topical meeting on nuclear reactor thermal-hydraulics (Nureth-11), Popes' palace conference center, Avignon, France, October 2–6, 2005, 2005, p. 20 pages, cd-rom.

Purhonen, H., Puustinen, M., Riikonen, V., Kyrki-Rajamäki, R., Vihavainen, J., 2006. PACTEL integral test facility—description of versatile applications, Annals of Nuclear Energy, 2006, vol. 33, p. 994–1009.

Puustinen, M., 2002. Natural circulation flow behavior at reduced inventory in a VVER geometry, Nuclear Engineering and Design 215 (2002) 99–110.

Regulatory Forum, [online document] [retrieved 06.10.2014], Available at http://www.regulatory.com/forum/article/test-val.html

RELAP5/MOD3.3, 2001. Code Manual Volume I: Code Structure, System Models and Solution Methods, NUREG/CR-5535/Rev 1-Vol I., December 2001.

Rempe, J. L., Knudson, D. L., 2013. TMI-2—A Case Study for PWR Instrumentation Performance during a Severe Accident, INL/EXT-13-28043, March 2013. [online document][retrieved 06.10.2014] Available at http://www.inl.gov/technicalpublications/Documents/5807657.pdf

Reyes, J.N., Wu, Q., King, J.B., 2003. Scaling Assessment for the Design of the OSU APEX-1000 Test Facility, OSU-APEX-03001, May 12, 2003. Prepared for US DOE.

Riikonen, V., Puustinen, M., Kouhia, J., 1995. RELAP5/MOD3.1 and APROS 3.0 analyses of SBLOCA in scaled VVER-440 geometry, Transactions of the American Nuclear Society; vol. 73; ISSN 0003-018X; p. 511–512; Winter meeting of the American Nuclear Society (ANS); San Francisco, CA (United States); 29 Oct–1 Nov 1995.

Riikonen, V., Kouhia, V., Vihavainen, J., 2011. Study of flow reversing in vertical heat exchange tubes, PAX 4/2011, 2011, p. 14 + app. 8 p., Lappeenranta, research report, Lappeenranta University of Technology, Nuclear Safety Research Unit.

Roache, P. J., 1998. Verification and Validation in Computational Science and Engineering. Albuquerque, NM: Hermosa Publishers, 1998.

Rosatom, 2011, [online document] [retrieved 06.10.2014] Available at http://www.atomproekt.com/resources/f3b59380478326aaa785ef9e1277e356/AES-2006_2011_EN_site.pdf

Routamo, T., Siltanen, S., Lundström, P., 2004, PSA Level 2 Source Term Approach in the Loviisa NPP, OECD/CSNI International Workshop on Level 2 PSA and Severe Accident Management. Köln, Germany, 29-31 March 2004.

Sanders, J., 1991. Methods of Heat Loss Measurement for a thermohydraulic Facility, Experimental Heat Transfer, vol. 4, pp. 127–151, 1991.

Schulz, T.L., 2006. Westinghouse AP1000 advanced passive plant, Nuclear Engineering and Design 236 (2006) 1547–1557.

Sargent, R.G., 2013. Verification and validation of simulation models, Journal of Simulation (2013) 7, pp. 12–24, doi:10.1057/jos.2012.20.

Sarrette, C., 2003. Effect of noncondensable gases on circulation of primary coolant in nuclear power plants in abnormal situations. Acta Universitatis Lappeenrantaensis 144, Diss., Lappeenranta University of Technology. Lappeenranta 2003. 114 p. ISBN 951-764-717-4.

Semken, R.S., Tuunanen, J., 1996. PACTEL Natural circulation Experiments in Low Primary Pressure (SIR-23, SIR-20 and SIR-21), Experimental Data Report, TEKOJA 4/95, VTT Energy, 1996.

Sonnenburg, H.G., Tuomisto, H., 1993. Analysis of a selected two-phase flow phenomenon in VVER reactors with horizontal steam generators, Nuclear Engineering and Design, Volume 145, Issues 1–2, 2 November 1993, pp. 261–269.

Spillner, A., 2004. The W-model—Strengthening the Bond between Development and Test. [online document][retrieved 06.10.2014] Available at http://www.stickyminds.com/article/w-model-strengthening-bond-between-development-and-test

STUK, 2003. Transient And Accident Analyses For Justification Of Technical Solutions At Nuclear Power Plants, GUIDE YVL 2.2, Helsinki 2005, ISSN 0783-2346.

STUK, 2013. Deterministic Safety Analyses For A Nuclear Power Plant, Guide YVL B.3, ISBN 978-952-309-074-3.

STUK, 2007. Safety assessment of the Loviisa nuclear power plant. Statement regarding the licence application by Fortum Power and Heat Oy concerning the operation of the Loviisa nuclear power plant. STUK-B 81. Helsinki 2007. 78 pp.

Szabados, L., Ezsöl, G., Perneczky, L., Toth, I., 2007. Final report on the PMK projects. Results of experiments performed in the PMK-2 facility for VVER safety studies, Tech. Rep. vol. I, Akademiai Kiado, Budapest, Hungary, 2007.

Szabados, L., Ezsöl, G., Perneczky, L., et al., 2009. Final report on the PMK projects. Major findings of PMK-2 test results and validation of thermohydraulic system codes for VVER safety studies, Tech. Rep. vol. II, Akademiai Kiado, Budapest, Hungary, 2009.

Technical Program Group, 1989. Quantifying Reactor Safety Margins: Application of Code Scaling, Applicability, and Uncertainty Evaluation Methodology to a Large Break Loss of Coolant Accident. Technical Report NUREG/CR-5249 EG&G, Idaho, Inc.

TMI-2 Analysis Exercise, 1991. Final Report, [online document] [retrieved 06.10.2014] Available at http://www.oecd-nea.org/nsd/docs/1991/csni-r91-8.pdf

Toth, I., 1988. Loop seal effects on core cooling in VVER type reactors, In: Proceedings of the International ENS/ANS Conference on Thermal Reactor Safety, NUCSAFE 88, Vol. 2. Avignon, France, pp. 1049–1058.

TRACE V5.0 User's Manual. Volume 1: Input Specification. USNRC, Division of System Analysis and Regulatory Effectiveness. PDF Document.

TRACE V5.0 User's Manual. Volume 1: Modeling Guidelines. USNRC, Division of System Analysis and Regulatory Effectiveness. PDF Document.

TRACE V5.830 User's Manual, 2013. Volume 2: Modeling Guidelines. USNRC, Division of System Analysis and Regulatory Effectiveness. PDF Document, 2013.

TRACE V5.840 Theory Manual, 2013. Field Equations, Solution Methods and Physical Models. USNRC, Division of System Analysis and Regulatory Effectiveness. PDF document.

Tuunanen, J., 1994. Thermal-hydraulic studies on the safety of VVER-440 type nuclear power plants, Lappeenranta University of Technology, Lappeenranta 1994.

Tuunanen, J., Kouhia, J., Purhonen, H., Riikonen, V., Puustinen, M., Semken, R.S., Partanen, H., Saure, I., Pylkkö, H., 1998. General description of the PACTEL test facility, Espoo, VTT, VTT Research Note No. 1929. 35 p. ISBN 951-38-5338-1.

Umminger, K., Dennhardt, L., Schollenberger, S., Schoen, B., 2012. Integral Test Facility PKL: Experimental PWR Accident Investigation, Science and Technology of Nuclear Installations, Volume 2012, Article ID 891056, 16 pages, doi:10.1155/2012/891056.

Vihavainen, J., Riikonen, V., Puustinen, M., Kyrki-Rajamäki, R., 2011. Modeling of the PACTEL Facility and Simulation of a Small Break LOCA Experiment with the TRACE v5.0 code, the 14th international topical meeting on nuclear reactor thermal hydraulics, Nureth-14, Toronto, Ontario, Canada, September 25–30, 2011, Cd-ROM, art nro. 463.

Vihavainen, J., Riikonen, V., Kyrki-Rajamäki, R., 2010. TRACE code modeling of the horizontal steam generator of the PACTEL facility and calculation of a loss-of-feedwater experiment, Annals of Nuclear Energy, 2010, vol. 37, No. 11, p. 1494–1501, ISSN 0306-4549.

Virtanen, E., Haapalehto, T., Kouhia, J., 1997. Analysis of steam generator loss-of-feedwater experiments with APROS and RELAP5:MOD3.1 computer codes, Nuclear Engineering and Design 177 (1997) 147–153.

Wilks, S.S., 1941, Determination of sample sizes for setting tolerance limits. Ann. Math. Statist. 12, pp. 91–96.

WWER-440/213 – The secondary circuit, [online document] [retrieved 06.10.2014], Available at
http://paksnuclearpowerplant.com/download/3460/The%20secondary%20circuit.pdf

Yang, R., Liu, R., Liu, J., Qin, S., 2008. Analysis of Reverse Flow in Inverted U-Tubes of Steam Generator under Natural Circulation Condition, Journal of Nuclear Science and Technology, Vol. 45, No. 12, p. 1252–1260 (2008).

Yonomoto, T., 2005. ROSA/LSTF Experiments on PWR Natural Circulation and Validation of RELAP5/MOD3.3, Japan Atomic Energy Research Institute, IAEA's Second Research Coordination Meeting on the CRP on Natural Circulation Phenomena, Modelling, and Reliability of Passive Safety Systems that Utilize Natural Circulation, Oregon State University, Corvallis, Oregon, USA, 2005.

Zarifi, E., Jahanfarnia, G.R., Mousavian, S.K., D'Auria, F., 2009. Semi 2D modeling of the horizontal steam generator PGV-1000 using the RELAP5 code, Progress in Nuclear Energy, 51 (2009) pp. 788–798.

Appendix 1: Additional tables

Experiments and test facilities in OECD validation matrices of VVERs.

- Matrix I is Cross Reference Matrix for Large Breaks in VVERs
- Matrix II is Cross Reference Matrix for Small and Intermediate Leaks
- Matrix III is Cross Reference Matrix for Transients

Extracts from:

Validation Matrix for the Assessment of Thermal-Hydraulic Codes for VVER LOCA and Transients, a Report by the OECD Support Group on the VVER Thermal-Hydraulic Code Validation Matrix, Nuclear Energy Agency,

Matrix 1: Cross Reference Matrix for Large Breaks in VVERs

- CSNI
  + covered by
  o partially covered
  - not covered

- **Phenomenon vs plant type**
  + fully specific to WWER
  o partially specific
  - not specific

- **Phenomenon vs test type**
  + occuring
  o partially occuring
  - not in list

- **Test facility vs phenomenon**
  + suitable for code assessment
  o limited suitability
  - not suitable
  x expected to be suitable

- **Test type vs test facility**
  + already performed
  o performed but of limited use
  - not performed

- **Plant type vs test facility**
  + covered by
  o partially covered
  - not covered

		Plant type			Test type			TEST FACILITY *1																
								System Tests				Separate Effects Tests												
		CSNI	WWER-440/213	WWER-1000	Blowdown	Reflood	Refill	PSB-WWER	PM-5	SB	ISB-WWER	Data bank (REFC)	LWL	REWET-II	IVO-CCFL	SKN	SVD-1	SVD-2	TVC-440	EVTUS	KS	TOPAZ	SG-NPP
Phenomena	Break flow	+	-	-	+	+	+	x		+	x	+												
	Phase separation	o	+	o	o	+	+	x			x				o									
	Mixing and condensation during injection	o	+	+	o	+	+	x			x													
	2--phase flow in SG primary and secondary side	-	o	o	o	o	o	x			x													
	Core wide void + flow distribution	o	+	+	o	+	+	x	o		-													
	ECC downcomer bypass and penetration	o	+	+	o	o	+	-			-													
	UP injection and penetration	-	+	+	0	+	+	x		+	x			+				+	+					
	CCFL (UCSP)	o	+	+	o	+	+	x	+		x				+									
	Steam binding (liquid carry over, ect.)	o	o	o	-	+	o	x		+	x													
	Pool formation in UP	o	+	+	-	+	+	x	+		x													
	Core heat transfer incl. DNB, dryout, RNB	o	+	+	+	+	+	x	o	+	x		+			+	+	+	o	o	+			
	Quench front propagation	o	+	+	o	+	o	x		+	x		+	+			+	x	+	o		+		
	Entrainment (Core, UP)	-	+	o	o	+	o	x	o	+	x			+				x	o					
	Deentrainment (Core, UP)	-	+	o	-	+	o	x	o	+	x			+				x	o					
	1 - and 2-phase pump behaviour	-	+	+	+	0	0	x			-													
	Noncondensible gas effects	-	o	o	-	+	+	x			x													x
Test Facility System Test	ISB-WWER		o	+	-	-	-																	
	PSB-WWER			+	-	-	-																	
	SB		+	+	+	+	+																	
	PM-5			+		+																		

important test parameter
- pumps off/pumps on
- ECC injection mode
- ACC-pressure

*1 refer to description of test facilities - leak location/leak size

Matrix II: Cross Reference Matrix for Small and Intermediate Leaks

- **CSNI**
  + covered by
  o partially covered
  - not covered

- **Phenomenon vs plant type**
  + fully specific to WWER
  o partially specific
  - not specific

- **Phenomenon vs test type**
  + occuring
  o partially occuring
  - not occuring

- **Test facility vs phenomenon**
  + suitable for code assessment
  o limited suitability
  - not suitable
  x expected to be suitable

- **Test type vs test facility**
  + already performed
  o performed but of limited use
  - not performed

- **Plant type vs test facility**
  + covered by
  o partially covered

		Plant Type			Test Type							System Tests						TEST FACILITY *1										
																		Separate Effects Tests										
		CSNI	WWER-440/213	WWER-1000	Stationary Test addressing energy transport on primary	Stationary Test addressing energy transport on secondary side	Small leak, overfeed by EBWS, secondary side necessary	Small leak without HPIS overfeeding, secondary side	Intermediate leak, secondary side not necessary	Pressurizer leak	SG-tube rupture	SG-header rupture	PACTEL	PMK-2	PSB-WWER	PM-5	SB	ISB-WWER	Data bank (IBEC)	IVO-Loop Seal *2	IVO-CCFL *2	HORUS-II	Thermal Mixing	SVD-1	SVD-2	EVTUS	KS-1	SG-NPI-NV AEP	IF-SC
		+	-	-	+	+	+	o	-	+	+	+	+	+	+	o		+		-	-							+
Phenomena	Natural circulation in 2-phase flow, primary side	o	o*	o*	+	-	o	+	+	o	-	+	+	+	+	o		+		-	-							+
	Reflux condenser mode and CCFL	o	-	-	+	-	-	+	+	+	-	+	-	-	-			-									x	
	Asymmetric loop behaviour	-*1	+	o	+	-	+	+	-	o	+	-	+	-	o			-		-	-								
	Leak flow	+	-	-	-	-	+	+	+	+	+	+	o	o	o			+	+										
	Phase separation without mixture level formation	o	+	o	+	-	o	+	+	+	o	+	o	o	x			o											
	Mixture level and entrainment in SG (SS+PS)	-	+	+	-	+	+	+	+	+	+	+	o	o	x	o		o		-	-	-							
	Mixture level and entrainment in the core	-	+	o	+	-	-	+	+	+	-	o	o	o	x			o		-	-			x					
	Stratification in horizontal pipes	+	-	-	+	-	-	+	+	-	-	o	o	o	x			-		o	-							x	
	ECC-mixing and condensation	o	+	+	-	-	o	+	+	+	+	+	o	o	o			o		-	-		+						
	Loop seal clearance (CL)	+	-	-	-	-	-	+	+	o	-	-	o	o	+	+	+	-		+	-								
	Pool formation in UP/CCFL (UCSP)	o	+	+	+	-	-	o	+	+	-	o	o	-	-	+		-		-	+			x					
	Core wide void and flow distribution	o	+	o	+	-	-	o	+	+	-	o	o	o	x	o		-		-	-				x				
	Heat transfer in covered core	+	o	-	+	+	+	+	+	+	+	+	+	+	x	+	+	+		-	-			x	x	o	+		
	Heat transfer in partly uncovered core	+	o	-	+	-	-	o	+	-	-	o	o	o	x	+	+	+		-	-			x	x		+		
	Heat transfer in SG primary side	-	+	+	+	o	o	+	+	o	o	+	o	o	x			o	o	-	-	+						o	
	Heat transfer in SG secondary side	-	+	+	o	+	+	+	+	+	+	+	o	o	o			-		-	-	-						+	
	Pressurizer thermohydraulics	-	+	+	o	-	o	o	+	+	+	o	o	o	x			o	o										
	Surgeline hydraulics	o	o	o	o	-	-	o	+	+	o	o	o	o	x			o		-	-								
	1- and 2-phase pump behaviour	-	+	+	-	-	-	o	+	-	-	o	x	-	x			-		-	-								
	Structural heat and heat losses	+	-	-	+	-	o	+	+	o	o	+	o	o	x			o		-	-								
	Noncondensible gas effects	o*3	+	+	+	-	-	-	-	-	-	-	x	+	x	x		x		-	-	x						x	
	Phase separation in T-junct. and effect on leakflow	+*3	-	-	-	-	-	+	+	-	-	o	-	-	-			-	o	-	-								
	Nat. circul., core-gap-downcomer, dummy elem.	-	+	+	o	+	+	-	-	-	+	o	-	-	-		+	-											
	Loop seal behaviour in HL	-	+	-	+	-	-	+	+	+	-	o	+	+	-		+	-											
	Recirculation in the SG primary side	-	+	+	+	-	-	+	o	o	-	-	+	x	x			x				-						x	
	Boron mixing and transport	-	+	+	-	-	-	+	+	+	o	o			o														
	Water accumulation in SG tubes	-	+	+	+	-	-	+	+	+	-	-	o	o	-	-	-	-				+						x	
Test Facility System Tests	WWER 1 : 1										+																		
	PMK-2		+		+	-	-	+	+	o	-	+																	
	REWET-III		+		+	+	+	-	-	-	o	-																	
	PACTEL		+		+	+	o	+	-	-	-	-																	
	ISB-WWER		o	+	-	-	-	o	-	-	-	-																	
	PSB-WWER		+		-	-	-	-	-	-	-	-																	
	SB		+	+			o	o	+																				
	PM-5		-	+	o		o																						

*1 refer todescription of test facilities

*2 included in the CSNI

*3 will be provided in the revised IT-matrix

Matrix III: Cross Reference Matrix for Transients

- CSNI
  - + covered by
  - o partially covered
  - - not covered
- Phenomenon vs plant type
  - + fully specific to WWER
  - o partially specific
  - - not specific
- Phenomenon vs test typ
  - + occuring
  - o partially occuring
  - - not occuring
- Test facility vs phenomenon
  - + suitable for code assessment
  - o limited suitability
  - - not suitable
  - x expected to be suitable
- Test type vs test facility
  - + already performed
  - o performed but of limited use
  - - not performed
- Plant type vs test facility
  - + covered by
  - o partially covered
  - - not covered

			Plant Type		Test Type									TEST FACILITY *6											
														System Tests							Separate Effects Tests				
		CSNI	WWER-440/213	WWER-1000	ATWS	Loss of feedwater, non	Loss of heat sink, non ATWS	Station blackout	Steam line break	Feed line break	Cooldown prim. feed and bleed	Reactivity disturbance	Over-cooling	WWER 1:1 *1	PACTEL	PMK-2	PSB-WWER	PM-5	ISB-WWER	BD	Data bank (EREC)	VEERA	REWET II	SVD-2	Mixing Model
Phenomena	Natural circulation in 1-phase flow	+	-	-	+	+	+	+	+	+	+	o	o	+	+	+	+	o	+			-	-		
	Natural circulation in 2-phase flow	o	o+	o+	+	+	+	+	-	-	o	o	-		+	+	+	o	+			-	-		
	Core thermohydraulics	o	+	o	+	+	+	+	o	o	o	+	o	+	+	+	x	o	+			+	+		
	Thermohydraulics on primary side of SG	-	+	+	+	o	o	+	o	o	+	o	+	+	o	o	x		o			-	-	+	
	Thermohydraulics on secondary side of SG	-	+	+	+	+	+	+	+	+	+	o	+	+	o	o	x		-			-	-		
	Pressurizer thermohydraulics *2	-	+	+	+	+	+	+	o	o	o	o	+	o	o	o	o		o		o	-	-		
	Surgeline hydraulics (CCFL, chocking) *2	o	o	o	+	+	+	+	o	o	o	o	o	o	o	o	x		o			-	-		
	1- and 2-phase pump behaviour	-	+	+	+	+	+	+	o	o	o	o	o		x	-	x		-			-	-		
	Thermohydraulic-nuclear feedback	o	+	+	+	-	-	-	+	-	-	+	- +	+	-	-	-		-			-	-		
	Structural heat and heat losses *3	+	-	-	o	o	o	o	o	o	o	o	o		o	o	o		+			-	-		
	Boron mixing and transport	o*5	+	+	-	-	-	-	o	-	-	-	o		x	-	x	-	-	+		+	+		+
Test Facility System Tests	WWER 1 : 1		+	+																					
	PMK-2		+		-	o	-	o	-	-	-	-	-												
	PACTEL		+		-	o	-	o	-	-	-	-	o												
	ISB-WWER		o	+	-	-	-	-	-	-	-	-	-												
	PSB-WWER			+	-	-	-	-	-	-	-	-	-												
	PM-5			+																					
	BD		+	+																					

Revision 6 - Status May 2000

*1 volumetric scaling

*2 for phenomena requiring separate effects test, e.g. pressurizer behaviour, refer to small leak cross reference matrix

*3 problem for scaled test facillities

*4 included in the CSNI SET matrix

*5 refer to descriptions of test facilities

ACTA UNIVERSITATIS LAPPEENRANTAENSIS

583. LANA, ANDREY. LVDC power distribution system: computational modelling. 2014. Diss.

584. PEKKARINEN, JOONAS. Laser cladding with scanning optics. 2014. Diss.

585. PELTOMAA, JYRKI. The early activities of front end of innovation in OEM companies using a new FEI platform as a framework for renewal. 2014. Diss.

586. ROZHANSKY, IGOR. Resonant tunneling effects in semiconductor heterostructures. 2014. Diss.

587. PHAM, THUY DUONG. Ultrasonic and electrokinetic remediation of low permeability soil contaminated with persistent organic pollutants. 2014. Diss.

588. HOKKANEN, SANNA. Modified nano- and microcellulose based adsorption materials in water treatment. 2014. Diss.

589. HINKKANEN, JUHA. Cooperative strategy in emerging markets – analysis of interfirm R&D cooperation and performance in Russian manufacturing companies. 2014. Diss.

590. RUSKOVAARA, ELENA. Entrepreneurship education in basic and upper secondary education – measurement and empirical evidence. 2014. Diss.

591. IKÄHEIMONEN, TUULI. The board of directors as a part of family business governance – multilevel participation and board development. 2014. Diss.

592. HAJIALI, ZUNED. Computational modeling of stented coronary arteries. 2014. Diss.

593. UUSITALO, VILLE. Potential for greenhouse gas emission reductions by using biomethane as road transportation fuel. 2014. Diss.

594. HAVUKAINEN, JOUNI. Biogas production in regional biodegradable waste treatment – possibilities for improving energy performance and reducing GHG emissions. 2014. Diss.

595. HEIKKINEN, JANNE. Vibrations in rotating machinery arising from minor imperfections in component geometries. 2014. Diss.

596. GHALAMCHI, BEHNAM. Dynamic analysis model of spherical roller bearings with defects. 2014. Diss.

597. POLIKARPOVA, MARIIA.Liquid cooling solutions for rotating permanent magnet synchronous machines. 2014. Diss.

598. CHAUDHARI, ASHVINKUMAR. Large-eddy simulation of wind flows over complex terrains for wind energy applications. 2014. Diss.

599. PURHONEN, MIKKO. Minimizing circulating current in parallel-connected photovoltaic inverters. 2014. Diss.

600. SAUKKONEN, ESA. Effects of the partial removal of wood hemicelluloses on the properties of kraft pulp. 2014. Diss.

601. GUDARZI, DAVOOD. Catalytic direct synthesis of hydrogen peroxide in a novel microstructured reactor. 2014. Diss.

602. VALKEAPÄÄ, ANTTI. Development of finite elements for analysis of biomechanical structures using flexible multibody formulations. 2014. Diss.

603. SSEBUGERE, PATRICK. Persistent organic pollutants in sediments and fish from Lake Victoria, East Africa. 2014. Diss.

604. STOKLASA, JAN. Linguistic models for decision support. 2014. Diss.

605. VEPSÄLÄINEN, ARI. Heterogenous mass transfer in fluidized beds by computational fluid dynamics. 2014. Diss.

606. JUVONEN, PASI. Learning information technology business in a changing industry landscape. The case of introducing team entreneurship in renewing bachelor education in information technology in a university of applied sciences. 2014. Diss.

607. MÄKIMATTILA, MARTTI. Organizing for systemic innovations – research on knowledge, interaction and organizational interdependencies. 2014. Diss.

608. HÄMÄLÄINEN, KIMMO. Improving the usability of extruded wood-plastic composites by using modification technology. 2014. Diss.

609. PIRTTILÄ, MIIA. The cycle times of working capital: financial value chain analysis method. 2014. Diss.

610. SUIKKANEN, HEIKKI. Application and development of numerical methods for the modelling of innovative gas cooled fission reactors. 2014. Diss.

611. LI, MING. Stiffness based trajectory planning and feedforward based vibration suppression control of parallel robot machines. 2014. Diss.

612. KOKKONEN, KIRSI. From entrepreneurial opportunities to successful business networks – evidence from bioenergy. 2014. Diss.

613. MAIJANEN-KYLÄHEIKO, PÄIVI. Pursuit of change versus organizational inertia: a study on strategic renewal in the Finnish broadcasting company. 2014. Diss.

614. MBALAWATA, ISAMBI SAILON. Adaptive Markov chain Monte Carlo and Bayesian filtering for state space models. 2014. Diss.

615. UUSITALO, ANTTI. Working fluid selection and design of small-scale waste heat recovery systems based on organic rankine cycles. 2014. Diss.

616. METSO, SARI. A multimethod examination of contributors to successful on-the-job learning of vocational students. 2014. Diss.

617. SIITONEN, JANI. Advanced analysis and design methods for preparative chromatographic separation processes. 2014. Diss.